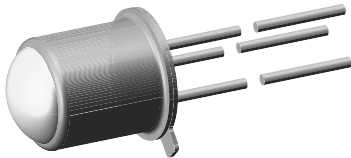


Silicon NPN Phototransistor, RoHS Compliant



94 8401

DESCRIPTION

BPW77 is a silicon NPN phototransistor with high radiant sensitivity in hermetically sealed TO-18 package with base terminal and glass lens. It is sensitive to visible and near infrared radiation.

FEATURES

- Package type: leaded
- Package form: TO-18
- Dimensions (in mm): Ø 4.7
- High photo sensitivity
- High radiant sensitivity
- Suitable for visible and near infrared radiation
- Fast response times
- Angle of half sensitivity: $\varphi = \pm 10^\circ$
- Base terminal connected
- Hermetically sealed package
- Lead (Pb)-free component in accordance with RoHS 2002/95/EC and WEEE 2002/96/EC



e4

RoHS
COMPLIANT

APPLICATIONS

- Detector in electronic control and drive circuits

PRODUCT SUMMARY

COMPONENT	I _{ca} (mA)	φ (deg)	$\lambda_{0.1}$ (nm)
BPW77NA	7.5 to 15	± 10	450 to 1080
BPW77NB	> 10	± 10	450 to 1080

Note

Test condition see table "Basic Characteristics"

ORDERING INFORMATION

ORDERING CODE	PACKAGING	REMARKS	PACKAGE FORM
BPW77NA	Bulk	MOQ: 1000 pcs, 1000 pcs/bulk	TO-18
BPW77NB	Bulk	MOQ: 1000 pcs, 1000 pcs/bulk	TO-18

Note

MOQ: minimum order quantity

ABSOLUTE MAXIMUM RATINGS

PARAMETER	TEST CONDITION	SYMBOL	VALUE	UNIT
Collector base voltage		V _{CBO}	80	V
Collector emitter voltage		V _{CEO}	70	V
Emitter base voltage		V _{EBO}	5	V
Collector current		I _C	50	mA
Collector peak current	t _p /T = 0.5, t _p ≤ 10 ms	I _{CM}	100	mA
Total power dissipation	T _{amb} ≤ 25 °C	P _V	250	mW
Junction temperature		T _j	125	°C
Operating temperature range		T _{amb}	- 40 to + 125	°C
Storage temperature range		T _{stg}	- 40 to + 125	°C
Soldering temperature	t ≤ 5 s	T _{sd}	260	°C
Thermal resistance junction/ambient	Connected with Cu wire, 0.14 mm ²	R _{thJA}	400	K/W
Thermal resistance junction/gase		R _{thJC}	150	K/W

Note

T_{amb} = 25 °C, unless otherwise specified

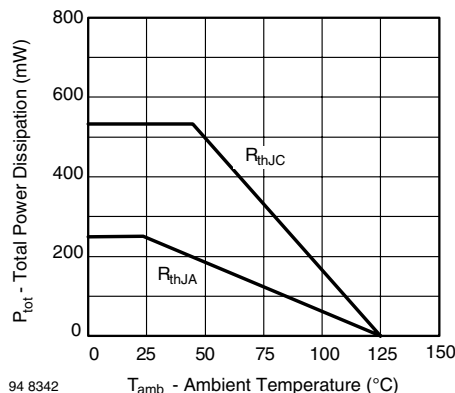


Fig. 1 - Power Dissipation Limit vs. Ambient Temperature

BASIC CHARACTERISTICS						
PARAMETER	TEST CONDITION	SYMBOL	MIN.	TYP.	MAX.	UNIT
Collector emitter breakdown voltage	I _C = 1 mA	V _{(BR)CEO}	70			V
Collector emitter dark current	V _{CE} = 20 V, E = 0	I _{CEO}		1	100	nA
Collector emitter capacitance	V _{CE} = 5 V, f = 1 MHz, E = 0	C _{CEO}		6		pF
Angle of half sensitivity		φ		± 10		deg
Wavelength of peak sensitivity		λ _p		850		nm
Range of spectral bandwidth		λ _{0.1}		450 to 1080		nm
Collector emitter saturation voltage	E _e = 1 mW/cm ² , λ = 950 nm, I _C = 1 mA	V _{CEsat}		0.15	0.3	V
Turn-on time	V _S = 5 V, I _C = 5 mA, R _L = 100 Ω	t _{on}		6		μs
Turn-off time	V _S = 5 V, I _C = 5 mA, R _L = 100 Ω	t _{off}		5		μs
Cut-off frequency	V _S = 5 V, I _C = 5 mA, R _L = 100 Ω	f _c		110		kHz

Note

 T_{amb} = 25 °C, unless otherwise specified

TYPE DEDICATED CHARACTERISTICS							
PARAMETER	TEST CONDITION	PART	SYMBOL	MIN.	TYP.	MAX.	UNIT
Collector light current	E _e = 1 mW/cm ² , λ = 950 nm, V _{CE} = 5 V	BPW77NA	I _{ca}	7.5		15	mA
		BPW77NB	I _{ca}	10			mA

BASIC CHARACTERISTICS

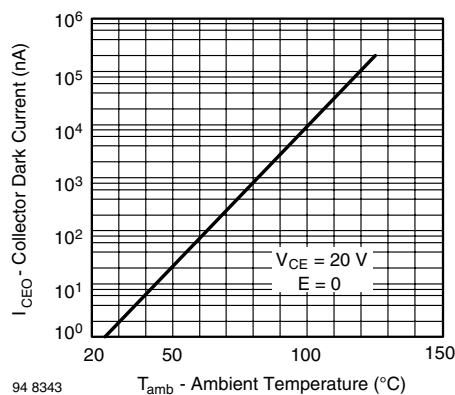
 T_{amb} = 25 °C, unless otherwise specified


Fig. 2 - Collector Dark Current vs. Ambient Temperature

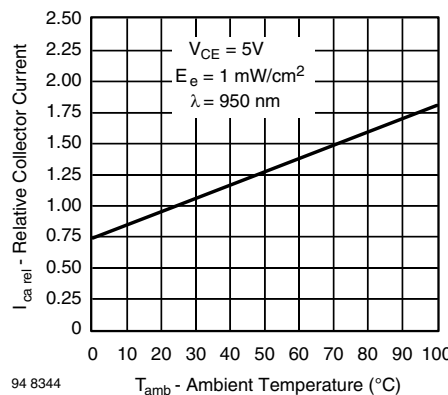


Fig. 3 - Relative Collector Current vs. Ambient Temperature

BPW77NA, BPW77NB

Vishay Semiconductors Silicon NPN Phototransistor, RoHS Compliant

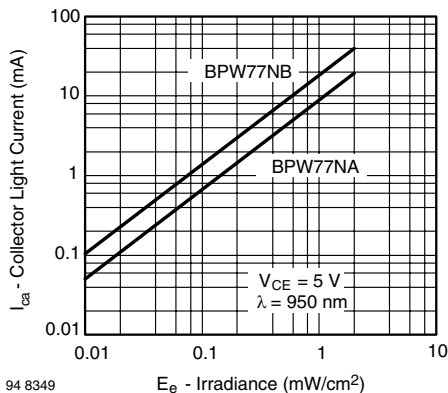


Fig. 4 - Collector Light Current vs. Irradiance

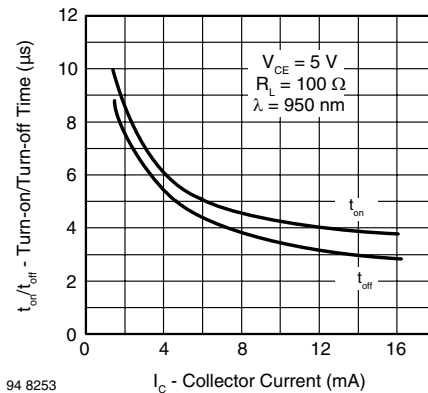


Fig. 7 - Turn-on/Turn-off Time vs. Collector Current

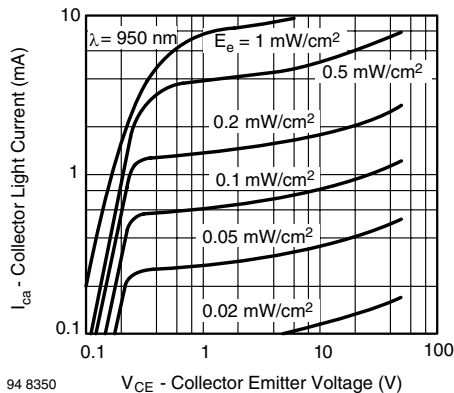


Fig. 5 - Collector Light Current vs. Collector Emitter Voltage

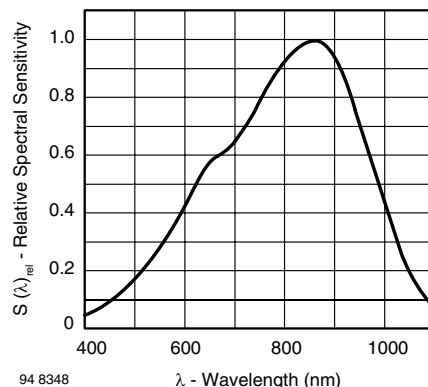


Fig. 8 - Relative Spectral Sensitivity vs. Wavelength

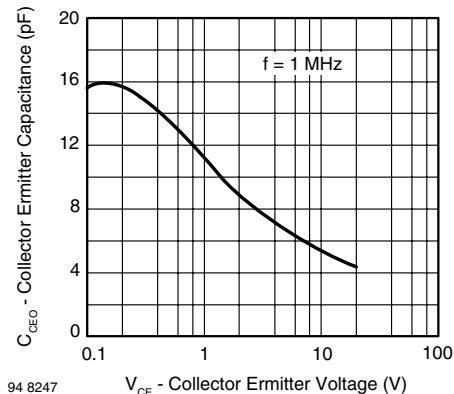


Fig. 6 - Collector Emitter Capacitance vs. Collector Emitter Voltage

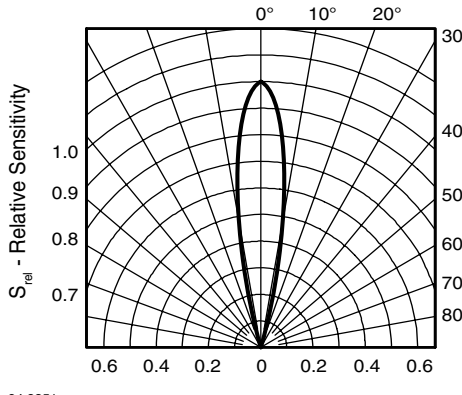
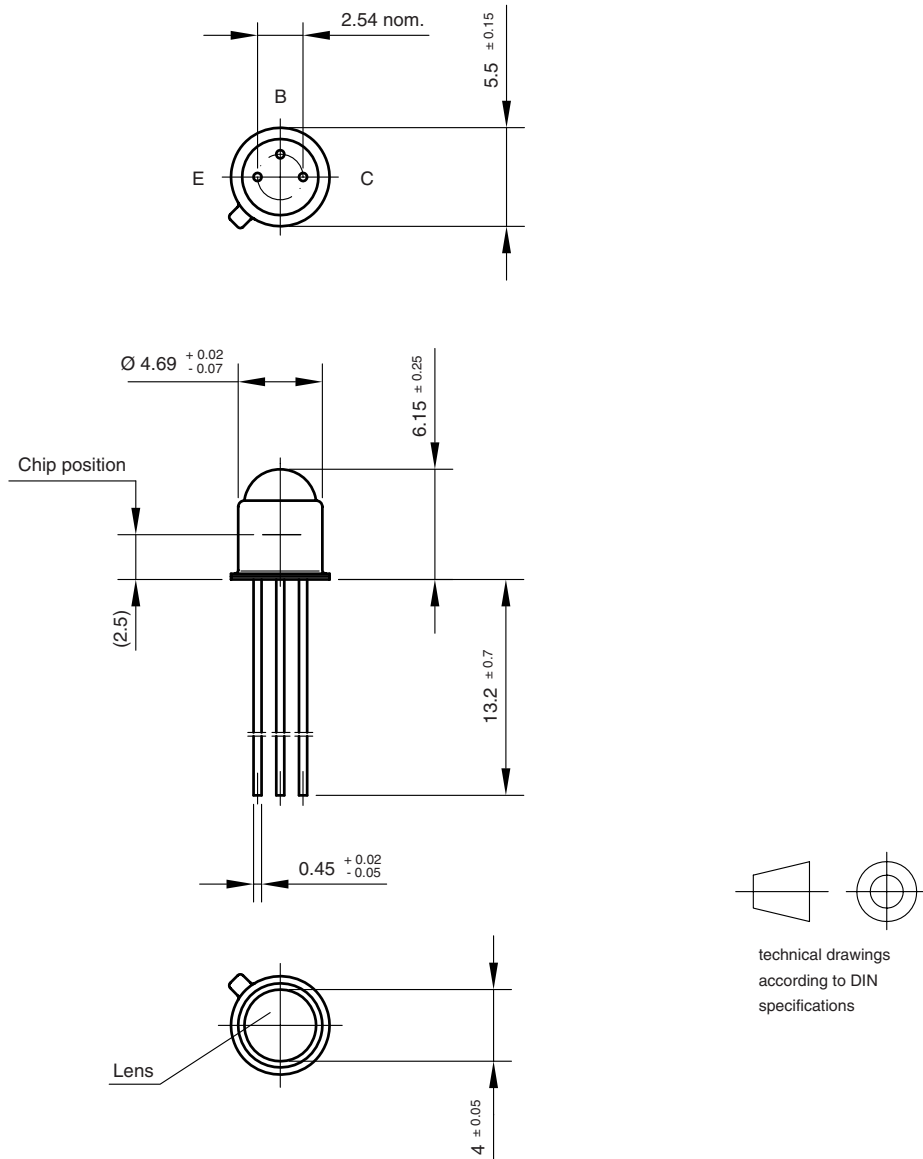


Fig. 9 - Relative Radiant Sensitivity vs. Angular Displacement

PACKAGE DIMENSIONS in millimeters


Drawing-No.: 6.503-5023.01-4

Issue:1; 01.07.96

96 12180

LEDs and 7-Segment Displays

Application Note

Processing Instructions for Mounting of Through-Hole LEDs

By Harald Lunt

INTRODUCTION

Through-hole LED cases usually consist of epoxy casting compounds with duroplastic properties. It is in the nature of things that optical semiconductor devices require transparent materials with the best possible optical features. Unlike standard IC mold compounds, which use reinforcing fillers like glass fibers to achieve better mechanical stability, these optical materials must not be filled. In addition, due to the very small component dimensions, the wall thickness of the casted resin body is also small. All this results in some special aspects regarding mechanical stability during the soldering process to be considered for the processing of leaded LEDs.

THERMAL PROPERTIES OF CURED EPOXY

The chemical cross-linking of thermosetting materials does not allow a real melting when reheated after curing. However, cross-linked materials suffer a softening at an elevated temperature, which is already far below the natural decomposition temperature. The corresponding softening temperature is called the glass transition temperature (T_G). The T_G is not a sharply defined thermodynamic transition, but rather a temperature range over which the mobility of the polymer chains increases significantly, and the base material changes from rigid / glassy to a more rubbery / soft state.

Above T_G , the coefficient of thermal expansion (CTE) of the epoxy increases significantly.

A typical value for T_G is ~ 130 °C and for the increase of CTE from ~ 60 ppm/K to ~ 180 ppm/K below and above T_G , which corresponds to an increase of three times.

KNOWN FAILURE MODES

If the T_G is exceeded too fast, package cracks could emerge, especially from edges of the lead frame, bond wire, or LED chip.

With increasing temperature, the epoxy softens around the highly heat-conductive lead frame, and could be partially detached from the metal so that a delamination could occur. At this stage, previously introduced mechanical tensions (e.g. due to spring effect) may be released, causing the lead frame to slightly move inside the casting resin, and thus bond wires could easily break.

Considering the filigree nature of the bond wire with only about one micro-inch diameter, it is easily comprehensible how important it is to avoid any mechanical stress that could be released during the soldering process.

The following pictures (Fig. 1 to Fig. 4) illustrate the failure modes, based on a practical example:

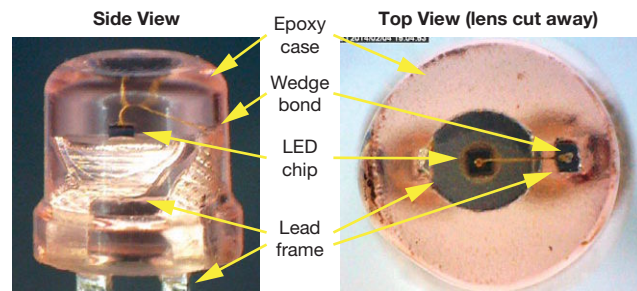


Fig. 1 - Overview Picture of the LEDs

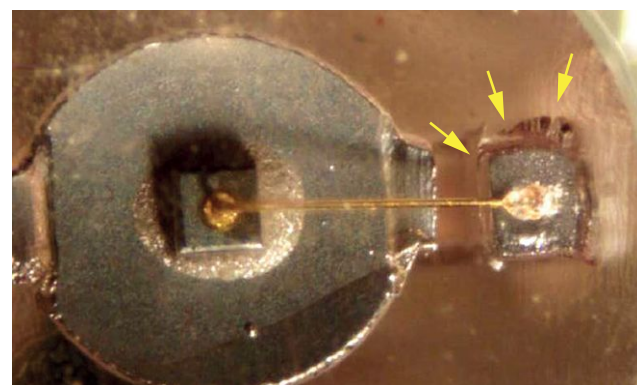


Fig. 2 - Detail View Showing Gaps and Cracks Around Leadframe Post, Indicated by Yellow Arrows

Processing Instructions for Mounting of Through-Hole LEDs

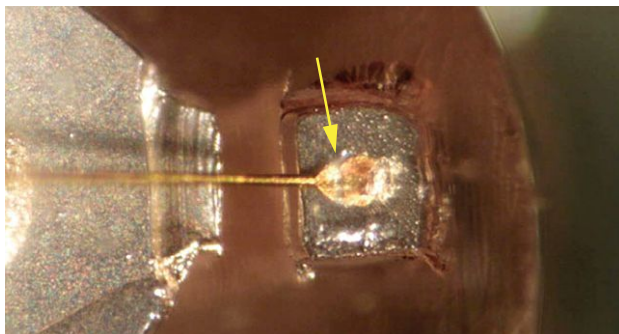


Fig. 3 - Detail View Showing Broken Wedge

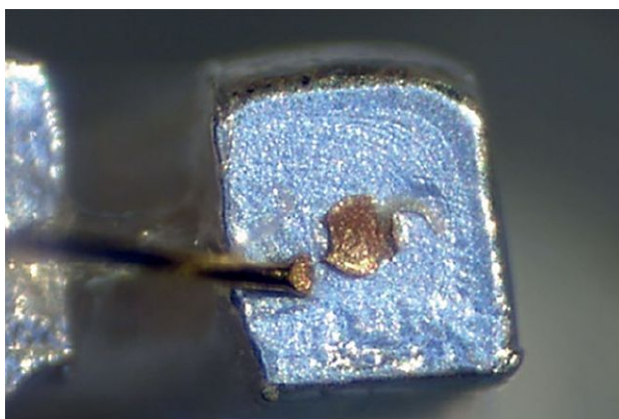


Fig. 4 - Another Example of Broken Wedge After Chemical De-Capsulation

This failure mode could cause immediate open rejects, intermittent behavior, or rather rarely, early fatigue break after some thermal cycles in less severe manifestation, where the bond wire is only pre-damaged after soldering.

ROOT CAUSES

In the example shown above, a plastic holder touching the lower rim of the epoxy case and additional crimping of the LED pins have been used to fix the LEDs on the PCB. Both a spring force applied by the plastic holder and a too-strong crimping of the LED pins contributed to the mechanical damages shown. Even if the maximum temperatures and timing of the soldering profile are within the allowed limits, the described mechanical forces could cause these failure modes.

Furthermore, considering the CTE = 13 ppm/K of steel as a typical lead frame material, an approximate elongation of $\Delta L = \alpha \times L \times \Delta T \approx 30 \mu\text{m}$ happens per 10 mm lead length during the soldering process with 260 °C peak temperature. If the LED is rigidly fixed at the epoxy case by a stiff holder, a pull force occurs during the cooling-down phase while the slower responding epoxy is still in a soft stage.

Further signs of damage could sometimes be observed in the form of cracks at the rim of the epoxy case, at the entry point of the leads into the epoxy case, and as bulging or cracks at points with small wall thickness of the epoxy case.

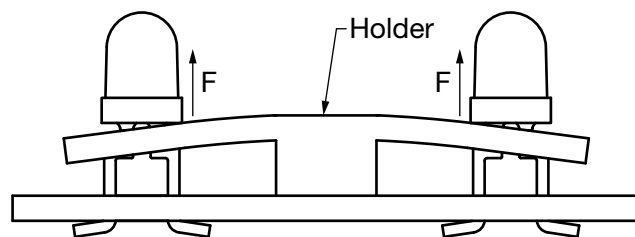


Fig. 5 - Very Critical Holder Design Applying Mechanical Spring Forces to the LEDs

PROCESSING INSTRUCTIONS

The following recommendations should be considered to prevent the LEDs from mechanical stress:

TABLE 1 - RECOMMENDATIONS FOR LED FORMING AND MOUNTING

REF.		
a)		
b)		
c)		
d)		

Processing Instructions for Mounting of Through-Hole LEDs

1. During cutting and lead forming, mechanical force must not be applied to the epoxy case. Suitable measures for strain relief have to be taken (Table 1, a):
 - Do not stress the LED case during lead forming. Use a bending tool, which securely holds the leads at their upper position without touching the epoxy case, so that no force will be transmitted to the epoxy case
 - Minimum 2 mm clearance between the epoxy case and bending point
 - Lead forming has to be done prior to soldering
 - Do not bend the leads more than twice at the same point
2. Generally, do not apply excessive force to the LEDs and allow cooling down of the LED below 50 °C before applying any force from outside
3. The distance between the lower epoxy rim and the closest solder point should be > 2 mm
4. A direct touch down of the epoxy case to the PCB should be avoided
5. The LED pins must be inserted mechanically tension-free into the solder holes (Table 1, a to d)
6. The mounting hole pitch must match the lead pitch of the LED. A proper lead forming according to item "1." may be done to meet this requirement (Table 1, c)
7. Pressure from the top or sides must not be applied to the LED during the whole soldering process, including the cooling-down phase
8. Holders must not create a stiff connection between the epoxy case and PCB, nor apply any spring force to the LED. Component covers or holders must leave some clearance to the epoxy case to avoid stress on the LED (Table 1, b)
9. Crimping should be avoided, or if it is really mandatory, the LED should still have a little clearance so that it could be slightly moved after crimping. The crimping angle should not exceed 45° (Table 1, b)

For further instructions, soldering methods, temperature profiles, and maximum ratings, please refer to individual datasheets and assembly instructions:

www.vishay.com/doc?80092

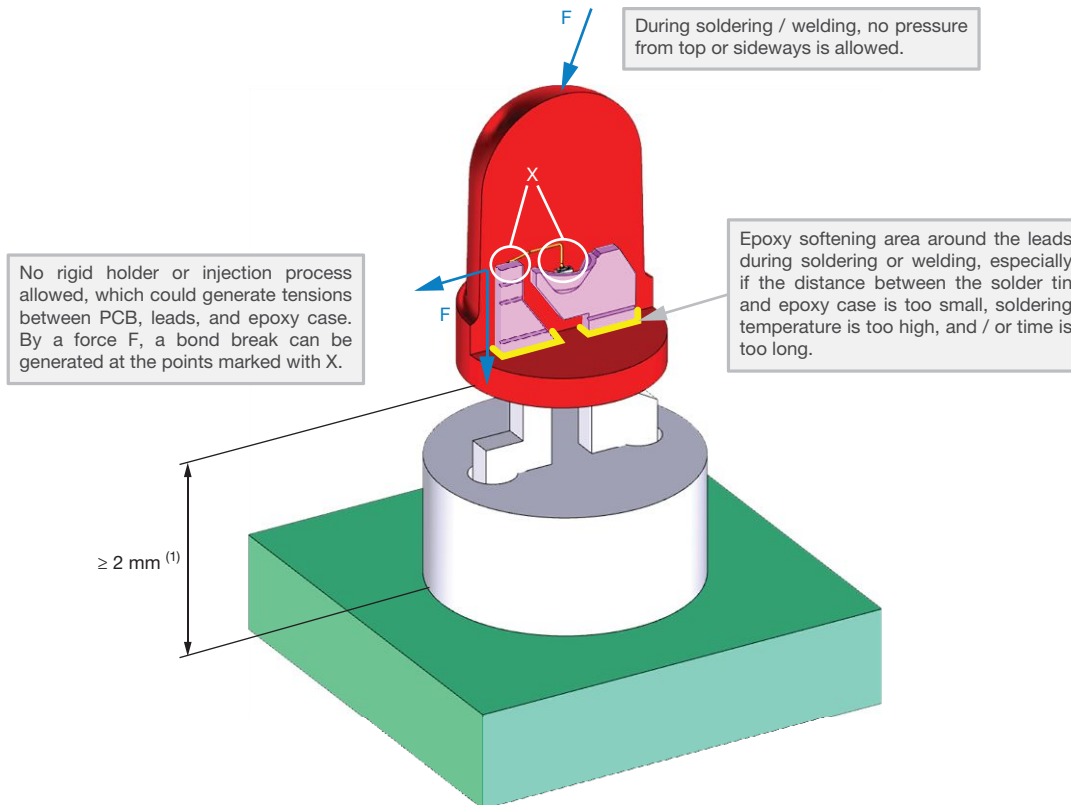


Fig. 6 - Basic Illustration of the Effects

Note

(1) If soldering distance is < 2 mm there is an increased risk to melt / delaminate the castingresin around the connections. Especially in the areas X, the bond connection can be impaired

Component Construction

Vishay Semiconductors

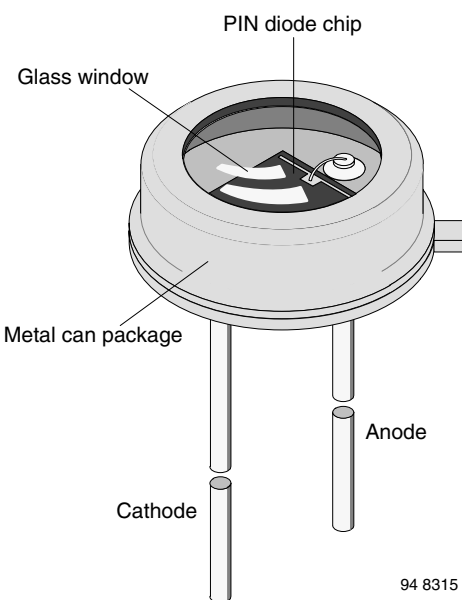
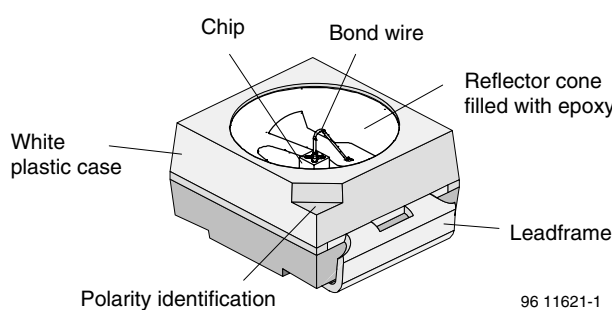
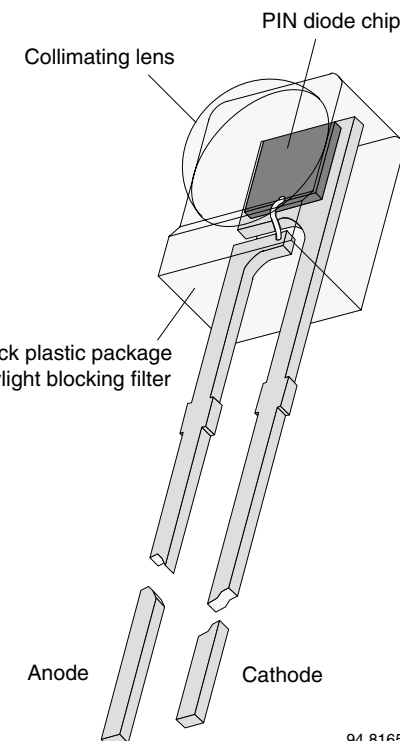
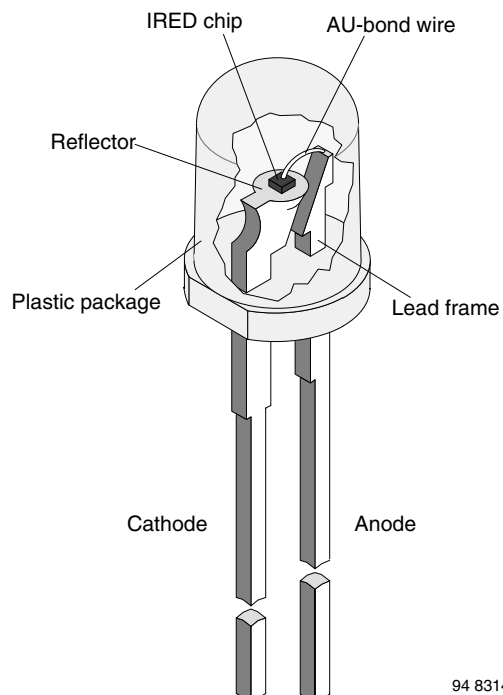


Component Construction

Photodetector and infrared emitter components are available in plastic or metal packages.

Plastic devices mostly include a lens to improve radiant sensitivity or radiant intensity. Detector chips are mounted on flat leadframe surfaces while leadframes for emitters have a silver plated reflector performing higher radiant intensity.

Devices in metal packages are hermetically sealed, are released for extended operating temperature range and have small optical and mechanical tolerances.



Measurement Techniques

INTRODUCTION

The characteristics of optoelectronics devices given in datasheets are verified either by 100 % production tests followed by statistic evaluation or by sample tests on typical specimens. These tests can be divided into following categories:

- Dark measurements
- Light measurements
- Measurements of switching characteristics, cut-off frequency and capacitance
- Angular distribution measurements
- Spectral distribution measurements
- Thermal measurements

Dark and light measurements limits are 100 % measurements. All other values are typical. The basic circuits used for these measurements are shown in the following sections. The circuits may be modified slightly to accommodate special measurement requirements.

Most of the test circuits may be simplified by use of a source measure unit (SMU), which allows either to source voltage and measure current or to source current and measure voltage.

DARK AND LIGHT MEASUREMENTS

EMITTER DEVICES

IR Diodes

Forward voltage, V_F , is measured either on a curve tracer or statically using the circuit shown in figure 1. A specified forward current (from a constant current source) is passed through the device and the voltage developed across it is measured on a high-impedance voltmeter.

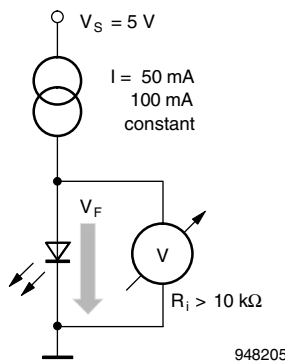


Fig. 1

To measure reverse voltage, V_R , a 10 μ A or 100 μ A reverse current from a constant current source is impressed through the diode (figure 2) and the voltage developed across is measured on a voltmeter of high input impedance ($\geq 10 \text{ M}\Omega$).

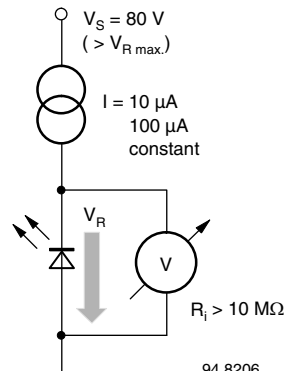


Fig. 2

For most devices, V_R is specified at 10 μ A reverse current. In this case either a high impedance voltmeter has to be used, or current consumption of DVM has to be calculated and added to the specified current. A second measurement step will then give correct readings.

In case of IR diodes, total radiant output power, Φ_e , is usually measured. This is done with a calibrated large-area photovoltaic cell fitted in a conical reflector with a bore which accepts the test item - see figure 3. An alternative test set uses a silicon photodiode attached to an integrating sphere. A constant DC or pulsating forward current of specified magnitude is passed through the IR diode. The advantage of pulse-current measurements at room temperature (25 °C) is that results can be reproduced exactly.

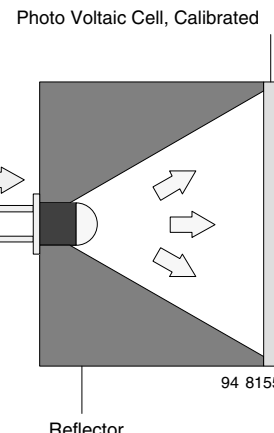


Fig. 3

If, for reasons of measurement economy, only DC measurements (figure 4) are to be made, then the energizing time should be kept short (below 1 s) and of uniform duration, to minimize any fall-off in light output due to internal heating.

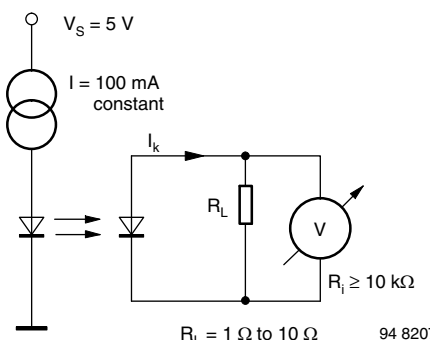


Fig. 4

To ensure that the relationship between irradiance and photocurrent is linear, the photodiode should operate near the short-circuit configuration. This can be achieved by using a low resistance load ($\leq 10 \Omega$) of such a value that the voltage dropped across is very much lower than the open circuit voltage produced under identical illumination conditions ($R_{\text{meas}} \ll R_i$). The voltage across the load should be measured with a sensitive DVM.

A knowledge of radiant intensity, I_e , produced by an IR emitter enables customers to assess the range of IR light barriers. The measurement procedure for this is more or less the same as the one used for measuring radiant power. The only difference is that in this case the photodiode is used without a reflector and is mounted at a specified distance from, and on the optical axis of, the IR diode (figure 5). This way, only the radiant power of a narrow axial beam is considered.

The radiant power within a solid angle of $\Omega = 0.01$ steradian (sr) is measured at a distance of 100 mm. Radiant intensity is then obtained by using this measured value for calculating the radiant intensity for a solid angle of $\Omega = 1$ sr.

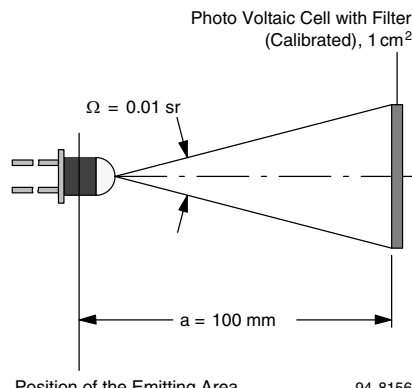


Fig. 5

DETECTOR DEVICES

Photovoltaic cells, photodiodes

- Dark measurements

The reverse voltage characteristic, V_R , is measured either on a curve tracer or statically using the circuit shown in figure 6. A high-impedance voltmeter, which draws only an insignificant fraction of device's reverse current, must be used.

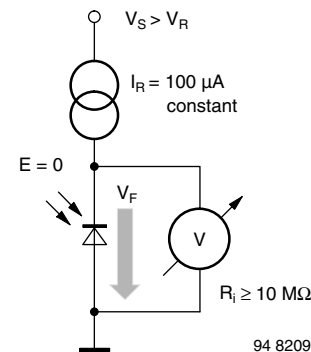


Fig. 6

Dark reverse current measurements, I_{ro} , must be carried out in complete darkness - reverse currents of silicon photodiodes are in the range of nanoamperes only, and an illumination of a few I_x is quite sufficient to falsify the test result. If a highly sensitive DVM is to be used, then a current sampling resistor of such a value that voltage dropped across it is small in comparison with supply voltage must be connected in series with the test item (figure 7). Under these conditions, any reverse voltage variations of the test samples can be ignored. Shunt resistance (dark resistance) is determined by applying a very slight voltage to the photodiode and then measuring dark current. In case of 10 mV or less, forward and reverse polarity will result in similar readings.

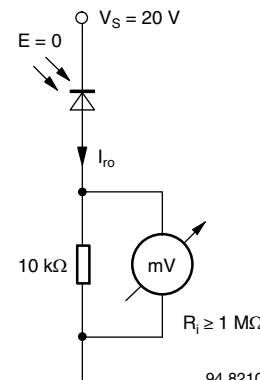


Fig. 7

- Light measurements

The same circuit as used in dark measurement can be used to carry out light reverse current, I_{ra} , measurements on photodiodes. The only difference is the diode is now irradiated and a current sampling resistor of lower value must be used (figure 8), because of the higher currents involved.

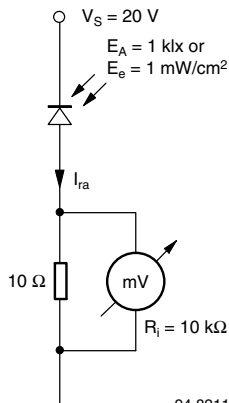


Fig. 8

The open circuit voltage, V_O , and short circuit current, I_k , of photovoltaic cells and photodiodes are measured by means of the test circuit shown in figure 9. The value of the load resistor used for the I_k measurement should be chosen so that the voltage dropped across it is low in comparison with the open circuit voltage produced under conditions of identical irradiation.

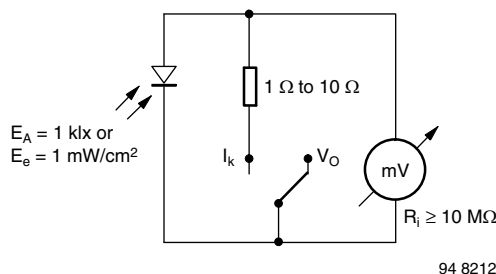


Fig. 9

The light source used for the light measurements is a calibrated incandescent tungsten lamp with no filters.

The filament current is adjusted for a color temperature of 2856 K (standard illuminant A to DIN 5033 sheet 7). A specified illumination, E_v , (usually 100 lx or 1000 lx) is produced by adjusting the distance, a , between the lamp and a detector on an optical bench. E_v can be measured on a $V(\lambda)$ -corrected luxmeter, or, if luminous intensity, I_v , of the lamp is known, E_v can be calculated using the formula: $E_v = I_v/a^2$.

It should be noted that this inverse square law is only strictly accurate for point light sources, that is for sources where the dimensions of the source (the filament) are small ($\leq 10\%$) in comparison with the distance between the source and detector.

Since lux is a measure for visible light only, near-infrared radiation (800 nm to 1100 nm) where silicon detectors have their peak sensitivity is not taken into account. Unfortunately, the near-infrared emission of filament lamps of various construction varies widely. As a result, light current measurements carried out with different lamps (but

the same lux and color temperature calibration) may result in readings that differ up to 20 %.

The simplest way to overcome this problem is to calibrate (measure the light current) some items of a photodetector type with a standard lamp (OSRAM WI 41/G) and then use these devices for adjustment of the lamp used for field measurements.

An IR diode is used as a radiation source (instead of a Tungsten incandescent lamp), to measure detector devices being used mainly in IR transmission systems together with IR emitters (e.g., IR remote control, IR headphone). Operation is possible both with DC or pulsed current.

The adjustment of irradiance, E_e , is similar to the above mentioned adjustment of illuminance, E_v . To achieve a high stability similar to filament lamps, consideration should be given to the following two points:

- The IR emitter should be connected to a good heat sink to provide sufficient temperature stability.
- DC or pulse-current levels as well as pulse duration have great influence on self-heating of IR diodes and should be chosen carefully.
- The radiant intensity, I_e , of the device is permanently controlled by a calibrated detector.

Phototransistors

The collector emitter voltage, V_{CEO} , is measured either on a transistor curve tracer or statically using the circuit shown in figure 10. Normal bench illumination does not change the measured result.

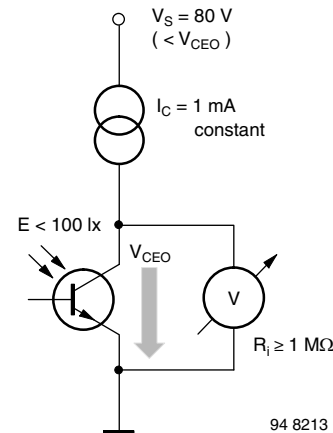


Fig. 10

In contrast, however, the collector dark current, I_{CEO} or I_{CO} , must be measured in complete darkness (figure 11). Even ordinary daylight illumination of the wire fed-through glass seals would falsify the measurement result.

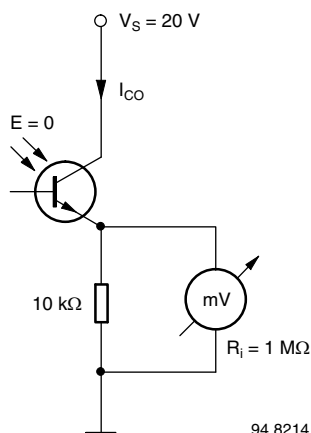


Fig. 11

The same circuit is used for collector light current, I_{ca} , measurements (figure 12). The optical axis of the device is aligned to an incandescent tungsten lamp with no filters, producing a CIE illuminance A of 100 lx or 1000 lx with a color temperature of $T_f = 2856$ K. Alternatively an IR irradiance by a GaAs diode can be used (refer to the photovoltaic cells and photodiodes section). Note that a lower sampling resistor is used, in keeping with the higher current involved.

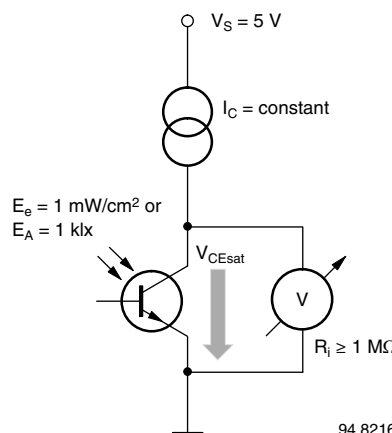


Fig. 13

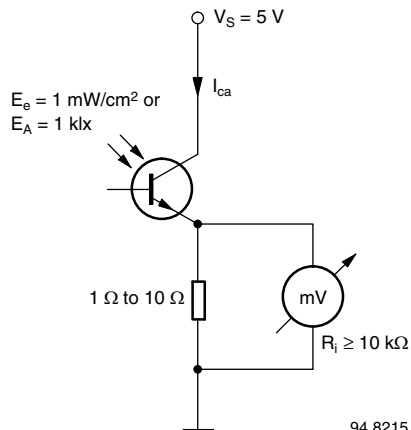


Fig. 12

To measure collector emitter saturation voltage, V_{CEsat} , the device is illuminated and a constant collector current is passed through. The magnitude of this current is adjusted below the level of the minimum light current, $I_{ca\ min}$, for the same illuminance (figure 13). The saturation voltage of the phototransistor (approximately 100 mV) is then measured on a high impedance voltmeter.

SWITCHING CHARACTERISTICS

Definition

Each electronic device generates a certain delay between input and output signals as well as a certain amount of amplitude distortion. A simplified circuit (figure 14) shows how input and output signals of optoelectronic devices can be displayed on a dual-trace oscilloscope.

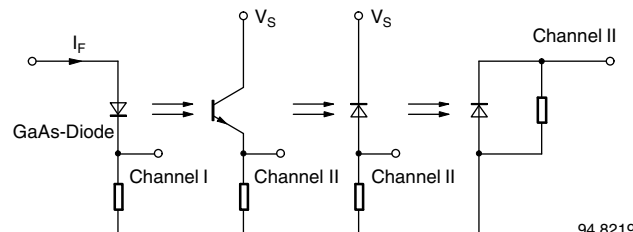
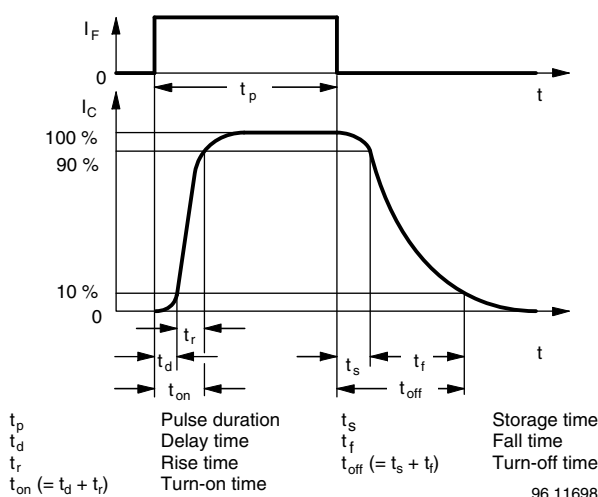


Fig. 14

The switching characteristics can be determined by comparing the timing of output current waveform with the input current waveform (figure 15).



These time parameters also include the delay existing in a luminescence diode between forward current (I_F) and radiant power Φ_θ .

Notes Concerning the Test Set-up

Circuits used for testing IR emitting, emitting sensitive and optically coupled isolator devices are basically the same (figure 14). The only difference is the way in which test device is connected to the circuit.

It is assumed that rise and fall times associated with the signal source (pulse generator) and dual trace oscilloscope are insignificant, and that the switching characteristics of any radiant sensitive device used in set-up are considerably shorter than those of the test item. The switching characteristics of IR emitters, for example ($t_r \approx 10 \text{ ns}$ to 1000 ns), are measured with aid of a PIN Photodiode detector ($t_r \approx 1 \text{ ns}$).

Photo- and darlington transistors and photo- and solar cells ($t_r \approx 0.5 \mu\text{s}$ to $50 \mu\text{s}$) are, as a rule, measured by use of fast IR diodes ($t_r < 30 \text{ ns}$) as emitters.

Red light-emitting diodes are used as light sources only for devices which cannot be measured with IR diodes because of their spectral sensitivity (e.g. BPW21R). These diodes emit only 1/10 of radiant power of IR diodes and consequently generate only very low signal levels.

Switching Characteristic Improvements on Phototransistors and Darlington Phototransistors

As in any ordinary transistor, switching times are reduced if drive signal level, and hence collector current, is increased. Another time reduction (especially in fall time t_f) can be achieved by use of a suitable base resistor, assuming there is an external base connection, although this can only be done at the expense of sensitivity.

TECHNICAL DESCRIPTION - ASSEMBLY

Emitter

Emitters are manufactured using the most modern liquid phase epitaxy (LPE) process. By using this technology, the number of undesirable flaws in the crystal is reduced. This results in a higher quantum efficiency and thus higher radiation power. Distortions in the crystal are prevented by using mesa technology which leads to lower degradation. A further advantage of the mesa technology is that each individual chip can be tested optically and electrically, even on the wafer.

DETECTOR

Vishay Semiconductor detectors have been developed to match perfectly to emitters. They have low capacitance, high photosensitivity, and extremely low saturation voltage. Silicon nitride passivation protects surface against possible impurities.

Assembly

Components are fitted onto lead frames by fully automatic equipment using conductive epoxy adhesive. Contacts are established automatically with digital pattern recognition using well-proven thermosonic techniques. All component are measured according to the parameter limits given in the datasheet.

Applications

Silicon photodetectors are used in manifold applications, such as sensors for radiation from near UV over visible to near infrared. There are numerous applications in measurement of light, such as dosimetry in UV, photometry, and radiometry. A well known application is shutter control in cameras.

Another large application area for detector diodes, and especially phototransistors, is position sensing.

Examples are differential diodes, optical sensors, and reflex sensors.

Other types of silicon detectors are built-in as parts of optocouplers.

One of the largest application areas is remote control of TV sets and other home entertainment appliances.

Different applications require specialized detectors and also special circuits to enable optimized functioning.

Equivalent circuit

Photodetector diodes can be described by the electrical equivalent circuit shown in figure 16.

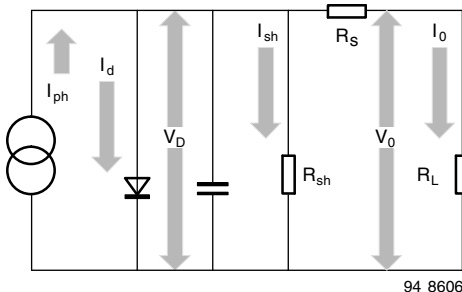


Fig. 16

$$I_O = I_{ph} - I_D - I_{sh} \quad (1)$$

$$I_O = I_{ph} - I_s \left(\exp \frac{qV_D}{kT} - 1 \right) - I_{sh}$$

$$V_{OC} = V_T \times \ln \left(\frac{S(\lambda) \times \phi_e - I_{sh}}{I_s} + 1 \right) \quad (2)$$

As described in the chapter "I-V Characteristics of illuminated pn junction", the incident radiation generates a photocurrent loaded by a diode characteristic and load resistor, R_L . Other parts of the equivalent circuit (parallel capacitance, C, combined from junction, C_j , and stray capacitances, serial resistance, R_s , and shunt resistance, R_{sh} , representing an additional leakage) can be neglected in most standard applications, and are not expressed in equations 5 and 7 (see "Physics and Technology"). However, in applications with high frequencies or extreme irradiation levels, these parts must be regarded as limiting elements.

Searching for the right detector diode type

The BPW 20 RF photodiode is based on rather highly doped n-silicon, while BPW34 is a PIN photodiode based on very lightly doped n-silicon. Both diodes have the same active area and spectral response as a function of wavelength is very similar. These diodes differ in their junction capacitance and shunt resistance. Both can influence the performance of an application.

Detecting very small signals is the domain of photodiodes with their very small dark currents and dark/shunt resistances.

With a specialized detector technology, these parameters are very well controlled in all Vishay photodetectors.

The very small leakage currents of photodiodes are offset by higher capacitances and smaller bandwidths in comparison to PIN photodiodes.

Photodiodes are often operated in photovoltaic mode, especially in light meters. This is depicted in figure 17, where a strong logarithmic dependence of the open circuit voltage on the input signal is used.

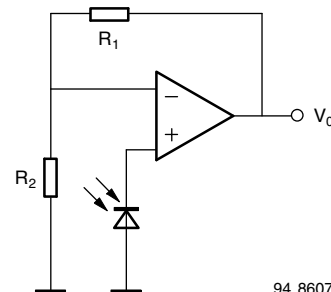


Fig. 17 - Photodiode in the Photovoltaic Mode Operating with a Voltage Amplifier

$$V_O \approx V_{OC} \times \left[1 + \frac{R_1}{R_2} \right] \text{ with} \quad (3)$$

$$V_{OC} = V_T \times \ln \left(\frac{S(\lambda) \times \phi_e - I_{sh}}{I_s} + 1 \right) \quad (2)$$

It should be noted that extremely high shunt/dark resistance (more than 15 GΩ) combined with a high-impedance operational amplifier input and a junction capacitance of about 1 nF can result in slow switch-off time constants of some seconds. Some instruments therefore have a reset button for shortening the diode before starting a measurement.

The photovoltaic mode of operation for precise measurements should be limited to the range of low ambient temperatures, or a temperature control of the diode (e.g., using a Peltier cooler) should be applied. At high temperatures, dark current is increased (see figure 18) leading to a non-logarithmic and temperature dependent output characteristic (see figure 19). The curves shown in figure 18 represent typical behavior of these diodes. Guaranteed leakage (dark reverse current) is specified with $I_{ro} = 30$ nA for standard types. This value is far from that one which is typically measured. Tighter customer specifications are available on request. The curve shown in figure 19 show the open circuit voltage as a function of irradiance with dark reverse current, I_S , as a parameter (in a first approximation increasing I_S and I_{sh} have the same effect). The parameter shown covers the possible spread of dark current. In combination with figure 18 one can project the extreme dependence of the open circuit voltage at high temperatures (figure 20).

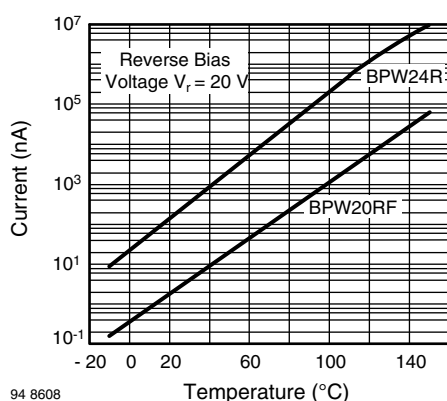


Fig. 18 - Reverse Dark Current vs. Temperature

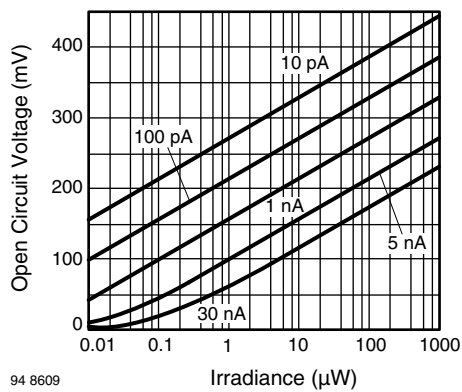


Fig. 19 - Open Circuit Voltage vs. Irradiance, Parameter: Dark Reverse Current, BPW20RF

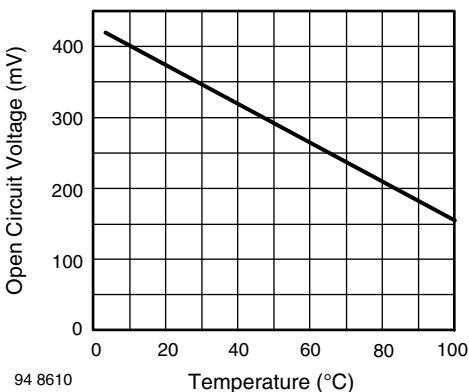


Fig. 20 - Open Circuit Voltage vs. Temperature, BPW46

Operating modes and circuits

The advantages and disadvantages of operating a photodiode in open circuit mode have been discussed.

For operation in short circuit mode (see figure 21) or photoconductive mode (see figure 22), current-to-voltage converters are typically used. In comparison with photovoltaic mode, the temperature dependence of the output signal is much lower. Generally, the temperature coefficient of the light reverse current is positive for irradiation with wavelengths > 900 nm, rising with increasing wavelength. For wavelengths < 600 nm, a negative temperature coefficient is found, likewise with increasing absolute value to shorter wavelengths.

Between these wavelength boundaries the output is almost independent of temperature. By using this mode of operation, the reverse biased or unbiased (short circuit conditions), output voltage, V_O , will be directly proportional to incident radiation, Φ_e (see equation in figure 21).

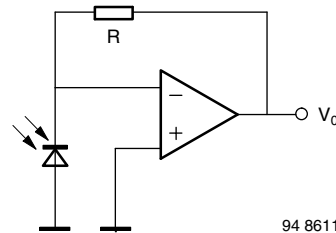


Fig. 21 - Transimpedance Amplifier, Current to Voltage Converter, Short Circuit Mode

$$V_O = -R \times \Phi_e \times S(\lambda) \quad (4)$$

$$V_{OC} = -I_{sc} \times R \quad (5)$$

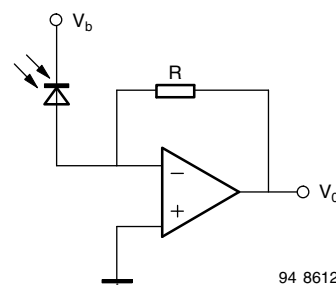


Fig. 22 - Transimpedance Amplifier, Current to Voltage Converter, Reverse Biased Photodiode

The circuit in figure 21 minimizes the effect of reverse dark current while the circuit in figure 22 improves the speed of the detector diode due to a wider space charge region with decreased junction capacitance and field increased velocity of the charge carrier transport.

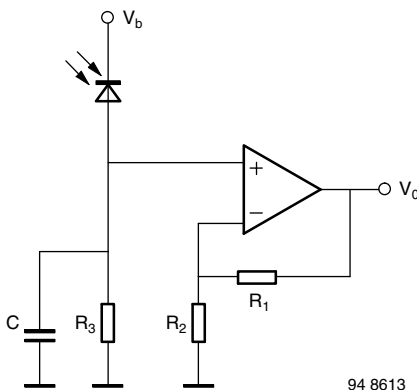


Fig. 23 - RC-Loaded Photodiode with Voltage Amplifier

Figure 23 shows photocurrent flowing into an RC load, where C represents junction and stray capacity while R_3 can be a real or complex load, such as a resonant circuit for the operating frequency.

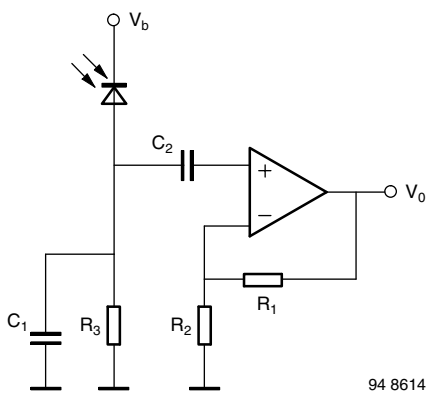


Fig. 24 - AC-Coupled Amplifier Circuit

$$V_O \approx \phi_e \times S(\lambda) \times R_3 \times \left[1 + \frac{R_1}{R_2} \right] \quad (6)$$

The circuit in figure 24 is equivalent to figure 23 with a change to AC coupling. In this case, the influence of background illumination can be separated from a modulated signal. The relation between input signal (irradiation, ϕ_e) and output voltage is given by the equation in figure 24.

Frequency response

The limitations of switching times in photodiodes are determined by carrier lifetime. Due to the absorption properties of silicon, especially in photodiodes, most of incident radiation at longer wavelengths is absorbed outside the space charge region. Therefore, a strong wavelength dependence of the switching times can be observed (figure 25).

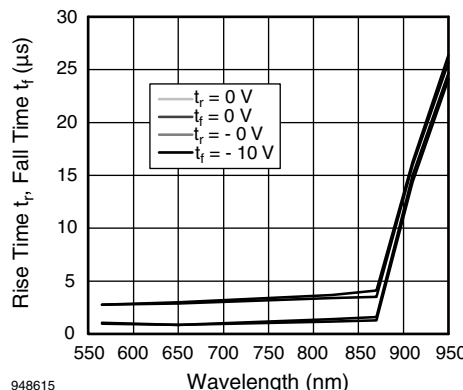


Fig. 25 - Switching Times vs. Wavelength for Photodiode BPW20RF

A drastic increase in rise and fall times is observed at wavelengths > 850 nm. Differences between unbiased and biased operation result from the widening of the space charge region.

However, for PIN photodiodes (BPW34/TEMD5000 family) similar results with shifted time scales are found. An example of such behavior, in this case in the frequency domain, is presented in figure 26 for a wavelength of 820 nm and figure 27 for 950 nm.

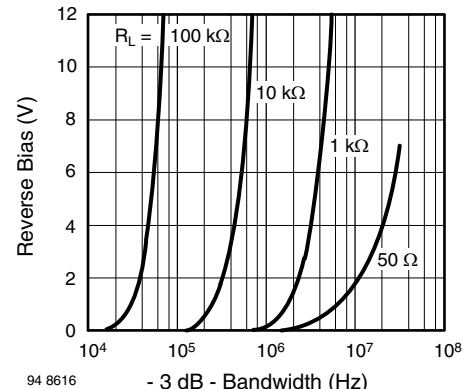


Fig. 26 - BPW34, TEMD5010X01, Bandwidth vs. Reverse Bias Voltage, Parameter: Load Resistance, $\lambda = 820$ nm

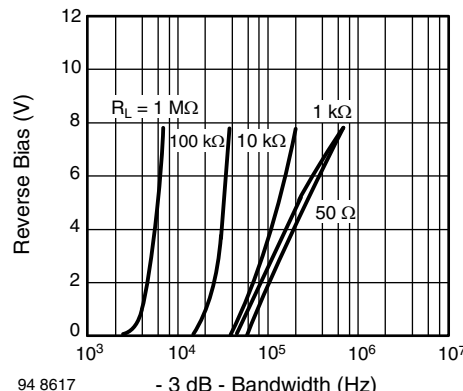


Fig. 27 - BPW41, TEMD5110X01, Bandwidth vs. Reverse Bias Voltage, Parameter: Load Resistance $\lambda = 950$ nm

Below about 870 nm, only slight wavelength dependence can be recognized, while a steep change of cut-off frequency takes place from 870 nm to 950 nm (different time scales in figure 26 and figure 27). Additionally, the influence of load resistances and reverse bias voltages can be taken from these diagrams.

For cut-off frequencies greater than 10 MHz to 20 MHz, depending on the supply voltage available for biasing the detector diode, PIN photodiodes are also used. However, for this frequency range, and especially when operating with low bias voltages, thin epitaxially grown intrinsic (i) layers are incorporated into PIN photodiodes.

As a result, these diodes (e.g., Vishay's TESP5700) can operate with low bias voltages (3 V to 4 V) with cut-off frequencies of 300 MHz at a wavelength of 790 nm. With application-specific optimized designs, PIN photodiodes with cut-off frequencies up to 1 GHz at only a 3 V bias voltage with only an insignificant loss of responsivity can be generated.

The main applications for these photodiodes are found in optical local area networks operating in the first optical window at wavelengths of 770 nm to 880 nm.

WHICH TYPE FOR WHICH APPLICATION?

In table 1, selected diode types are assigned to different applications. For more precise selection according to chip

sizes and packages, refer to the tables in introductory pages of this data book.

TABLE 1 - PHOTODIODE REFERENCE TABLE

DETECTOR APPLICATION	PIN PHOTODIODE	PHOTODIODE
Photometry, light meter		BPW21R
Radiometry	TEM5010X01, BPW34, BPW24R, ...	BPW20RF
Light barriers	BPV10NF, BPW24R	
Remote control, IR filter included, $\lambda > 900$ nm	BPV20F, BPV23F, BPW41N, S186P, TEMD5100X01	
IR Data Transmission $f_c < 10$ MHz IR filter included, $\lambda > 820$ nm	BPV23NF, BPW82, BPW83, BPV10NF, TEMD1020, TEMD5110X01	
IR Data Transmission, $f_c > 10$ MHz, no IR filter	BPW34, BPW46, BPV10, TEMD5010X01	
Densitometry	BPW34, BPV10, TEMD5010X01	BPW20RF, BPW21R
Smoke detector	BPV22NF, BPW34, TEMD5010X01	

PHOTOTRANSISTOR CIRCUITS

A phototransistor typically operates in a circuit shown in figure 28. Resistor R_B can be omitted in most applications. In some phototransistors, the base terminal is not connected. R_B can be used to suppress background radiation by setting a threshold level (see equation 7 and 8)

$$V_O = V_S - B \times \phi_e \times S(\lambda) \times R_L \quad (7)$$

$$V_{OC} \approx V_S - \left(B \times \phi_e \times S(\lambda) - \frac{0.6}{R_B} \right) \times R_L \quad (8)$$

For the dependence of rise and fall times on load resistance and collector-base capacitance, see the chapter "Properties of Silicon Phototransistors".

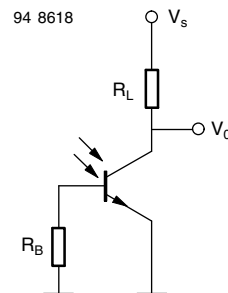


Fig. 28 - Phototransistor with Load Resistor and Optional Base Resistor

Physics and Technology

EMITTERS

Materials

Infrared emitting diodes (IREDs) can be produced from a range of different III-V compounds. Unlike the elemental semiconductor silicon, compound III-V semiconductors consist of two or more different elements of group three (e.g., Al, Ga, In) and five (e.g., P, As) of periodic table. The bandgap energies of these compounds vary between 0.18 eV and 3.4 eV. However, the IREDs considered here emit in the near infrared spectral range between 800 nm and 1000 nm, and, therefore, the selection of materials is limited to GaAs and mixed crystal $\text{Ga}_{1-x}\text{Al}_x\text{As}$, $0 \leq X \leq 0.8$, made from pure compounds GaAs and AlAs.

Infrared radiation is produced by the radiative recombination of electrons and holes from the conduction and valence bands. Emited photon energy, therefore, corresponds closely to bandgap energy E_g . The emission wavelength can be calculated according to the formula $\lambda (\mu\text{m}) = 1.240/E_g (\text{eV})$. Internal efficiency depends on band structure, doping material and doping level. Direct bandgap materials offer high efficiencies, because no phonons are needed for recombination of electrons and holes. GaAs is a direct gap material and $\text{Ga}_{1-x}\text{Al}_x\text{As}$ is direct up to $X = 0.44$. Doping species Si provides the best efficiencies and the shifts emission wavelength below the bandgap energy into the infrared spectral range by about 50 nm typically. Charge carriers are injected into the material via pn junctions. Junctions of high injection efficiency are readily formed in GaAs and $\text{Ga}_{1-x}\text{Al}_x\text{As}$. P-type conductivity can be obtained with metals of valency two, such as Zn and Mg, and n-type conductivity with elements of valency six, such as S, Se and Te. However, silicon of valency four can occupy sites of III-valence and V-valence atoms, and, therefore, acts as donor and as acceptor. Conductivity type depends primarily on material growth temperature. By employing exact temperature control, pn junctions can be grown with the same doping species Si on both sides of the junction. Ge, on the other hand, also has a valency of four, but occupies group V sites at high temperatures i.e., p-type.

Only mono crystalline material is used for IRED production. In the mixed crystal system $\text{Ga}_{1-x}\text{Al}_x\text{As}$, $0 \leq X \leq 0.8$, lattice constant varies only by about 1.5×10^{-3} . Therefore, mono crystalline layered structures of different $\text{Ga}_{1-x}\text{Al}_x\text{As}$ compositions can be produced with extremely high structural quality. These structures are useful because the bandgap can be shifted from 1.40 eV (GaAs) to values beyond 2.1 eV which enables transparent windows and heterogeneous structures to be fabricated. Transparent windows are another suitable means to increase efficiency, and heterogeneous structures can provide shorter switching times and higher efficiency. Such structures are termed single hetero (SH) or double hetero structures (DH). DH structures consist normally of two layers that confine a layer with a much smaller bandgap.

The best production method for all materials needed is liquid phase epitaxy (LPE). This method uses Ga-solutions containing As, possibly Al, and a doping substance. The solution is saturated at a high temperature, typically 900 °C, and GaAs substrates are dipped into the liquid. The solubility of As and Al decreases with decreasing temperature. In this way epitaxial layers can be grown by slow cooling of the solution. Several layers differing in composition may be obtained using different solutions one after another, as needed e.g. for DHs.

In liquid phase epitaxial reactors, production quantities of up to 50 wafers, depending on type of structure required, can be handled.

IRED CHIPS AND CHARACTERISTICS

In the past IRED chips are made only from GaAs. The structure of the chip is displayed in figure 1.

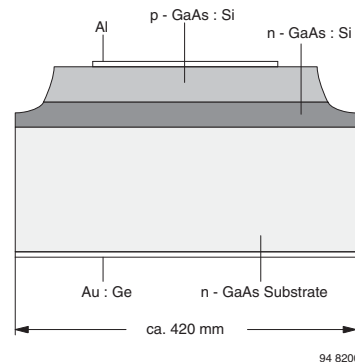


Fig. 1

On an n-type substrate, two Si-doped layers are grown by liquid phase epitaxy from the same solution producing an emission wavelength of 950 nm. Growth starts as n-type at high temperature and becomes p-type below about 820 °C. A structured Al-contact on p-side and a large area Au:Ge contact on back side provide a very low series resistance.

The angular distribution of emitted radiation is displayed in figure 2.

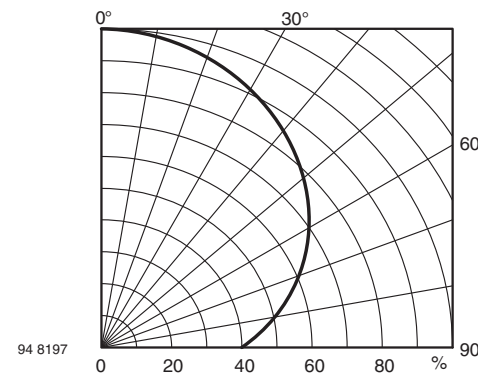


Fig. 2

The package of the chip has to provide good collection efficiency of radiation emitted sideways, and has to diminish the refractive index step between the chip ($n = 3.6$) and the air ($n = 1.0$) with an epoxy of refractive index of 1.55. In this way, the output power of chip is increased by a factor of 3.5 for the assembled device.

The chip described is the most cost-efficient one. Its forward voltage at $I_F = 1.5$ A has the lowest possible value. Total series resistance is typically only 0.60Ω ; output power and linearity (defined as optical output power increase, divided by current increase between 0.1 A and 1.5 A) are high. Relevant data on chip and a typical assembled device are given in table 1.

The technology used for a chip emitting at 880 nm eliminates the absorbing substrate and uses only a thick epitaxial layer. The chip is shown in figure 3.

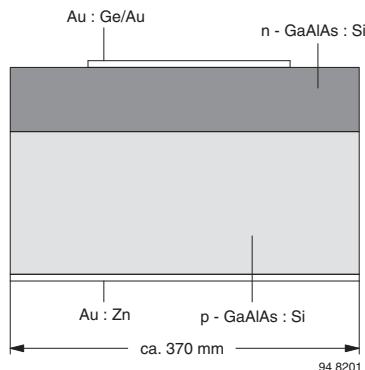


Fig. 3

Originally, the GaAs substrate was adjacent to the n-side. Growth of $\text{Ga}_{0.7}\text{Al}_{0.3}\text{As}$ started as n-type and became p-type - as in the first case - through the specific properties of the doping material Si. A characteristic feature of the Ga-Al-As phase system causes the Al-content of growing epitaxial layer to decrease. This causes the Al-concentration at the junction to drop to 8 % ($\text{Ga}_{0.92}\text{Al}_{0.08}\text{As}$), producing an emission wavelength of 880 nm. During further growth the Al-content approaches zero. The gradient of the Al-content and correlated gradient of bandgap energy produce an emission band of a relatively large half width. The transparency of the large bandgap material results in a high external efficiency on this type of chip.

The chip is mounted n-side up, and the front side metallization is Au:Ge/Au, whereas the reverse side metallization is Au:Zn.

The angular distribution of the emitted radiation is displayed in figure 4.

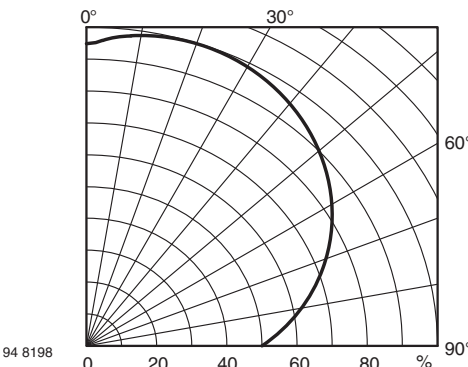


Fig. 4

Due to its shorter wavelength, $\text{Ga}_{1-x}\text{Al}_x\text{As}$ chip described above offers specific advantages in combination with a Si detector. Integrated opto ICs, like amplifiers or Schmitt Triggers, have higher sensitivities at shorter wavelengths. Similarly, phototransistors are also more sensitive. Finally, the frequency bandwidth of pin diodes is higher at shorter wavelengths. This chip also has the advantage of having high linearity up to and beyond 1.5 A. The forward voltage, however, is higher than the voltage of a GaAs chip. Table 2 (see "Symbols and Terminology") provides more data on the chip.

A technology combining some of the advantages of the two technologies described above is summarized in figure 5.

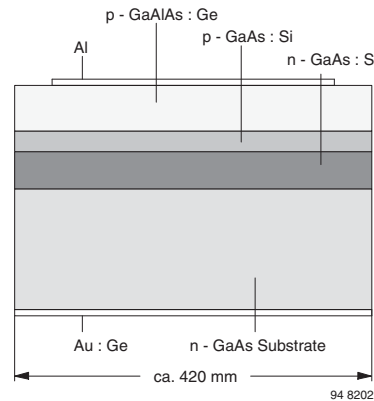


Fig. 5

Starting with n-type substrate, n- and p-type GaAs layers are grown in a similar way to the epitaxy of a standard GaAs:Si diode. After this, a highly transparent window layer of $\text{Ga}_{1-x}\text{Al}_x\text{As}$, doped p-type is grown. The upper contact to the p-side is made of Al and the rear side contact is Au:Ge. The angular distribution of emitted radiation is shown in figure 6.

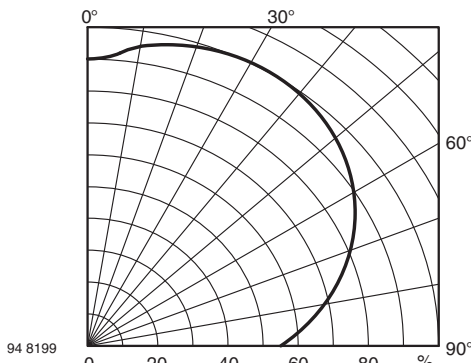


Fig. 6

This chip type combines a relatively low forward voltage with a high electro-optical efficiency, offering an optimized combination of the advantageous characteristics of the two other chips. Refer again to table 2 (see "Symbols and Terminology") for more details.

As mentioned in the previous section, double heterostructures (DH) provide even higher efficiencies and faster switching times. A schematic representation of such a chip is shown in figure 7.

BULK AND SURFACE EMITTER TECHNOLOGY

A more recent technology, the surface emitter chip technology, involves bonding the Infrared emitting diode structure to a metalized conducting carrier substrate, after which the substrate, which was originally used for the epitaxial growth of the Infrared emitting crystal layers, is chemically removed. The layer structure of these diodes is extremely thin which has the favorable consequence that side wall emission is minimized.

The layers of the surface emitter IRED structures are deposited by metal-organic chemical vapor deposition (MOVPE) on suitable substrates. The active region consists of a multiple-quantum-well (MQW) or a DH structure. MQW active regions for Infrared emitting diodes contain typically one or more 5 nm thick InGaAs quantum wells which are separated by 15 nm thick GaAlAsP barriers.

High electro-optical efficiencies are achieved by the implementation of a metallic mirror on the back side of the layer structure which redirects the incident radiation effectively towards the top surface as well as a treatment of the top surface to increase the extraction efficiency. As sidewall emission is negligible radiance scales with chip area and large devices can be realized without significant increase of reabsorption losses.

In order to provide a good current spreading and a uniform current distribution surface emitter diodes are grown n-side up. Both contacts, the structured top electrode to the n-side and the large area back side contact, are made of gold.

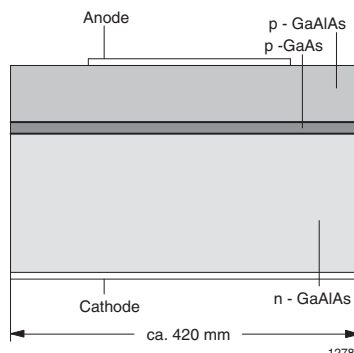


Fig. 7

The active layer is depicted as the thin layer between the p- and n-type $\text{Ga}_{1-x}\text{Al}_x\text{As}$ confinement layers.

The contacts are dependent on the polarity of the chip. If p is up, then the p-side contact is Al and the back side Au:Ge; if n is up, then this side has an Au:Ge contact and the back side Au:Zn. Two such chips that are also very suitable for IrDA applications are given in table 1.

The angular distribution of the emitted radiation corresponds nearly perfectly to the lambertian emission pattern of point sources $I_0 = I(\phi) \times \cos \phi$ and enables an efficient coupling of the output power into optical systems.

Exemplary data on chip and assembled device are given in table 1.

A further Infrared emitter chip technology, which makes use of metal organic chemical vapor deposition, is the bulk emitter chip technology. On an n-type GaAs substrate a MQW structure similar to the one described above is grown producing an emission wavelength of 940 nm. As the substrate is transparent at this wavelength the bulk emitter technology offers the high efficiencies of double hetero structures in combination with exceptional low forward voltages and very fast response times. With these favorable characteristics bulk emitter chips can substitute conventional GaAlAs/GaAs chips in many technical applications. As electrode material for the top p-type contact Al or Au are in use, whereas the back side contact consists of an Au alloy. The angular distribution of the emitted radiation resembles the one shown in figure 6. Relevant chip and device data are given in table 1.

TABLE 1: CHARACTERISTICS DATA OF IRED CHIPS

TECHNOLOGY	TYPICAL CHIP DATA				TYPICAL DEVICE	TYPICAL DEVICE DATA			
	Φ_e at 0.1 A (mW)	λ_p (nm)	$\Delta\lambda$ (nm)	POLARITY		Φ_e at 0.1 A (mW)	V_F at 0.1 A (V)	V_F at 1.0 A (V)	t_r at 0.1 A (ns)
GaAs	7.7	950	50	p up	TSUS540.	20	1.3	2.1	800
GaAlAs	12.8	875	80	n up	TSHA550.	27	1.5	3.4	600
GaAlAs (DDH)	20	890	40	p up	TSHF5410	45	1.5	2.3	30
GaAlAs (DDH)	26	870	40	p up	TSFF5410	50	1.5	2.3	15
Bulk Emitter	21	940	30	p up	VSLB3940	40	1.35	2.1	15
GaAlAs MQW	22	940	30	p up	TSAL6200	40	1.35	2.2	15
Surface Emitter	30	850	25	n up	VSLY5850	55	1.65	2.9	10

UV, VISIBLE, AND NEAR IR SILICON PHOTODETECTORS

(adapted from "Sensors, Vol 6, Optical Sensors, Chapt. 8, VCH - Verlag, Weinheim 1991")

Silicon Photodiodes (PN and PIN Diodes)

The physics of silicon detector diodes

Absorption of radiation is caused by the interaction of photons and charge carriers inside a material. The different energy levels allowed and the band structure determine the likelihood of interaction and, therefore, the absorption characteristics of the semiconductors. The long wavelength cutoff of the absorption is given by the bandgap energy. The slope of the absorption curve depends on the physics of interaction and is much weaker for silicon than for most other semiconducting materials. This results in a strong wavelength-dependent penetration depth which is shown in figure 8. (The penetration depth is defined as that depth where $1/e$ of the incident radiation is absorbed.)

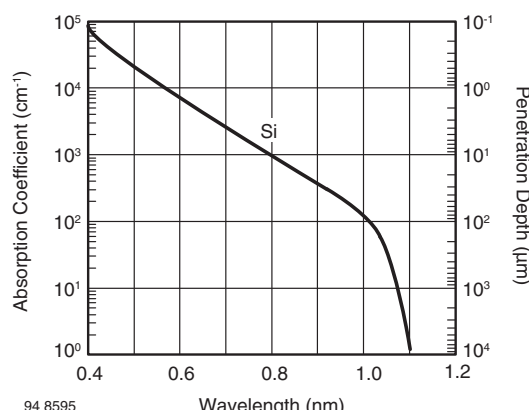


Fig. 8 - Absorption and Penetration Depth of Optical Radiation in Silicon

Depending on the wavelength, the penetration depth varies from tenths of a micron at 400 nm (blue) to more than 100 μm at 1 μm (IR). For detectors to be effective, an interaction length of at least twice the penetration depth should be realized (equivalent to $1/e^2 = 86\%$ absorbed radiation). In the pn diode, generated carriers are collected by the electrical field of the pn junction. Effects in the vicinity of a pn junction are shown in figure 9 for various types and

operating modes of the pn diode. Incident radiation generates mobile minority carriers - electrons on the p-side, holes on the n-side. In the short circuit mode shown in figure 9 (top), the carriers drift under the field of the built-in potential of the pn junction. Other carriers diffuse inside the field-free semiconductor along a concentration gradient, which results in an electrical current through the applied load, or without load, in an external voltage, open circuit voltage, V_{OC} , at contact terminals. Bending of the energy bands near the surface is caused by surface states. An equilibrium is established between generation, recombination of carriers, and current flow through the load.

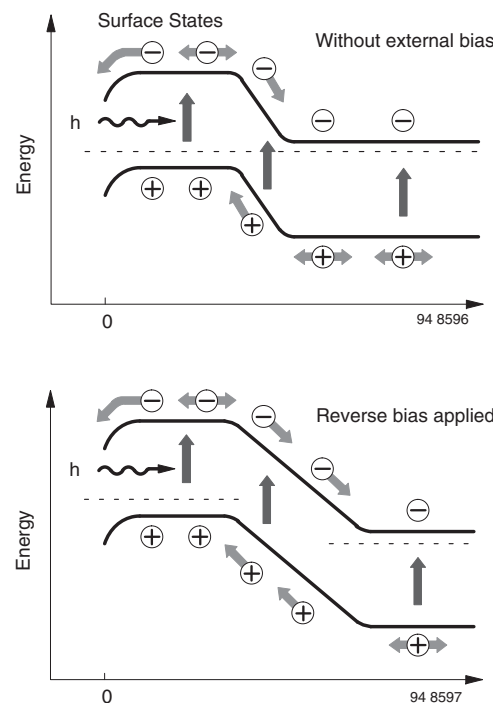


Fig. 9 - Generation-Recombination Effects in the Vicinity of a PN Junction
Top: Short Circuit Mode, Bottom: Reverse Biased

Recombination takes place inside the bulk material with technology- and process-dependent time constants which are very small near the contacts and surfaces of the device. For short wavelengths with very small penetration depths, carrier recombination is the efficiency limiting process. To achieve high efficiencies, as many carriers as possible should be separated by the electrical field inside the space charge region. This is a very fast process, much faster than typical recombination times (for data, see chapter 'Operating modes and circuits').

The width, W, of the space charge is a function of doping the concentration N_B and applied voltage V:

$$W = \sqrt{\frac{2 \times \epsilon_s \times \epsilon_0 \times (V_{bi} + V)}{q \times N_B}} \quad (1)$$

(for a one-sided abrupt junction), where V_{bi} is built-in voltage, ϵ_s dielectric constant of Si, ϵ_0 vacuum dielectric constant and q is electronic charge. The diode's capacitance (which can be speed limiting) is also a function of the space charge width and applied voltage. It is given by

$$C = \frac{\epsilon_s \times \epsilon_0 \times A}{W} \quad (2)$$

where A is the area of the diode. An externally applied bias will increase the space charge width (see figure 8) with the result that a larger number of carriers are generated inside this zone which can be flushed out very fast with high efficiency under the applied field. From equation (1), it is evident that the space charge width is a function of the doping concentration N_B . Diodes with a so-called pin structure show according to equation (1) a wide space charge width where i stands for intrinsic, low doped. This zone is also sometimes nominated as n or p rather than low doped n, n- or p, p-zone indicating the very low doping. Per equation (2), the junction capacitance C, is low due to the large space charge region of PIN photodiodes. These photodiodes are mostly used in applications requiring high speed.

Figure 10 shows a cross section of PIN photodiodes and PN diodes. The space charge width of the PIN photodiodes (bottom) with a doping level ($n = N_B$) as low as $N_B = 5 \times 10^{11} \text{ cm}^{-3}$ is about 80 μm wide for a 2.5 V bias in comparison with a pn diode with a doping (n) of $N_B = 5 \times 10^{15} \text{ cm}^{-3}$ with only 0.8 mm.

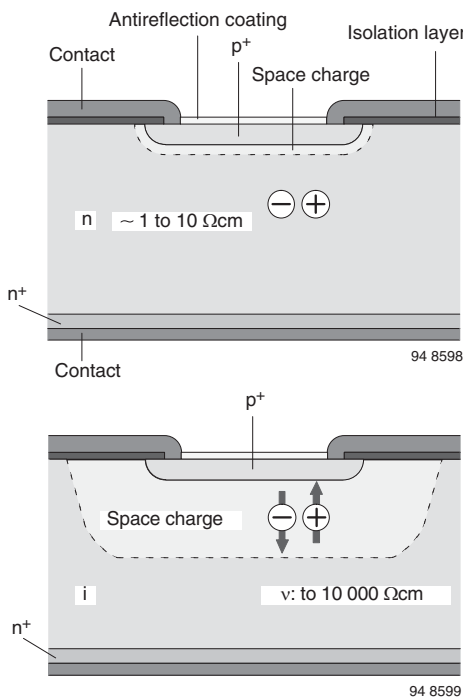


Fig. 10 - Comparison of PN Diode (Top) and PIN Photodiode (Bottom)

PROPERTIES OF SILICON PHOTODIODES

I-V Characteristics of illuminated pn junction

The cross section and I-V-characteristics of a photodiode are shown in figure 11 and 12. The characteristic of the illuminated diode is identical to the characteristic of a standard rectifier diode. The relationship between current, I, and voltage, V, is given by

$$I = I_S \times \left(\frac{\exp(V)}{V_T - 1} \right) \quad (3)$$

with $V_T = kT/q$

$k = 1.38 \times 10^{-23} \text{ JK}^{-1}$, Boltzmann constant

$q = 1.6 \times 10^{-19} \text{ As}$, electronic charge.

I_S , the dark-reverse saturation current, is a material- and technology-dependent quantity. The value is influenced by the doping concentrations at pn junction, by carrier lifetime, and especially by temperature. It shows a strongly exponential temperature dependence and doubles every 8 °C.

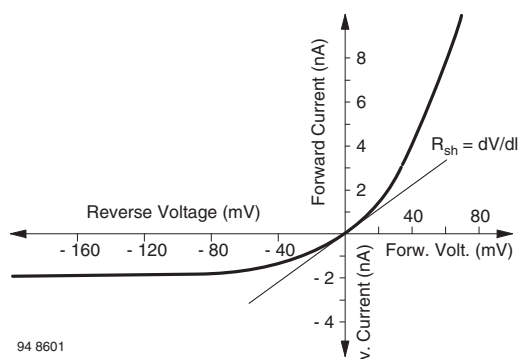


Fig. 11 - Measured I-V-Characteristics of an Si Photodiode in the Vicinity of the Origin

The typical dark currents of Si photodiodes are dependent on size and technology and range from less than picoamps up to tens of nanoamps at room temperature conditions. As noise generators, dark current I_{D0} and the resistance R_{sh} (defined and measured at a voltage of 10 mV forward or reverse, or peak-to-peak) are limiting quantities when detecting very small signals.

The photodiode exposed to optical radiation generates a photocurrent I_r exactly proportional to incident radiant power Φ_e .

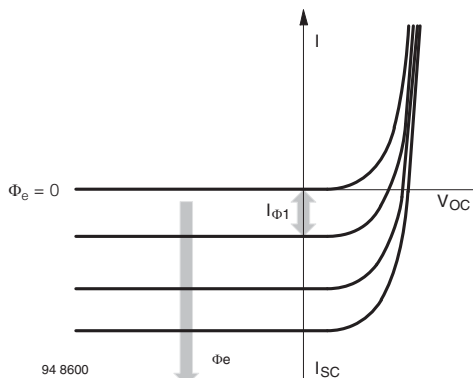


Fig. 12 - I-V-Characteristics of an Si Photodiode under Illumination. Parameter: Incident Radiant Flux

The quotient of both is spectral responsivity $s(\lambda)$,

$$S(\lambda) = \frac{I_r}{\Phi_e [A/W]} \quad (4)$$

The characteristic of the irradiated photodiode is then given by

$$I = I_s \times \left(\frac{\exp V}{V_T - 1} \right) - S(\lambda) \times \Phi_e \quad (5)$$

and in case $V \approx 0$, zero or reverse bias we find,

$$I = -I_s - S(\lambda) \times \Phi_e \quad (6)$$

Dependent on load resistance, R_L , and applied bias, different operating modes can be distinguished. An unbiased diode operates in photovoltaic mode. Under short circuit conditions (load $R_L = 0 \Omega$), short circuit current, I_{SC}

flows into the load. When R_L increases to infinity, the output voltage of the diode rises to the open circuit voltage, V_{OC} , given by

$$V_{OC} = V_T \times \left(\frac{S(\lambda) \times \Phi_e}{I_S + 1} \right) \quad (7)$$

Because of this logarithmic behavior, the open circuit voltage is sometimes used for optical light meters in photographic applications. The open circuit voltage shows a strong temperature dependence with a negative temperature coefficient. The reason for this is the exponential temperature coefficient of the dark reverse saturation current I_S . For precise light measurement, a temperature control of the photodiode is employed. Precise linear optical power measurements require small voltages at the load, typically smaller than about 5 % of the corresponding open circuit voltage. For less precise measurements, an output voltage of half the open circuit voltage can be allowed. The most important disadvantage of operating in photovoltaic mode is the relatively large response time. For faster response, it is necessary to implement an additional voltage source reverse-biasing the photodiode. This mode of operation is termed photoconductive mode. In this mode, the lowest detectable power is limited by the shot noise of the dark current, I_S , while in photovoltaic mode, the thermal (Johnson) noise of shunt resistance, R_{sh} , is the limiting quantity.

SPECIAL RESPONSITIVITY

Efficiency of Si photodiodes:

The spectral responsivity, s_λ , is given as the number of generated charge carriers ($\eta \times N$) per incident photons N of energy $h \times v$ (η is percent efficiency, h is the Planck's constant, and v is the radiation frequency). Each photon will generate one charge carrier at the most. The photocurrent I_{re} is then given as

$$I_{re} = \eta \times N \times q \quad (8)$$

$$S(\lambda) = \left(\frac{I_{re}}{\Phi_e} \right) = \frac{\eta \times N \times q}{h \times v \times N} = \frac{\eta \times q}{h \times v} \quad (9)$$

$$S(\lambda) = \frac{\lambda (\mu\text{m})}{1.24} [\text{A}/\text{W}]$$

At fixed efficiency, a linear relationship between wavelength and spectral responsivity is valid.

Figure 8 shows that the semiconductors absorb radiation similar to a cut-off filter. At wavelengths smaller than the cut-off wavelength, the incident radiation is absorbed. At larger wavelengths the radiation passes through the material without interaction. The cut-off wavelength corresponds to the bandgap of the material. As long as the energy of the photon is larger than the bandgap, carriers can be generated by absorption of photons, provided that the material is thick enough to propagate photon-carrier interaction. Bearing in mind that the energy of photons decreases with increasing wavelength, we can see, that the curve of the spectral responsivity vs. wavelength in ideal

case (100 % efficiency) will have a triangular shape (see figure 13). For silicon photodetectors, the cut-off wavelength is near 1100 nm.

In most applications, it is not necessary to detect radiation with wavelengths larger than 1000 nm. Therefore, designers use a typical chip thickness of 200 μm to 300 μm , which results in reduced sensitivity at wavelengths larger than 950 nm. With a typical chip thickness of 250 μm , an efficiency of about 35 % at 1060 nm is achieved. At shorter wavelengths (blue-near UV, 500 nm to 300 nm) sensitivity is limited by recombination effects near the surface of the semiconductor. A reduction in efficiency starts near 500 nm and increases as the wavelength decreases. Standard detectors designed for visible and near IR radiation may have poor UV/blue sensitivity and poor UV stability. Well designed sensors for wavelengths of 300 nm to 400 nm can operate with fairly high efficiencies. At shorter wavelengths (< 300 nm), efficiency decreases strongly.

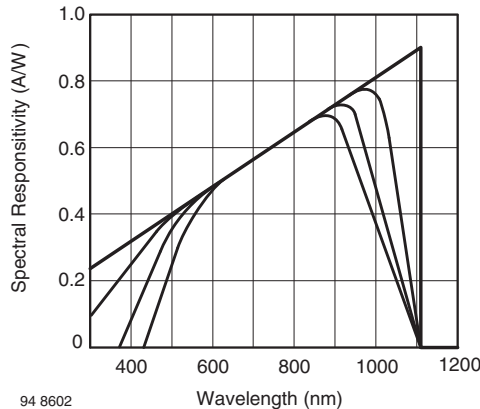


Fig. 13 - Spectral Responsivity as a Function of Wavelength of a Si Photodetector Diode, Ideal and Typical Values

Temperature dependence of spectral responsivity

The efficiency of carrier generation by absorption and the loss of carriers by recombination are the factors which influence spectral responsivity. The absorption coefficient increases with temperature. The radiation of the long wavelength is therefore more efficiently absorbed inside the bulk and results in increased response. For shorter wavelengths (< 600 nm), reduced efficiency is observed with increasing temperature because of increased recombination rates near the surface. These effects are strongly dependent on technological parameters and therefore cannot be generalized to the behavior at longer wavelengths.

Uniformity of spectral responsivity

Inside the technologically defined active area of photodiodes, spectral responsivity shows a variation of sensitivity on the order of < 1 %. Outside the defined active area, and especially at lateral edges of the chips, local spectral response is sensitive to applied reverse voltage. Additionally, this effect depends on wavelength. Therefore, the relation between power (W) related spectral responsivity, s_λ (A/W), and power density (W/cm²) related

spectral responsivity, s_λ [A/(W/cm²)] is not a constant. Rather, this relation is a function of wavelength and reverse bias

Stability of spectral responsivity

Si detectors for wavelengths between 500 nm and 800 nm appear to be stable over very long periods of time. In the literature concerned here, remarks can be found on instabilities of detectors in blue, UV, and near IR under certain conditions. Thermal cycling reversed the degradation effects.

Surface effects and contamination are possible causes but are technologically well controlled.

Angular dependence of responsivity

The angular response of Si photodiodes is given by the optical laws of reflection. The angular response of a detector is shown in figure 14.

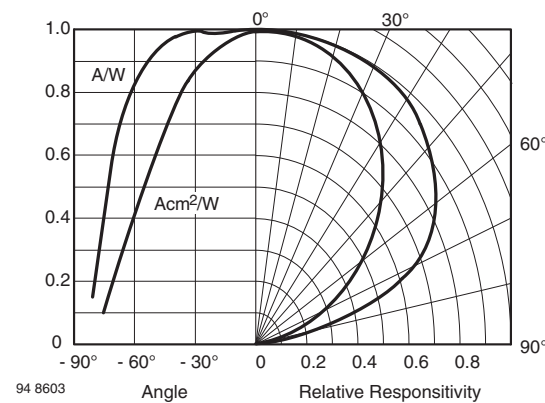


Fig. 14 - Responsivity of Si Photodiodes as a Function of the Angle of Incidence

Semiconductor surfaces are covered with quarter wavelength anti-reflection coatings. Encapsulation is performed with uncoated glass or sapphire windows.

The bare silicon response can be altered by optical imaging devices such as lenses. In this way, nearly every arbitrary angular response can be achieved.

Dynamic Properties of Si Photodiodes

Si photodiodes are available in many different variations. The design of diodes can be tailored to meet special needs. Si photodiodes may be designed for maximum efficiency at given wavelengths, for very low leakage currents, or for high speed. The design of a photodiode is nearly always a compromise between various aspects of a specification.

Inside the absorbing material of the diode, photons can be absorbed in different regions. For example at the top of a p⁺n-diode there is a highly doped layer of p⁺-Si. Radiation of shorter wavelengths will be effectively absorbed, but for larger wavelengths only a small amount is absorbed. In the vicinity of the pn junction, there is the space charge region, where most of the photons should generate carriers. An electric field accelerates the generated carrier in this part of the detector to a high drift velocity. Carriers which are not

absorbed in these regions penetrate into field-free region where the motion of the generated carriers fluctuates by a slow diffusion process.

The dynamic response of the detector is composed of different processes which transport carriers to contacts. The dynamic response of photodiodes is influenced by three fundamental effects:

- Drift of carriers in an electric field
- Diffusion of carriers
- Capacitance x load resistance

Carrier drift in the space charge region occurs rapidly with very small time constants. Typically, transit times in an electric field of $0.6 \text{ V}/\mu\text{m}$ are on the order of $16 \text{ ps}/\mu\text{m}$ and $50 \text{ ps}/\mu\text{m}$ for electrons and holes, respectively. At (maximum) saturation velocity, the transit time is on the order of $10 \text{ ps}/\mu\text{m}$ for electrons in p-material. With a $10 \mu\text{m}$ drift region, traveling times of 100 ps can be expected. Response time is a function of the distribution of the generated carriers and is therefore dependent on wavelength.

The diffusion of the carriers is a very slow process. Time constants are on the order of some ms. The typical pulse response of the detectors is dominated by these two processes. Obviously, carriers should be absorbed in large space charge regions with high internal electrical fields. This requires material with an adequate low doping level.

Furthermore, a reverse bias of rather large voltage is useful. Radiation of shorter wavelength is absorbed in smaller penetration depths. At wavelengths shorter than 600 nm , decreasing wavelength leads to an absorption in the diffused top layer. The movement of carriers in this region is also diffusion limited. Because of the small carrier lifetimes, the time constants are not as large as in homogeneous substrate material.

Finally, capacitive loading of output in combination with load resistance limits frequency response.

PROPERTIES OF SILICON PHOTOTRANSISTORS

The phototransistor is equivalent to a photodiode in conjunction with a bipolar transistor amplifier (figure 15). Typically, the current amplification, B , is between 100 and 1000 depending on type and application. The active area of phototransistor is usually about $0.5 \times 0.5 \text{ mm}^2$.

The data of spectral responsivity are equivalent to those of photodiodes, but must be multiplied by the factor current amplification, B .

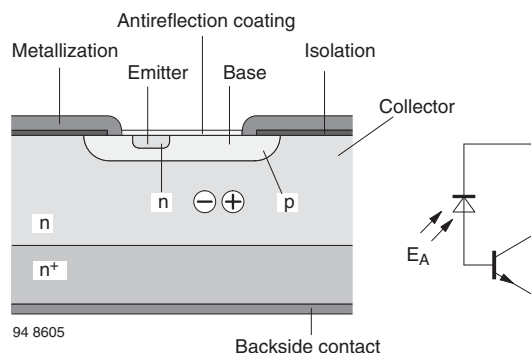


Fig. 15 - Phototransistor, Cross Section and Equivalent Circuit

The switching times of phototransistors are dependent on current amplification and load resistance and are between 30 ms and 1 ms. The resulting cut-off frequencies are a few hundred kHz.

The transit times, t_r and t_f , are given by

$$t_{r,f} = \sqrt{\left(\frac{1}{2 \times f_t}\right)^2 + b \times (R C_B \times V)^2} \quad (10)$$

f_t : Transit frequency

R : Load resistance, 1.6

C_B : Base-collector capacitance, $b = 4$ to 5

V : Amplification

Phototransistors are most frequently applied in transmissive and reflective optical sensors.

Symbols and Terminology

Vishay Semiconductors



Symbols and Terminology

A	Anode , anode terminal	E _{A amb}	standard illuminant A, unit: Ix (Lux) or klx
A	Ampere , SI unit of electrical current	echo-off	Ambient illumination at standard illuminant A
A	Radiant sensitive area , that area which is radiant sensitive for a specified range		Unprecise term to describe the behavior of the output of IrDA® transceivers during transmission. "Echo-off" means that by blocking the receiver the output RXD is quiet during transmission
a	Distance , e.g. between the emitter (source) and the detector	echo-on	Unprecise term to describe the behavior of the output of IrDA® transceivers during transmission. "Echo-on" means that the receiver output RXD is active but often undefined during transmission. For correct data reception after transmission the receiver channel must be cleared during the latency period
B	Base , base terminal		
BER	Bit Error Rate		
bit/s	Data rate or signaling rate 1000 bit/s = 1 kbit/s, 10 ⁶ bit/s = 1 Mbit/s		
C	Capacitance , unit: F (farad) = C/V	E _e , E	Irradiance (at a point of a surface), quotient of the radiant flux dΦ _e incident on an element of the surface containing the point, by the area dA of that element. Equivalent definition. Integral, taken over the hemisphere visible from the given point, of the expression L _e · cosθ · dΩ, where L _e is the radiance at the given point in the various directions of the incident elementary beams of solid angle dΩ, and θ is the angle between any of these beams and the normal to the surface at the given point
C	Coulomb , C = s x A		
C	Cathode , cathode terminal		
C	Collector , collector terminal		
°C	Degree Celsius , Celsius temperature, symbol t, and is defined by the quantity equation t = T - T ₀ . The unit of Celsius temperature is the degree Celsius, symbol °C. The numerical value of a Celsius temperature t expressed in degrees Celsius is given by t/°C = T/K - 273.15 It follows from the definition of t that the degree Celsius is equal in magnitude to the Kelvin, which in turn implies that the numerical value of a given temperature difference or temperature interval whose value is expressed in the unit degree Celsius (°C) is equal to the numerical value of the same difference or interval when its value is expressed in the unit Kelvin (K).		
C _{CEO}	Collector emitter capacitance , Capacitance between the collector and the emitter with open base	E _v , E	Illuminance (at a point of a surface), quotient of the luminous flux dΦ _v incident on an element of the surface containing the point, by the area dA of that element. Equivalent definition. Integral, taken over the hemisphere visible from the given point, of the expression L _v · cosθ · dΩ, where L _v is the luminance at the given point in the various directions of the incident elementary beams of solid angle dΩ, and θ is the angle between any of these beams and the normal to the surface at the given point
cd	Candela , SI unit of luminous intensity. The candela is the luminous intensity, in a given direction, of a source that emits monochromatic radiation of frequency 540 Hz x 10 ¹² Hz and that has a radiant intensity in that direction of 1/683 W per steradian. (16 th General Conference of Weights and Measures, 1979), 1 cd = 1 lm · sr ⁻¹		
C _D	Diode capacitance , total capacitance effective between the diode terminals due to case, junction and parasitic capacitances		
C _j	Junction capacitance , capacitance due to a p-n junction of a diode, decreases with increasing reverse voltage		
d	Apparent (of virtual) source size (of an emitter), the measured diameter of an optical source used to calculate the eye safety laser class of the source. See IEC 60825-1 and EN ISO 11146-1	F	Farad , unit: F = C/V
D*	Detectivity √A/NEP	f	Frequency , unit: s ⁻¹ , Hz (Hertz)
E	Emitter , Emitter terminal (phototransistor)	f _c , f _{cd}	Cut-off frequency - detector devices, the frequency at which, for constant signal modulation depth of the input radiant power, the demodulated signal power has decreased to ½ of its low frequency value. Example: The incident radiation generates a photocurrent or a photo voltage 0.707 times the value of radiation at f = 1 kHz (3 dB signal drop, other references may occur as e.g. 6 dB or 10 dB)
E _A	Illumination at standard illuminant A , according to DIN 5033 and IEC 306-1, illumination emitted from a tungsten filament lamp with a color temperature T _f = 2855.6 K, which is equivalent to		

f_s	Switching frequency	IRED	Infrared emitting diode , solid state device embodying a p-n junction, emitting infrared radiation when excited by an electric current. See also LED: solid state device embodying a p-n junction, emitting optical radiation when excited by an electric current.
FIR	Fast infrared , as SIR, data rate 4 Mbit/s		
I_a	Light current , general: current which flows through a device due to irradiation/illumination	I_{ro}	Reverse dark current, dark current , reverse current flowing through a photoelectric device in the absence of irradiation
I_B	Base current	IRPHY	Version 1.0, SIR IrDA® , data communication specification covering data rates from 2.4 kbit/s to 115.2 kbit/s and a guaranteed operating range more than one meter in a cone of $\pm 15^\circ$
I_{BM}	Base peak current	IRPHY	Version 1.1, MIR and FIR were implemented in the IrDA® standard with the version 1.1, replacing version 1.0
I_C	Collector current	IRPHY	Version 1.2, added the SIR low power standard to the IrDA® standard, replacing version 1.1. The SIR low power standard describes a current saving implementation with reduced range (min. 20 cm to other low power devices and min. 30 cm to full range devices).
I_{ca}	Collector light current , collector current under irradiation. Collector current which flows at a specified illumination/irradiation	IRPHY	Version 1.3, extended the low power option to the higher bit rates of MIR and FIR replacing version 1.2.
I_{CEO}	Collector dark current, with open base , collector emitter dark current. For radiant sensitive devices with open base and without illumination/radiation ($E = 0$)	IRPHY	Version 1.4, VFIR was added, replacing version 1.3
I_{CM}	Repetitive peak collector current		Quiescent current
idle	Mode of operation where the device (e.g. a transceiver) is fully operational and expecting to receive a signal for operation e.g in case of a transceiver waiting to receive an optical input or to send an optical output as response to an applied electrical signal.		Supply current in dark ambient
I_e, I	Radiant intensity (of a source, in a given direction), quotient of the radiant flux $d\Phi_e$ leaving the source and propagated in the element of solid angle $d\Omega$ containing the given direction, by the element of solid angle. $I_e = d\Phi_e/d\Omega$, unit: $W \cdot sr^{-1}$ Note: The radiant intensity I_e of emitters is typically measured with an angle < 0.01 sr on mechanical axis or off-axis in the maximum of the irradiation pattern.		Supply current in bright ambient
I_F	Continuous forward current , the current flowing through a diode in the forward direction		Luminous intensity (of a source, in a given direction), quotient of the luminous flux $d\Phi_v$ leaving the source and propagated in the element of solid angle $d\Omega$ containing the given direction, by the element of solid angle. $I_v = d\Phi_v/d\Omega$, unit: $cd \cdot sr^{-1}$ Note: The luminous intensity I_v of emitters is typically measured with an angle < 0.01 sr on mechanical axis or off-axis in the maximum of the irradiation pattern.
I_{FAV}	Average (mean) forward current	K	luminous efficacy of radiation, quotient of the luminous flux Φ_v by the corresponding radiant flux Φ_e : $K = \Phi_v / \Phi_e$, unit: $lm \cdot W^{-1}$
I_{FM}	Peak forward current		Note: When applied to monochromatic radiations, the maximum value of $K(\lambda)$ is denoted by the symbol K_m .
I_{FSM}	Surge forward current		$K_m = 683 lm \cdot W^{-1}$ for $\nu_m = 540 \times 10^{12} Hz$ ($\lambda_m \approx 555 nm$) for photopic vision.
I_k	Short-circuit current , that value of the current which flows when a photovoltaic cell or a photodiode is short circuited ($R_L \ll R_i$) at its terminals		$K'_m = 1700 lm \cdot W^{-1}$ for $\lambda'_m \approx 507 nm$ for scotopic vision. For other wavelengths : $K(\lambda) = K_m V(\lambda)$ and $K'(\lambda) = K'_m V'(\lambda)$
I_o	DC output current	K	Kelvin , SI unit of thermodynamic temperature, is the fraction 1/273.15 of the thermodynamic temperature of the triple point of water (13 th CGPM (1967), Resolution 4). The unit Kelvin and its symbol K should be used to express an interval or a difference of temperature.
I_{ph}	Photocurrent , that part of the output current of a photoelectric detector, which is caused by incident radiation.		Note: In addition to the thermodynamic
I_R	Reverse current, leakage current , current which flows through a reverse biased semiconductor p-n-junction		
IR	Abbreviation for infrared		
I_{ra}	Reverse current under irradiation , reverse light current which flows due to a specified irradiation/illumination in a photoelectric device $I_{ra} = I_{ro} + I_{ph}$		
IrDA®	Infrared Data Association , no profit organization generating infrared data communication standards		

Symbols and Terminology

Vishay Semiconductors

Symbols and Terminology



temperature (symbol T), expressed in Kelvins, use is also made of Celsius temperature (symbol t) defined by the equation $t = T - T_0$, where $T_0 = 273.15$ K by definition. To express Celsius temperature, the unit "degree Celsius", which is equal to the unit "Kelvin" is used; in this case, "degree Celsius" is a special name used in place of "Kelvin". An interval or difference of Celsius temperature can, however, be expressed in Kelvins as well as in degrees Celsius.

Latency **Receiver latency allowance** (in ms or μ s) is the maximum time after a node ceases transmitting before the node's receiving recovers its specified sensitivity

LED and IRED

Light Emitting Diode, LED: solid state device embodying a p-n junction, emitting optical radiation when excited by an electric current. The term LED is correct only for visible radiation, because light is defined as visible radiation (see Radiation and Light). For infrared emitting diodes the term IRED is the correct term. Nevertheless it is common but not correct to use "LED" also for IREDS.

L_e ; L **Radiance** (in a given direction, at a given point of a real or imaginary surface).

Quantity defined by the formula

$$L_e = \frac{d\Phi_v}{dA \cdot \cos\theta \cdot d\Omega} ,$$

where $d\Phi_e$ is the radiant flux transmitted by an elementary beam passing through the given point and propagating in the solid angle $d\Omega$ containing the given direction; dA is the area of a section of that beam containing the given point; θ is the angle between the normal to that section and the direction of the beam, unit: $W \cdot m^{-2} \cdot sr^{-1}$

lm **Lumen**, unit for luminous flux

lx **Lux**, unit for illuminance

m **Meter**, SI unit of length

M_e ; M **Radiant exitance** (at a point of a surface) - Quotient of the radiant flux $d\Phi_e$ leaving an element of the surface containing the point, by the area dA of that element. Equivalent definition. Integral, taken over the hemisphere visible from the given point, of the expression $L_e \cdot \cos\theta \cdot d\Omega$, where L_e is the radiance at the given point in the various directions of the emitted elementary beams of solid angle $d\Omega$, and θ is the angle between any of these beams and the normal to the surface at the given point.

$$M_e = \frac{d\Phi_e}{dA} = \int_{2\pi sr} L_e \cdot \cos\theta \cdot d\Omega$$

unit: $W \cdot m^{-2}$

MIR **Medium speed IR**, as SIR, with the data rate 576 kbit/s to 1152 kbit/s

Mode	Electrical input or output port of a transceiver device to set the receiver bandwidth
N.A.	Numerical Aperture , N.A. = $\sin \alpha/2$ Term used for the characteristic of sensitivity or intensity angles of fiber optics and objectives
NEP	Noise equivalent power
P_{tot}	Total power dissipation
P_v	Power dissipation, general
Radiation and Light	Visible radiation , any optical radiation capable of causing a visual sensation directly. Note: There are no precise limits for the spectral range of visible radiation since they depend upon the amount of radiant power reaching the retina and the responsivity of the observer. The lower limit is generally taken between 360 nm and 400 nm and the upper limit between 760 nm and 830 nm.
Radiation and Light	Optical radiation , electromagnetic radiation at wavelengths between the region of transition to X-rays ($\lambda = 1$ nm) and the region of transition to radio waves ($\lambda = 1$ mm)
Radiation and Light IR	Infrared radiation , optical radiation for which the wavelengths are longer than those for visible radiation. Note: For infrared radiation, the range between 780 nm and 1 mm is commonly sub-divided into: IR-A 780 nm to 1400 nm IR-B 1.4 μ m to 3 μ m IR-C 3 μ m to 1 mm
R_D	Dark resistance
R_F	Feedback resistor
R_i	Internal resistance
R_{is}	Isolation resistance
R_L	Load resistance
R_S	Serial resistance
R_{sh}	Shunt resistance , the shunt resistance of a detector diode is the dynamic resistance of the diode at zero bias. Typically it is measured at a voltage of 10 mV forward or reverse, or peak-to-peak
R_{thJA}	Thermal resistance , junction to ambient
R_{thJC}	Thermal resistance , junction to case
RXD	Electrical data output port of a transceiver device
s	Second , SI-unit of time 1 h = 60 min = 3600 s
S	Absolute sensitivity Ratio of the output value Y of a radiant-sensitive device to the input value X of a physical quantity: $S = Y/X$, units: e.g. A/lx, A/W, A/(W/m ²)
$s(\lambda_p)$	Spectral sensitivity at a wavelength λ_p

$s(\lambda)$	Absolute spectral sensitivity at a wavelength λ , the ratio of the output quantity y to the radiant input quantity x in the range of wavelengths λ to $\lambda + \Delta\lambda$ $s(\lambda) = dy(\lambda)/dx(\lambda)$ E.g., the radiant power $\Phi_e(\lambda)$ at a specified wavelength λ falls on the radiationsensitive area of a detector and generates a photocurrent $I_{ph} \cdot s(\lambda)$ is the ratio between the generated photocurrent I_{ph} and the radiant power $\Phi_e(\lambda)$ which falls on the detector. $s(\lambda) = I_{ph} / \Phi_e(\lambda)$, unit: A/W	shape of the area does not matter at all. Any shape on the surface of the sphere that holds the same area will define a solid angle of the same size. The unit of the solid angle is the steradian (sr) . Mathematically, the solid angle is dimensionless, but for practical reasons, the steradian is assigned.
$s(\lambda)_{rel}$	Spectral sensitivity, relative , ratio of the spectral sensitivity $s(\lambda)$ at any considered wavelength to the spectral sensitivity $s(\lambda_0)$ at a certain wavelength λ_0 taken as a reference $s(\lambda)_{rel} = s(\lambda)/s(\lambda_0)$	Standby Mode of operation where a device is prepared to be quickly switched into an idle or operating mode by an external signal.
$s(\lambda_0)$	Spectral sensitivity at a reference wavelength λ_0	Period of time (duration)
SC	Electrical input port of a transceiver device to set the receiver sensitivity	Temperature, 0 K = - 273.15 °C, unit: K (Kelvin)
SD	Electrical input port of a transceiver device to shut down the transceiver	Temperature, °C (degree Celsius). Instead of t sometimes T is used not to mix up temperature T with time t
Shutdown	Mode of operation where a device is switched to a sleep mode (shut down) by an external signal or after a quiescent period keeping some functions alive to be prepared for a fast transition to operating mode. Might be in some cases identical with "standby"	Time Ambient temperature , if self-heating is significant: temperature of the surrounding air below the device, under conditions of thermal equilibrium. If self-heating is insignificant: air temperature in the surroundings of the device
SIR	Serial Infrared , term used by IrDA® to describe infrared data transmission up to and including 115.2 kbit/s. SIR IrDA® data communication covers 2.4 kbit/s to 115.2 kbit/s, equivalent to the basic serial infrared standard introduced with the physical layer version IrPhy version 1.0	Ambient temperature range , as an absolute maximum rating: the maximum permissible ambient temperature range
Split power supply	Term for using separated power supplies for different functions in transceivers. Receiver circuits need well-controlled supply voltages. IRED drivers do not need a controlled supply voltage but need much higher currents. Therefore it safes cost not to control the IRED current supply and have a separated supply. For that some modified design rules have to be taken into account for designing the ASIC. This is used in nearly all Vishay transceivers and is described in US-Patent no. 6,157,476	Temperature coefficient , the ratio of the relative change of an electrical quantity to the change in temperature (ΔT) which causes it under otherwise constant operating conditions
sr	Steradian (sr) , SI unit of solid angle Ω . Solid angle that, having its vertex at the centre of a sphere, cuts off an area of the surface of the sphere equal to that of a square with sides of length equal to the radius of the sphere. (ISO, 31/1-2.1, 1978) Example: The unity solid angle, in terms of geometry, is the angle subtended at the center of a sphere by an area on its surface numerically equal to the square of the radius (see figures below). Other than the figures might suggest, the	Colour temperature (BE) , the temperature of a Planckian radiator whose radiation has the same chromaticity as that of a given stimulus, unit: K Note: The reciprocal colour temperature is also used, unit K^{-1} (BE).
		Case temperature , the temperature measured at a specified point on the case of a semiconductor device. Unless otherwise stated, this temperature is given as the temperature of the mounting base for devices with metal can
		Delay time Fall time , the time interval between the upper specified value and the lower specified value on the trailing edge of the pulse. Note: It is common to use a 90 % value of the signal for the upper specified value and a 10 % value for the lower specified value.
		Junction temperature , the spatial mean value of the temperature during operation. In the case of phototransistors, it is mainly the temperature of the collector junction because its inherent temperature is the maximum.
		Turn-off time , the time interval between the upper specified value on the trailing edge of the applied input pulse and the lower specified value on the trailing edge of the output pulse. $t_{off} = t_{d(off)} + t_f$

Symbols and Terminology

Vishay Semiconductors

Symbols and Terminology



t_{on}	Turn-on time , the time interval between the lower specified value on the trailing edge of the applied input pulse and the upper specified value on the trailing edge of the output pulse. $t_{on} = t_{d(on)} + t_f$	V_{CC}	Supply voltage (positive)
t_p	Pulse duration , the time interval between the specified value on the leading edge of the pulse and the specified value on the trailing edge of the output pulse. Note: In most cases the specified value is 50 % of the signal	V_{CE}	Collector emitter voltage
t_{pi}	Input pulse duration	V_{CEO}	Collector emitter voltage, open base ($I_B = 0$)
t_{po}	Output pulse duration	V_{CEsat}	Collector emitter saturation voltage , the saturation voltage is the DC voltage between collector and emitter for specified (saturation) conditions, i.e., I_C and E_V (E_e or I_B), whereas the operating point is within the saturation region.
t_r	Rise time , the time interval between the lower specified value and the upper specified value on the trailing edge of the pulse. Note: It is common to use a 90 % value of the signal for the upper specified value and a 10 % value for the lower specified value	V_{dd}	Supply voltage (positive)
t_s	Storage time	V_{EBO}	Emitter base voltage, open collector
T_{sd}	Soldering temperature , maximum allowable temperature for soldering with a specified distance from the case and its duration	V_{ECO}	Emitter collector voltage, open base
T_{stg}	Storage temperature range , the temperature range at which the device may be stored or transported without any applied voltage	V_F	Forward voltage , the voltage across the diode terminals which results from the flow of current in the forward direction
TXD	Electrical data input port of a transceiver device	VFIR	As SIR, data rate 16 Mbit/s
V	Volt	V_{logic}	Reference voltage for digital data communication ports
$V(\lambda)$	Standard luminous efficiency function for photopic vision (relative human eye sensitivity)	V_{no}	Signal-to-noise ratio
$V(\lambda), V'(\lambda)$	Spectral luminous efficiency (of a monochromatic radiation of wavelength λ); $V(\lambda)$ for photopic vision; $V'(\lambda)$ for scotopic vision). Ratio of the radiant flux at wavelength λ_m to that at wavelength λ such that both radiations produce equally intense luminous sensations under specified photometric conditions and λ_m is chosen so that the maximum value of this ratio is equal to 1	V_O	Output voltage
V_{BEO}	Base emitter voltage, open collector	ΔV_O	Output voltage change (differential output voltage)
$V_{(BR)}$	Breakdown voltage , reverse voltage at which a small increase in voltage results in a sharp rise of reverse current. It is given in technical data sheets for a specified current	V_{oc}	Open circuit voltage , the voltage measured between the photovoltaic cell or photodiode terminals at a specified irradiance/illuminance (high impedance voltmeter!)
$V_{(BR)}$	CEO Collector emitter breakdown voltage, open base	V_{OH}	Output voltage high
$V_{(BR)EBO}$	Emitter base breakdown voltage, open collector	V_{OL}	Output voltage low
$V_{(BR)ECO}$	Emitter collector breakdown voltage, open base	V_{ph}	Photovoltage , the voltage generated between the photovoltaic cell or photodiode terminals due to irradiation/ illumination
V_{CBO}	Collector-base voltage, open emitter , generally, reverse biasing is carried out by applying a voltage to any of two terminals of a transistor in such a way that one of the junctions operates in reverse direction, whereas the third terminal (second junction) is specified separately.	V_R	Reverse voltage (of a junction), applied voltage such that the current flows in the reverse direction
		V_R	Reverse (breakdown) voltage , the voltage drop which results from the flow of a defined reverse current
		V_S	Supply voltage
		V_{ss}	(Most negative) supply voltage (in most cases: ground)
		$\pm \varphi_{1/2}$	Angle of half transmission distance
		η	Quantum efficiency
		$\theta_{1/2}; \pm \varphi = \alpha/2$	Half-intensity angle , in a radiation diagram, the angle within which the radiant (or luminous) intensity is greater than or equal to half of the maximum intensity. Note: IEC 60747-5-1 is using $\theta_{1/2}$. In Vishay datasheets mostly $\pm \varphi = \alpha/2$ is used
		$\theta_{1/2}; \pm \varphi = \alpha/2$	Half-sensitivity angle , in a sensitivity diagram, the angle within which the sensitivity is greater than or equal to half of the maximum sensitivity. Note: IEC 60747-5-1 is using $\theta_{1/2}$. In Vishay datasheets mostly $\pm \varphi = \alpha/2$ is used

Ω	Solid angle , see sr, steradian for IEC 60050(845)-definition. The space enclosed by rays, which emerge from a single point and lead to all the points of a closed curve. If it is assumed that the apex of the cone formed in this way is the center of a sphere with radius r and that the cone intersects with the surface of the sphere, then the size of the surface area (A) of the sphere subtending the cone is a measure of the solid angle Ω . $\Omega = A/r^2$. The full sphere is equivalent to 4π sr. A cone with an angle of $\alpha/2$ forms a solid angle of $\Omega = 2\pi(1 - \cos \alpha/2) = 4\pi \sin^2 \alpha/4$, unit: sr	observer. For photopic vision $\Phi_v = K_m \int_0^\infty \frac{d\Phi_e \lambda}{d\lambda} \cdot V(\lambda) d\lambda,$ where $\frac{d\Phi_e \lambda}{d\lambda}$ is the spectral distribution of the radiant flux and $V(\lambda)$ is the spectral luminous efficiency, unit : lm, lm: lumen, $K_m = 683 \text{ lm/W}$: Note: For the values of K_m (photopic vision) and $K'm$ (scotopic vision), see IEC 60050 (845-01-56).
λ_m	Wavelength of the maximum of the spectral luminous efficiency function $V(\lambda)$	λ_c
$\Delta\lambda$	Range of spectral bandwidth (50 %) , the range of wavelengths where the spectral sensitivity or spectral emission remains within 50 % of the maximum value	λ_c
$\Phi_e; \Phi; P$	Radiant flux; radiant power , power emitted, transmitted or received in the form of radiation. unit: W, W = Watt	λ_D
$\Phi_v; \Phi$	Luminous flux , quantity derived from radiant flux Φ_e by evaluating the radiation according to its action upon the CIE standard photometric	λ_p

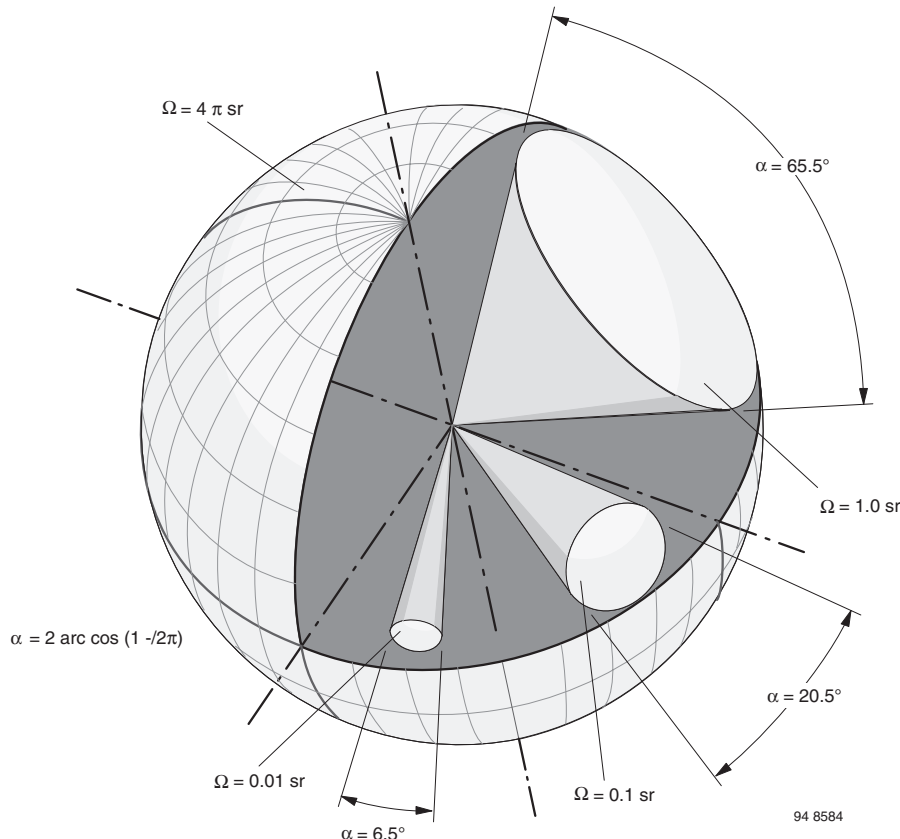


Fig. 1

Symbols and Terminology

Vishay Semiconductors

Symbols and Terminology



DEFINITIONS

Databook Nomenclature

The nomenclature, symbols, abbreviations and terms inside the Vishay Semiconductors data book is based on ISO and IEC standards.

The special optoelectronic terms and definitions are referring to the IEC Multilingual Dictionary (Electricity, Electronics and Telecommunications), Fourth edition (2001-01), IEC 50 (Now: IEC 60050). The references are taken from the current editions of IEC 60050 (845), IEC 60747-5-1 and IEC 60747-5-2. Measurement conditions are based on IEC and other international standards and especially guided by IEC 60747-5-3.

Editorial notes: Due to typographical limitations variables cannot be printed in an italics format, which is usually mandatory. Our booklet in general is using American spelling. International standards are written in UK English. Definitions are copied without changes from the original text. Therefore these may contain British spelling.

Radiant and Luminous Quantities and Their Units

These two kinds of quantities have the same basic symbols, identified respectively, where necessary, by the subscript e (energy) or v (visual), e.g. Φ_e , Φ_v . See note.

Note: Photopic and scotopic quantities. Luminous (photometric) quantities are of two kinds, those used for photopic vision and those used for scotopic vision. The wording of the definitions in the two cases being almost identical, a single definition is generally sufficient with the appropriate adjective, photopic or scotopic added where necessary.

The symbols for scotopic quantities are prime (Φ'_v , I'_v , etc), but the units are the same in both cases.

In general, optical radiation is measured in radiometric units. Luminous (photometric) units are used when optical radiation is weighted by the sensitivity of the human eye, correctly spoken, by the CIE standard photometric observer

(Ideal observer having a relative spectral responsivity curve that conforms to the $V(\lambda)$ function for photopic vision or to the $V'(\lambda)$ function for scotopic vision, and that complies with the summation law implied in the definition of luminous flux).

Note: With a given spectral distribution of a radiometric quantity the equivalent photometric quantity can be evaluated. However, from photometric units without knowing the radiometric spectral distribution in general one cannot recover the radiometric quantities.

Radiometric Terms, Quantities and Units

The radiometric terms are used to describe the quantities of optical radiation.

The relevant radiometric units are:

TABLE 1 - RADIOMETRIC QUANTITIES AND UNITS

RADIOMETRIC TERM	SYMBOL	UNIT	REFERENCE
Radiant power, radiant flux	Φ_e	W	IEC 50 (845-01-24)
Radiant intensity	I_e	W/sr	IEC 50 (845-01-30)
Irradiance	E_e	W/m ²	IEC 50 (845-01-37)
Radiant exitance	M_e	W/m ²	IEC 50 (845-01-47)
Radiance	L_e	W/(sr · m ²)	IEC 50 (845-01-34)

Photometric Terms, Quantities and Units

The photometric terms are used to describe the quantities of optical radiation in the wavelength range of visible radiation (generally assumed as the range from 380 nm to 780 nm). The relevant photometric terms are:

TABLE 2 - PHOTOMETRIC QUANTITIES AND UNITS

PHOTOMETRIC TERM	EQUIVALENT RADIOMETRIC TERM	SYMBOL	UNIT	REFERENCE
Luminous power or luminous flux	Radiant power or radiant flux Φ_e	Φ_v	lm	Φ_v : IEC 50 (845-01-25) lm : IEC 50 (845-01-51)
Luminous intensity	Radiant intensity I_e	I_v	lm/sr = cd	I_v : IEC 50 (845-01-31) cd : IEC 50 (845-01-50)
Illuminance	Irradiance E_e	E_v	lm/m ² = lx (lux)	E_v : IEC 50 (845-01-38) lx : IEC 50 (845-01-52)
Luminous exitance	Radiant exitance M_e	M_v	lm/m ²	IEC 50 (845-01-48)
Luminance	Radiance L_e	L_v	cd/m ²	IEC 50 (845-01-35)

Photometric units are derived from the radiometric units by weighting them with a wavelength dependent standardized human eye sensitivity $V(\lambda)$ - function, the so-called CIE-standard photometric observer. There are different functions for photopic vision ($V(\lambda)$) and scotopic vision ($V'(\lambda)$).

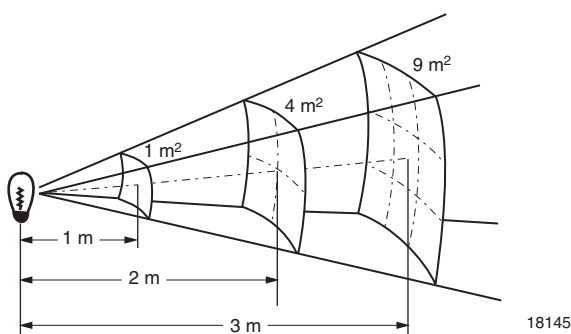
In the following is shown, how the luminous flux is derived from the radiant power and its spectral distribution. The equivalent other photometric terms can be derived from the radiometric terms in the same way.

Relation between distance r, irradiance (illuminance) E_e (E_V) and intensity I_e (I_V)

The relation between intensity of a source and the resulting irradiance in the distance r is given by the basic square root rule law.

An emitted intensity I_e generates in a distance r the irradiance $E_e = I_e/r^2$.

This relationship is not valid under near field conditions and should be used not below a distance d smaller than 5 times the emitter source diameter.



18145

Fig. 2

Using a single radiation point source, one gets the following relation between the parameter E_e , Φ_e , r :

$$E_e = \frac{d\Phi_e}{dA} \left[\frac{W}{m^2} \right]$$

use

$$I_e = \frac{d\Phi}{d\Omega}, \quad \Omega = \frac{A}{r^2} \quad \text{and get}$$

$$E_e = \frac{d\Phi_e}{dA} = I_e \frac{d\Omega}{dA} = \frac{I_e}{r^2} \left[\frac{W}{m^2} \right]$$

Examples

1. Calculate the irradiance with given intensity and distance r :

Transceivers with specified intensity of $I_e = 100 \text{ mW/sr}$ will generate in a distance of 1 m an irradiance of $E_e = 100/1^2 = 100 \text{ mW/m}^2$. In a distance of 10 m the irradiance would be $E_e = 100/10^2 = 1 \text{ mW/m}^2$.

2. Calculate the range of a system with given intensity and irradiance threshold. When the receiver is specified with a sensitivity threshold irradiance $E_e = 20 \text{ mW/m}^2$, the transmitter with an intensity $I_e = 120 \text{ mW/sr}$ the resulting range can be calculated as

$$r = \sqrt{\frac{I_e}{E_e}} = \sqrt{\frac{120}{20}} = \sqrt{6} = 2.45 \text{ m}$$

Assembly Instructions: Optoelectronic Semiconductors (IR Emitters, Detectors)

GENERAL

Optoelectronic semiconductor devices can be mounted in any position. Connection wires may be bent provided the bend is not less than 1.5 mm from bottom of case. During bending, no forces must be transmitted from pins to case (e.g., by spreading the pins).

If the device is to be mounted near heat generating components, the resultant increase in ambient temperature should be taken into account.

SOLDERING INSTRUCTIONS

Protection against overheating is essential when a device is being soldered. It is recommended, therefore, that the connection wires be left in place as long as possible. The maximum permissible device junction temperature should be exceeded for as little time as possible, and for no longer than specified in the solder profiles, during the soldering process. In case of plastic encapsulated devices, the maximum permissible soldering temperature is governed by the maximum permissible heat that may be applied to encapsulants rather than by the maximum permissible junction temperature.

Maximum soldering iron (or solder bath) temperatures are given in table 1. During soldering, no forces must be transmitted from pins to case (e.g., by spreading pins).

SOLDERING METHODS

There are several methods in use to solder devices onto the substrate. Some of them are listed in the following sections.

Vapor Phase Soldering

Soldering in saturated vapor is also known as condensation soldering. This soldering process is used as a batch system (dual vapor system) or as a continuous single vapor system. Both systems may also include preheating of the assemblies to prevent high-temperature shock and other undesired effects.

Infrared soldering

With infrared (IR) reflow soldering the heating is contact-free and the energy for heating the assembly is derived from direct infrared radiation and from convection (Refer to CECC00802).

The heating rate in an IR furnace depends on the absorption coefficients of the material surfaces and on the ratio of component's mass to its irradiated surface.

The temperature of components in an IR furnace, with a mixture of radiation and convection, cannot be determined in advance. Temperature measurement may be performed by measuring the temperature of a certain component while it is being transported through furnace.

The temperatures of small components, soldered together with larger ones, may rise up to 280 °C.

The following parameters influence the internal temperature of a component:

- Time and power
- Mass of component
- Size of component
- Size of printed circuit board
- Absorption coefficient of surfaces
- Packaging density
- Wavelength spectrum of radiation source
- Ratio of radiated and convected energy

Temperature-time profiles of the entire process and the above parameters are given in Fig. 1 and Fig. 2.

TABLE 1 - MAXIMUM SOLDERING TEMPERATURES

	IRON SOLDERING			WAVE SOLDERING		
	IRON TEMPERATURE	DISTANCE OF THE SOLDERING POSITION FROM THE LOWER EDGE OF THE CASE	MAXIMUM ALLOWABLE SOLDERING TIME	SOLDERING TEMPERATURE SEE TEMPERATURE TIME PROFILES	DISTANCE OF THE SOLDERING POSITION FROM THE LOWER EDGE OF THE CASE	MAXIMUM ALLOWABLE SOLDERING TIME
Devices in metal case	≤ 245 °C	≥ 1.5 mm	5 s	245 °C	≥ 1.5 mm	5 s
	≤ 245 °C	≥ 5.0 mm	10 s	-	-	-
	≤ 350 °C	≥ 5.0 mm	5 s	300 °C	≥ 5.0 mm	3 s
Devices in plastic case > 3 mm	≤ 260 °C	≥ 2.0 mm	5 s	235 °C	≥ 2.0 mm	8 s
	≤ 300 °C	≥ 5.0 mm	3 s	260 °C	≥ 2.0 mm	5 s
Devices in plastic case ≤ 3 mm	≤ 300 °C	≥ 5.0 mm	3 s	260 °C	≥ 2.0 mm	3 s

Wave soldering

In wave soldering, one or more continuously replenished waves of molten solder are generated, while the substrates to be soldered are moved in one direction across the wave's crest.

Temperature-time profiles of the entire process are given in Fig. 3.

Iron soldering

This process cannot be carried out in a controlled way.

It should not be considered for use in applications where reliability is important. There is no SMD classification for this process.

Laser soldering

This is an excess heating soldering method. The energy absorbed may heat device to a much higher temperature than desired. There is no SMD classification for this process at the moment.

Resistance soldering

This is a soldering method which uses temperature controlled tools (thermodes) for making solder joints. There is no SMD classification for this process at the moment.

WARNING

Surface-mount devices are sensitive to moisture release if they are subjected to infrared reflow or a similar soldering process (e.g. wave soldering). After opening the bag, they must be:

1. Stored at ambient of < 20 % relative humidity (RH)
2. Mounted within floor life specified on MSL sticker under factory conditions of $T_{amb} < 30^{\circ}\text{C}/\text{RH} < 60\%$

Devices require baking before mounting if 1. or 2. is not met and the humidity indicator card is > 20 % at $23 \pm 5^{\circ}\text{C}$. If baking is required, devices may be baked for 192 h at $40^{\circ}\text{C} + 5^{\circ}\text{C} - 0^{\circ}\text{C}$ and < 5 % RH.

TEMPERATURE-TIME PROFILES

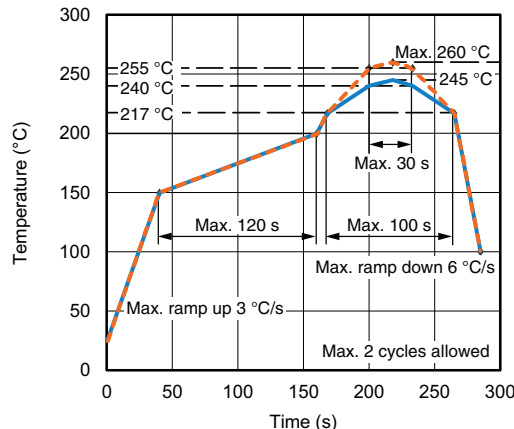


Fig. 1 - Lead (Pb)-free (Sn) Infrared Reflow Solder Profile
acc. J-STD020D for Surface-Mount Components

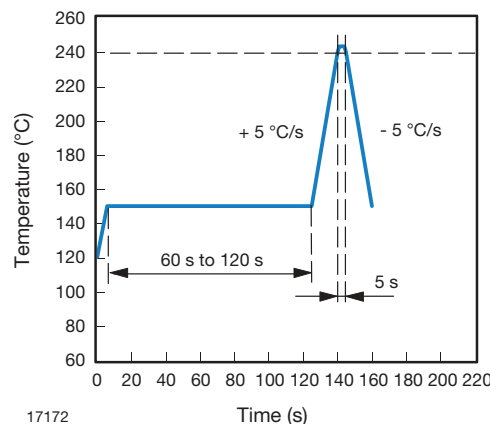


Fig. 2 - Infrared Reflow SnPb Solder Profile for Surface-Mount Components like TEMx1xxx and TSMx1xxx

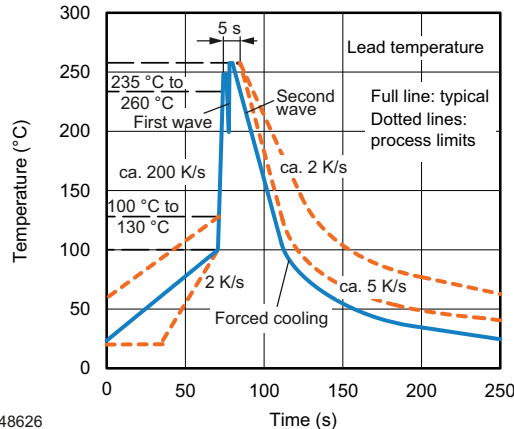


Fig. 3 - Double Wave Solder Profile for Leaded Components

HEAT REMOVAL

To maintain thermal equilibrium, the heat generated in the semiconductor junction(s) must be removed to keep the junction temperature below specified maximum.

In case of low-power devices, the natural heat conductive path between the case and surrounding air is usually adequate for this purpose. The heat generated in the junction is conveyed to the case or the header by conduction rather than convection. A measure of the effectiveness of heat conduction is the inner thermal resistance or the junction-to-case thermal resistance, R_{thJC} , which is governed by the device construction.

Any heat transfer from the case to the surrounding air involves radiation convection and conduction, the effectiveness of transfer being expressed in terms of an R_{thCA} value, i.e., external or case ambient thermal resistance. The total junction-to-ambient thermal resistance is consequently:

$$R_{thJA} = R_{thJC} + R_{thCA}$$

The total maximum power dissipation, P_{totmax} , of a semiconductor device can be expressed as follows:

$$P_{totmax} = \frac{T_{j\ max.} - T_{amb}}{R_{thJA}} = \frac{T_{j\ max.} - T_{amb}}{R_{thJC} + R_{thCA}}$$

where:

$T_{j\ max.}$ the maximum allowable junction temperature

T_{amb} the highest ambient temperature likely to be reached under the most unfavorable conditions

R_{thJC} junction-to-case thermal resistance

R_{thJA} the junction-to-ambient thermal resistance, is specified for the components. The following diagram shows how the different installation conditions effect the thermal resistance

R_{thCA} the case-to-ambient thermal resistance, R_{thCA} , depends on cooling conditions. If a heat dissipator or sink is used, R_{thCA} depends on the thermal contact between the case and heat sink, upon the heat propagation conditions in the sink, and upon the rate at which heat is transferred to the surrounding air

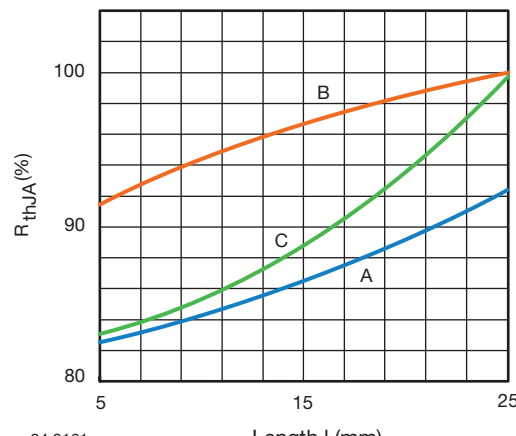


Fig. 4 - Junction-to-Ambient Thermal Resistance vs.
Lead Length at Different Assembly

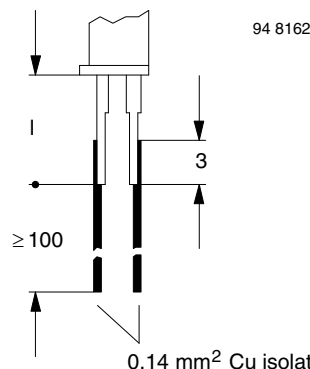


Fig. 5 - In Case of Wire Contacts (Curve B, Fig. 4)

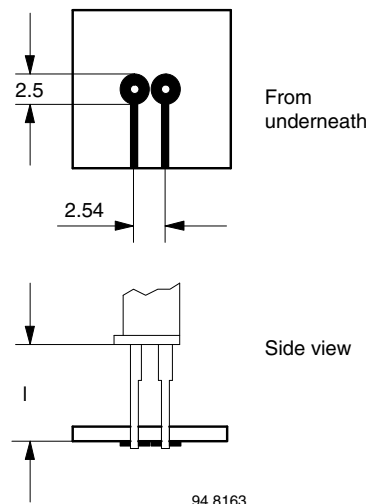


Fig. 6 - In Case of Assembly on PC Board, no Heatsink
(Curve C, Fig. 4)

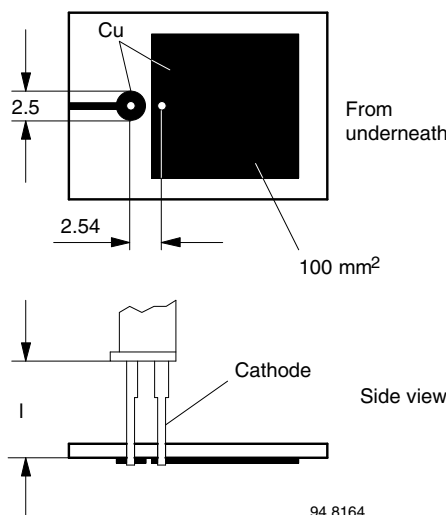
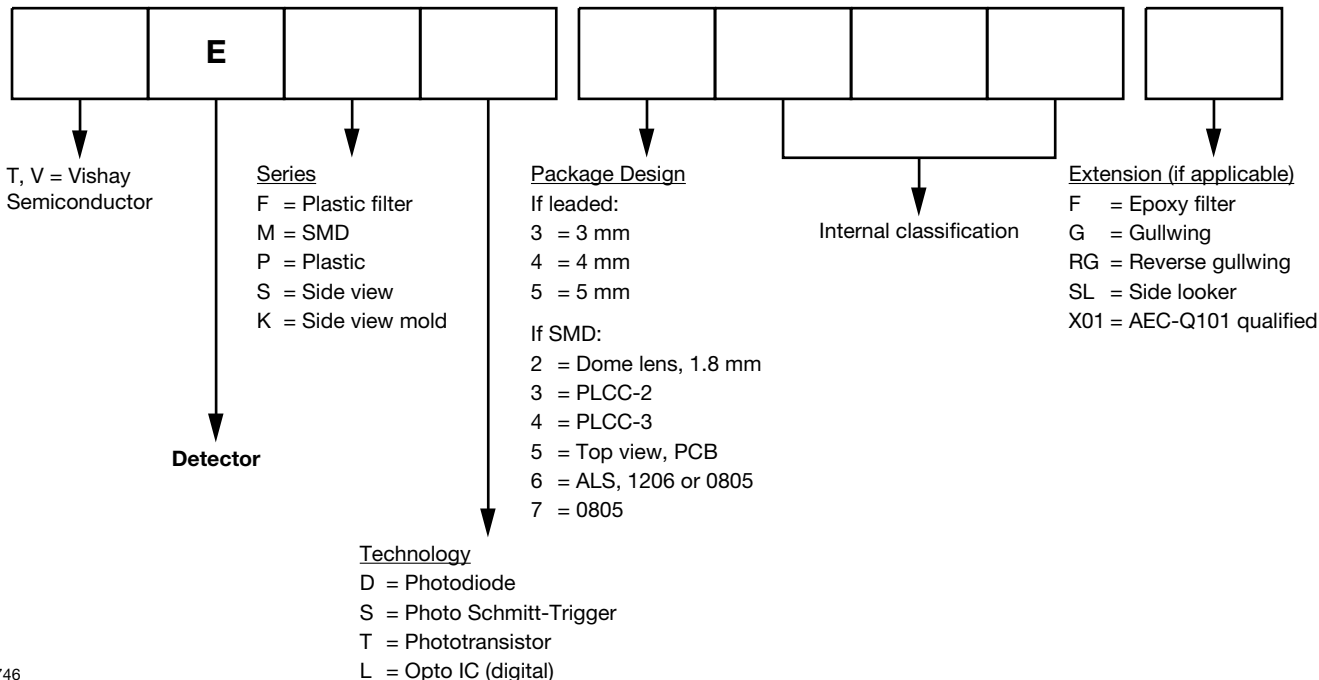


Fig. 7 - In Case of Assembly on PC Board, with Heatsink
(Curve A, Fig. 4)

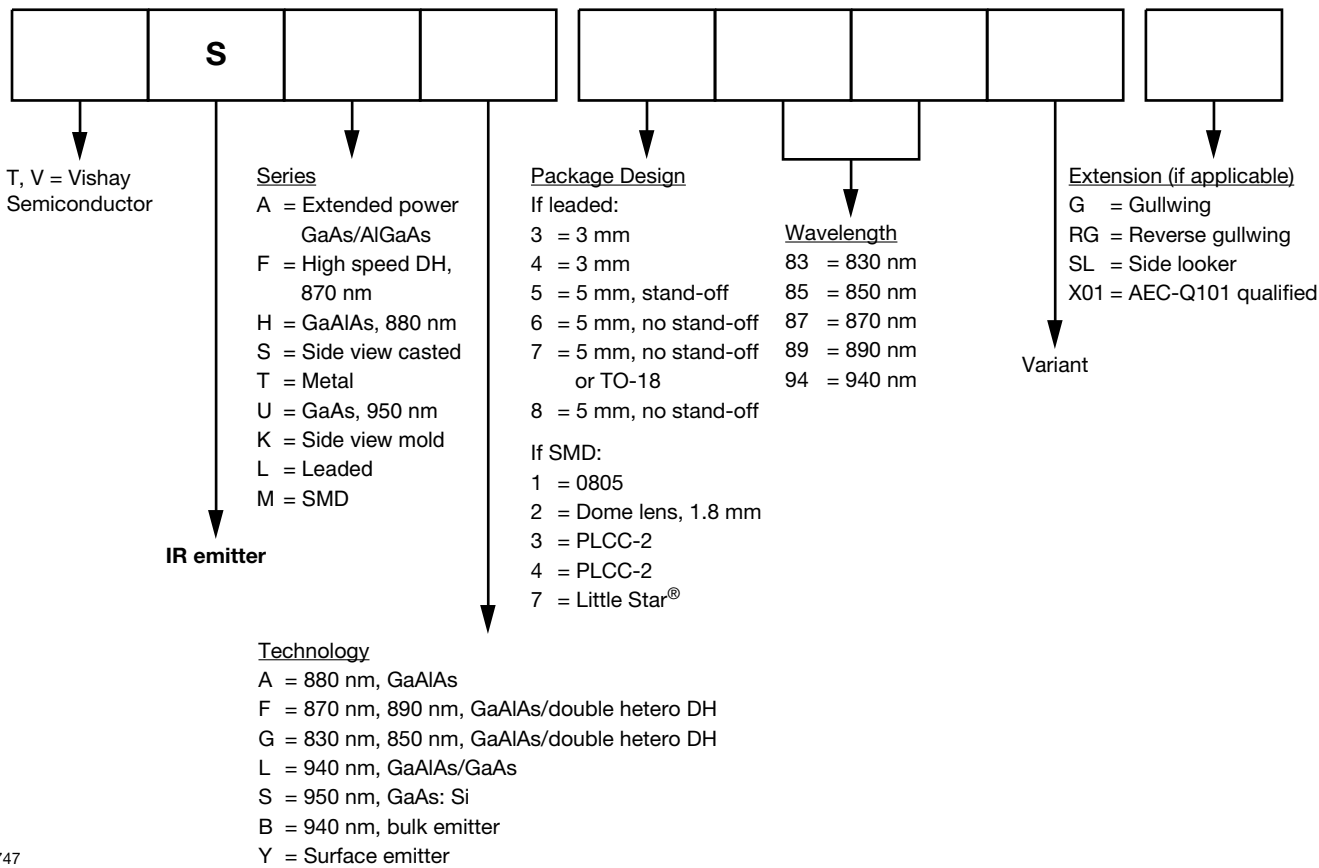
Type Designation Code

DETECTORS



18746

IR EMITTERS



18747

Packaging and Order Information

PACKAGING SURVEY

TABLE 1 - PACKAGING OPTIONS OF DETECTOR AND Emitter DEVICES					
PACKAGE FORM	SERIES	PACKAGING OPTION			
		BULK	TAPE	BLISTER TAPE	TUBE
Metal can	BPW./TS.	X			
Side view lens	TEKS5400.		X		
	TEKS5400S				
	TEKT5400S	X	X		
	TSKS5400S				
	TSKS542.X01		X		
SMD	TEM./TSM./VEM./VSM.			X	
Top view mold	BP104				
	BPW34	X			
	BP104S				X
	BPW34S				
Other leaded packages	BP./TE./TS.	X	X		

MOISTURE PROOF PACKAGING

The reel is packed in a moisture proof aluminum bag to protect devices from absorbing moisture during transportation and storage.

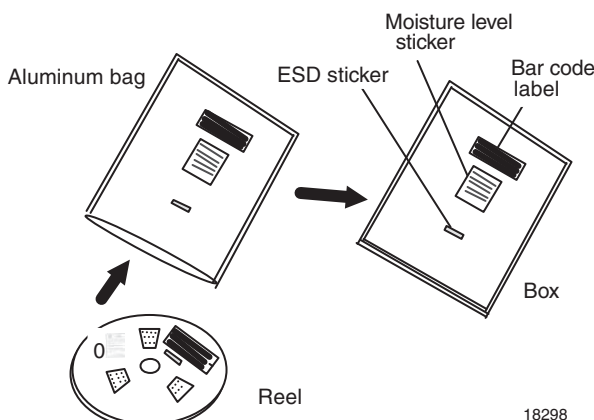


Fig. 1 - Moisture Proof Packaging

18298

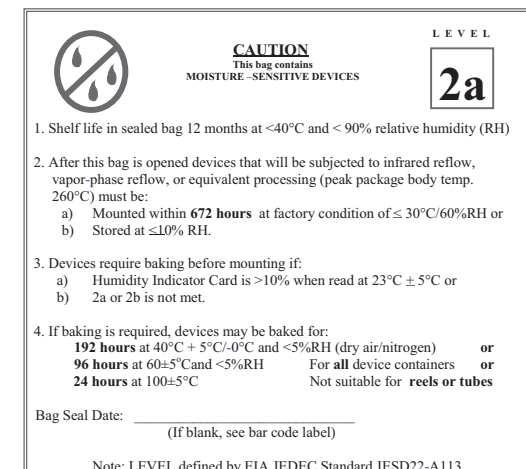


Fig. 2 - Example of MSL Sticker

19786

TABLE 2 - MOISTURE SENSITIVITY LEVEL, FLOOR LIFE AND FLOOR CONDITIONS

MSL	FLOOR LIFE	CONDITIONS
1	No limit	$\leq 30^{\circ}\text{C}/60\% \text{ RH}$
2	1 year	
2a	672 h	
3	168 h	
4	72 h	
5	24h/48 h	
6	6 h	

TABLE 3 - MOQ/DELIVERY UNIT SURVEY

PACKAGE FORM/DEVICE TYPE	MINIMUM ORDER QUANTITY	DELIVERY UNIT
LEADED		
5 mm		
Bulk e.g. TSAL, TSHF, BPV	4000	4000/bulk
Tape e.g. TSHF5210-ES21	5000	1000/reel
3 mm		
Bulk e.g. TSAL, VSLB, TEFT	5000	5000/bulk
Tape e.g. VSLB3940-MSZ	10 000	2000/reel
1.8 mm		
Bulk e.g. CQY37N, BPW17N	5000	5000/bulk
Tape e.g. CQY37N-CS12	4000	2000/reel
Side View Lens		
Bulk e.g. TSKS, TEKT	2000	2000/bulk
Tape e.g. TSKS5400S-ASZ	2000	2000/reel
Side View Micro		
Bulk e.g. TEST2600, TSSS2600	5000	5000/bulk
Tape e.g. TEST2600-MS21	5000	1000/reel
Top View Detector		
Bulk e.g. BP104, BPW34	3000	3000/bulk
Tube e.g. BP104S	1800	45/tube
Side View Detector		
Bulk e.g. BPV22F, BPW46	4000	4000/bulk
Tape e.g. BPV22F-AS12	5000	1000/reel
Metal Can TO-5		
Bulk e.g. BPW21R, BPW20RF	500	500/bulk
Metal Can TO-18		
Bulk e.g. BPW76, TSTS7100	1000	1000/bulk
SMD		
PLCC-2		
e.g. VSMF3710-GS08	7500	1500/reel
e.g. VSMF3710-GS18	8000	8000/reel
0805		
e.g. TEMT6200FX01	3000	3000/reel
1206		
e.g. TEMT6000X01	3000	3000/reel
SMD Top View		
e.g. TEMD5010X01	1500	1500/reel
SMD Gullwing, Reverse Gullwing		
e.g. VBP104S, VBPW34FASR	1000	1000/reel
Little Star		
e.g. VSMY7850X01	2000	2000/reel
Dome Lens 1.8 mm		
e.g. VSMB2020X01, VEMD2020X01	6000	6000/reel
Dome Lens 1.8 mm, Side Looker		
e.g. VSMB2943SLX01, VEMD2023SLX01	3000	3000/reel
Dome Lens 1.9 mm		
e.g. TSML1020, TEMT1020	1000	1000/reel

ESD PRECAUTION

Proper storage and handling procedures should be followed to prevent ESD damage to the devices, especially when they are removed from the antistatic shielding bag.

BAR CODE LABELS

Vishay Semiconductor standard bar code labels are printed on the final package. Labels containing Vishay Semiconductor specific data are affixed to each package unit.

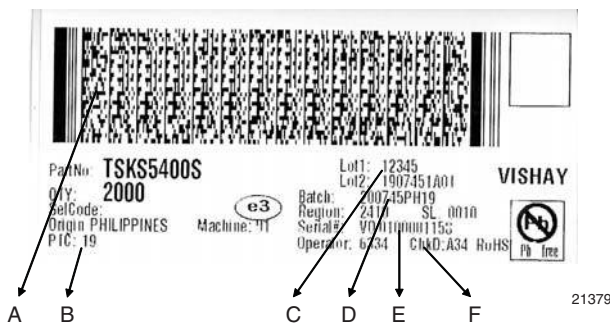


Fig. 3 - Bar code design and information

- A) PDF417 barcode including 325 char
- B) Plant code according TQD9021
http://intra.hn.vishay.com/quality/docs/tqd/tqd_9021.htm
- C) Lot1 and Lot2 reflects the lot numbers. Lot2 is a combination of 19 (PTC), 0745 (YYWW), 1 (production day MO=1, TU=2), A (Shift A,B,C) and 01 as production equipment
- D) Batch contains the datecode 200745 (YYYYWW), origin (PH=Philippines), 19 (PTC)
- E) Unique label serial number: VO production location (ISO), 01=label station ID, 00001158 (serial number)
- F) Check digit: counting number starting at A00 up to Z99 to give e.g. a manufactured reel a serial number (track and trace information)

TAPING OF SMD

Vishay SMD IR emitters and detectors are packed in antistatic blister tapes (in accordance with DIN IEC 40 (CO) 564) for automatic component insertion. The blister tapes are plastic strips with impressed component cavities, which are covered by a glued top tape.

Missing Devices

A maximum of 0.5 % of the total number of components per reel may be missing, excluding missing components at the beginning and at the end of reel. A maximum of three consecutive components may be missing. This gap is followed by ≥ 6 consecutive components (minimum).

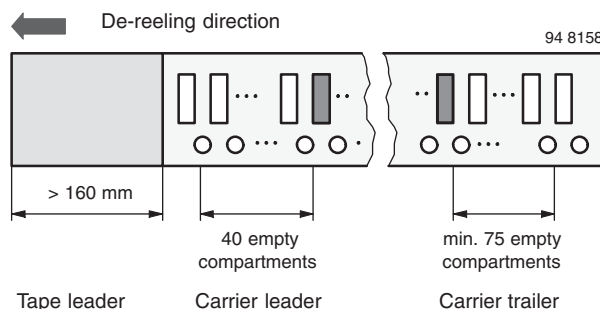


Fig. 4 - Beginning and End of Reel

TAPING SMD PLCC-2 PACKAGE

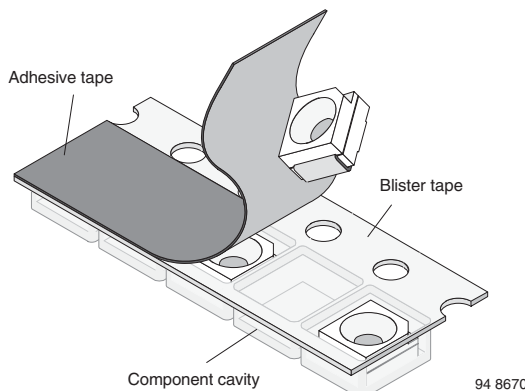


Fig. 5 - Blister Tape

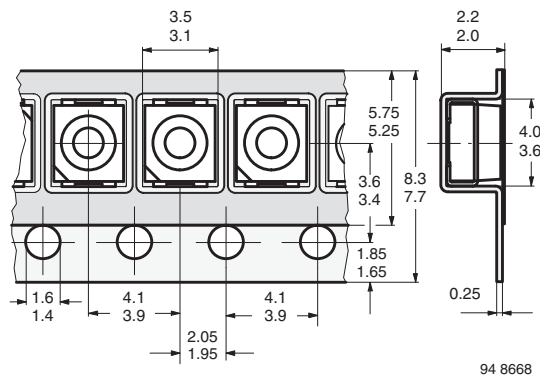


Fig. 6 - Tape Dimensions in mm for PLCC-2

TAPING STANDARDS GS08 AND GS18

GS08: 1500 pcs/reel

GS18: 8000 pcs/reel

The tape leader is at least 160 mm and is followed by a carrier tape leader with at least 40 empty compartments (figure 3). The tape leader may include carrier tape as long as the cover tape is not connected to carrier tape.

The last component is followed by a carrier tape trailer with at least 75 empty compartments, sealed with cover tape.

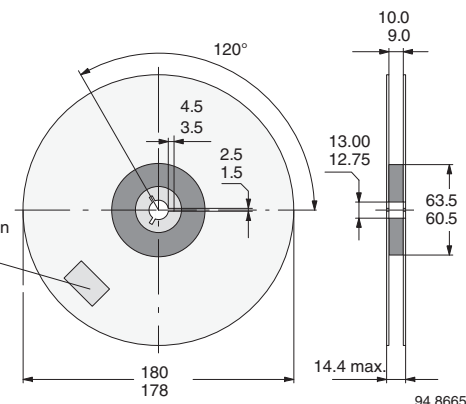


Fig. 7 - Reel Dimensions: GS08

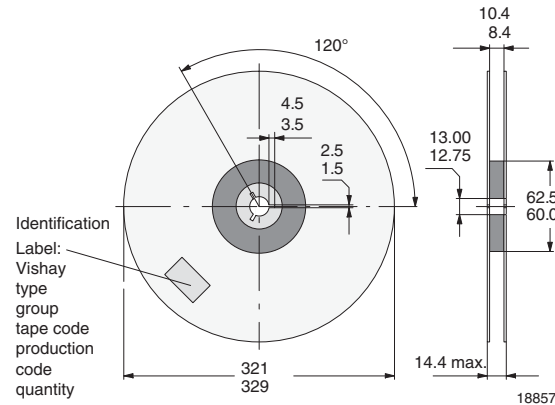


Fig. 8 - Reel Dimensions: GS18

COVER TAPE REMOVAL FORCE

The removal force may vary in strength between 0.1 N and 1.0 N at a removal speed of 5 mm/s.

In order to prevent components from popping out of blisters, the cover tape must be pulled off at an angle of 180° relative to the feed direction.

TAPING SMD WITH PCB OR DOME PACKAGE

Dimensions in millimeters

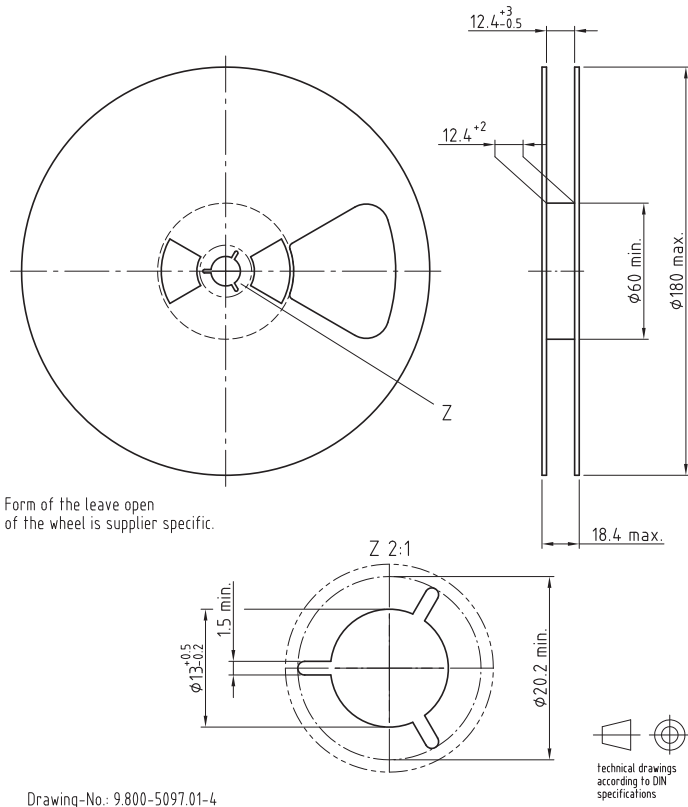


Fig. 9 - Reel of TEMD5010X01, TEMD5020X01, TEMD5110X01, TEMD5120X01, and TEMD5510FX01

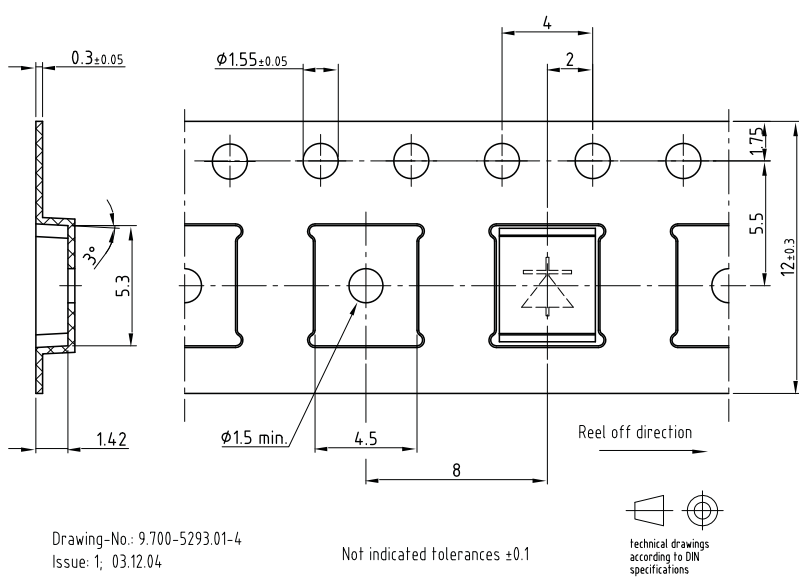


Fig. 10 - Blister Tape of TEMD5010X01, TEMD5020X01, TEMD5110X01, TEMD5120X01, and TEMD5510FX01

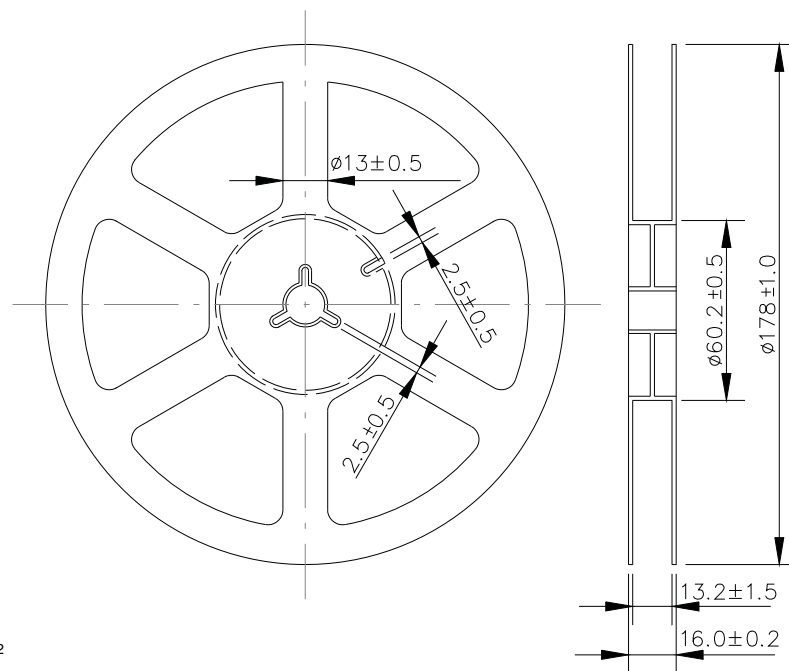


Fig. 11 - Reel of VBP104S, VPB104SR Series and VBPW34S, VBPW34SR Series

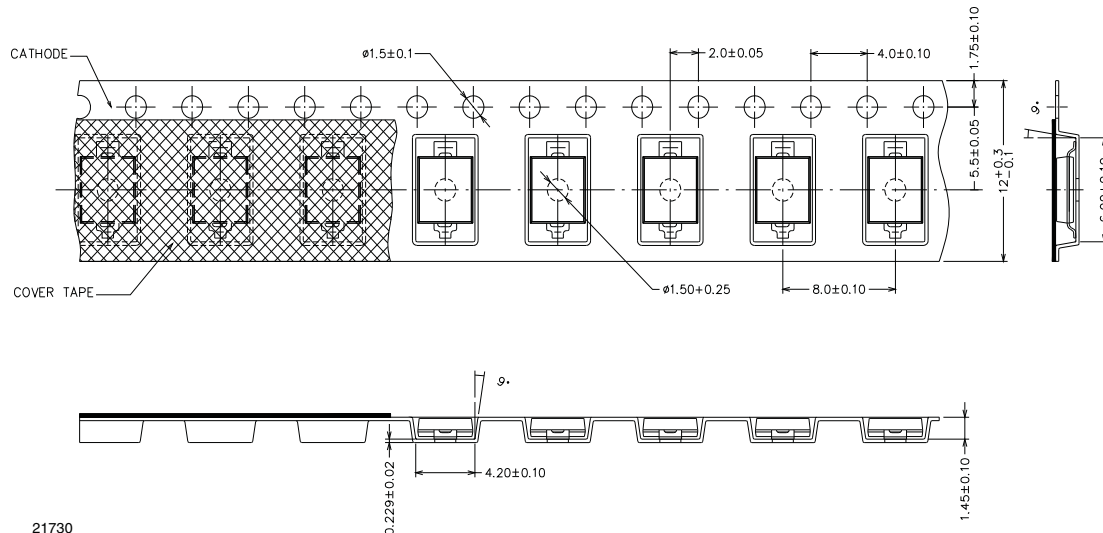


Fig. 12 - Blister Tape VBP104S Series and VBPW34S Series

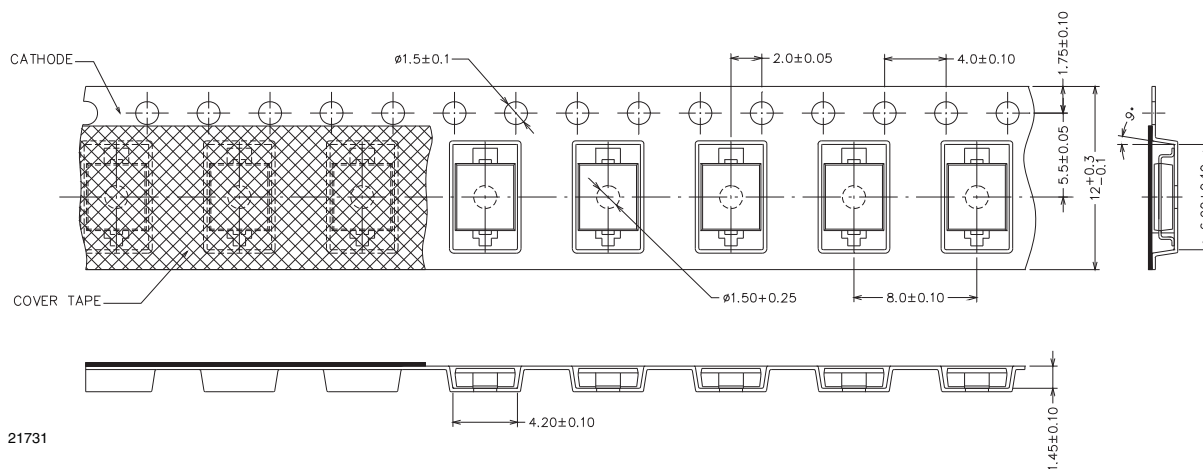
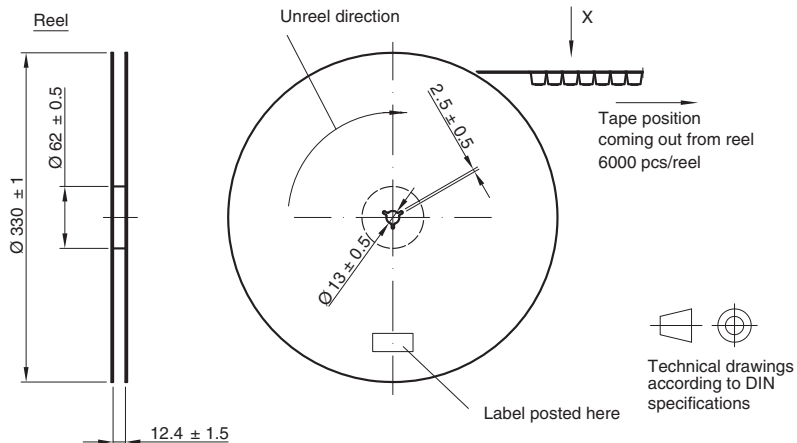
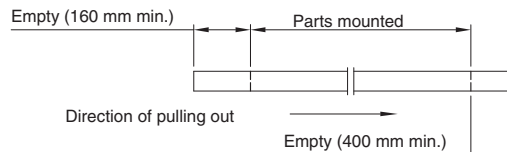


Fig. 13 - Blister Tape VBP104SR Series and VBPW34SR Series

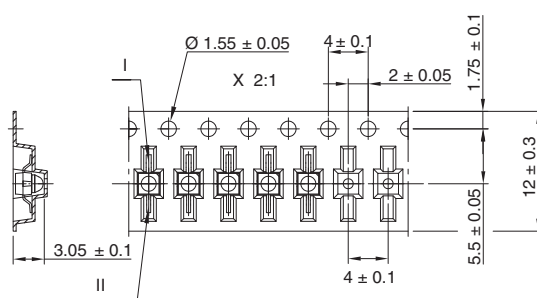


Leader and trailer tape:



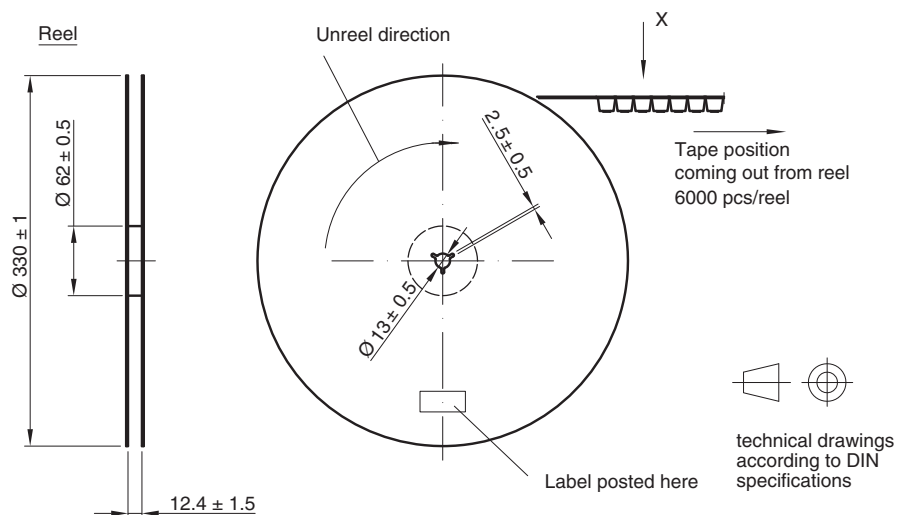
Terminal position in tape

Device	Lead I	Lead II
VEMT2000		
VEMT2500	Collector	Emitter
VEMD2000		
VEMD2500		
VSMB2000	Cathode	Anode
VSMG2000		
VSMY2850RG	Anode	Cathode

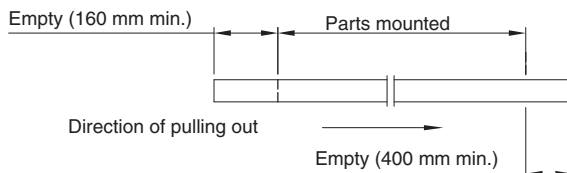


Drawing-No.: 9.800-5100.01-4
Issue: 2; 18.03.10
21572

Fig. 14 - Reel and Blister Tape of SMD Dome Lens, 1.8 mm, Reverse Gullwing

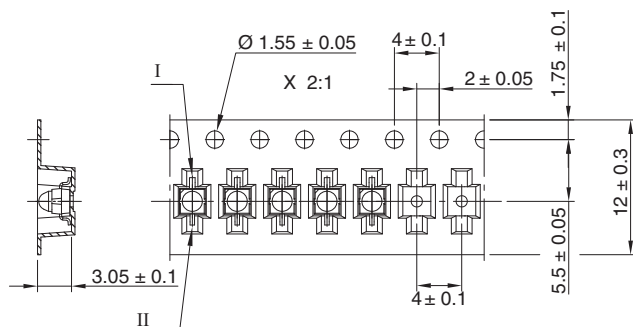


Leader and trailer tape:



Terminal position in tape

Device	Lead I	Lead II
VEMT2020		
VEMT2520	Collector	Emitter
VSMB2020		
VSMG2020		
VEMD2020	Cathode	Anode
VEMD2520		
VSMY2850G	Anode	Cathode

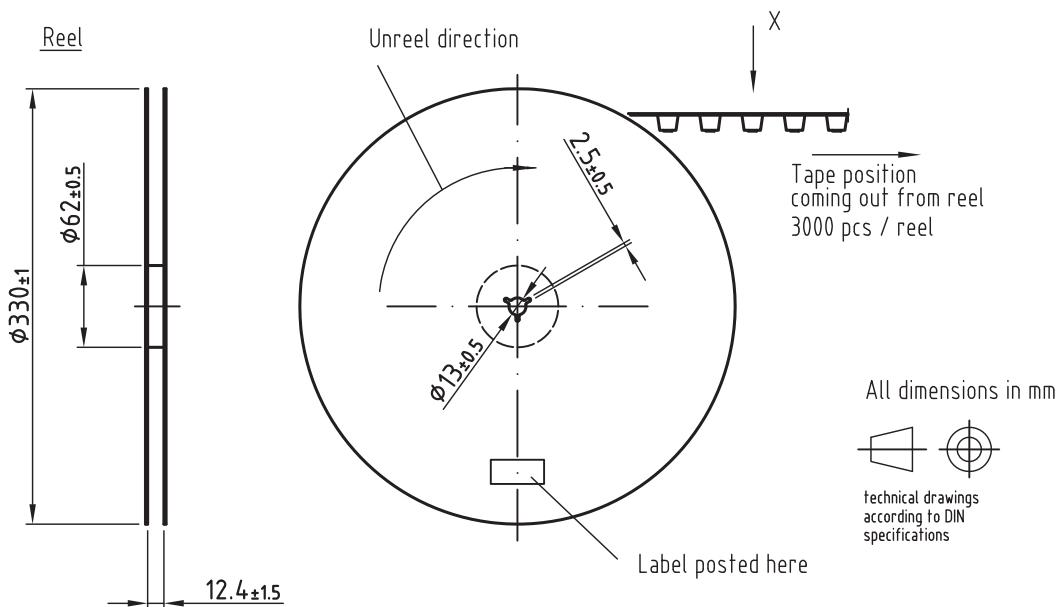


Drawing-No.: 9.800-5091.01-4

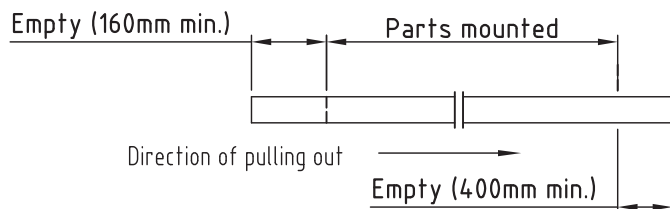
Issue: 3; 18.03.10

21571

Fig. 15 - Reel and Blister Tape of SMD Dome Lens, 1.8 mm, Gullwing

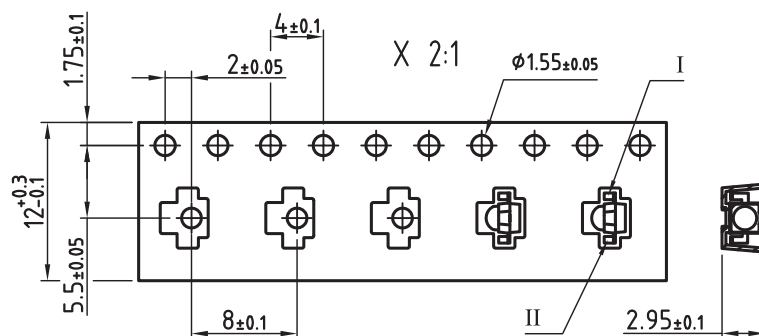


Leader and trailer tape:



Terminal position in tape

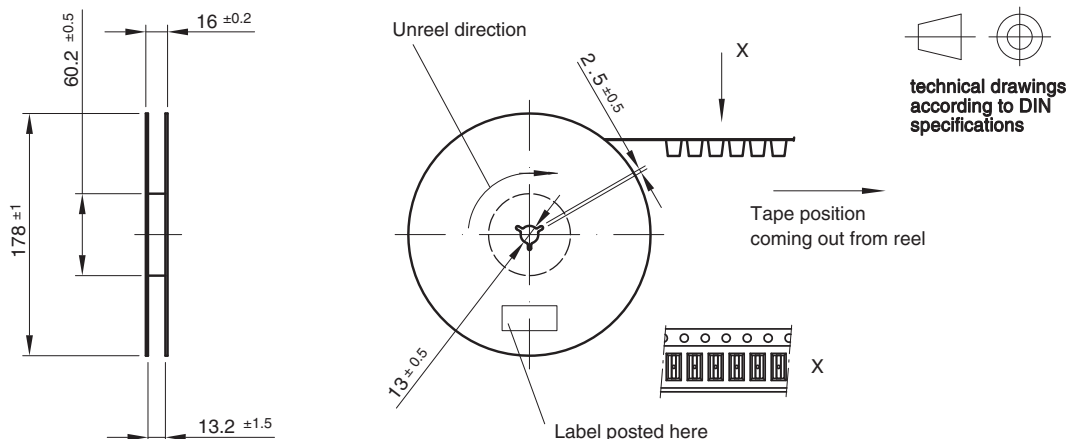
Device	Lead I	Lead II
VSMB2943SLX01	Cathode	Anode
VSMF2893SLX01		
VSMB2948SL		
VEMD2023SLX01		
VEMD2523SLX01		
VEMT2023SLX01	Collector	Emitter
VEMT2523SLX01		
VSMY2853SL	Anode	Cathode



Drawing refers to following types: see table
Reel dimensions and tape

Drawing-No.: 9.800-5123.01-4
Issue: prel; 03.08.12

Fig. 16 - Reel and Blister Tape of SMD Dome Lens, 1.8 mm, Side Looker



Leader and trailer tape:

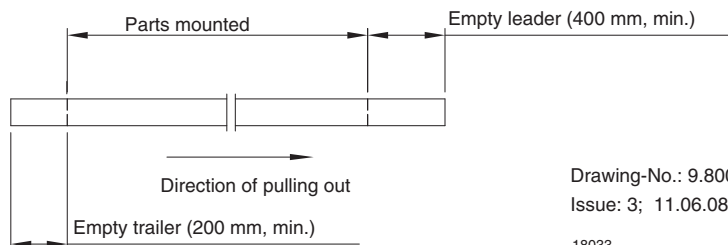


Fig. 17 - Reel of TEMx1000 Series and TSMx1000 Series
Quantity per Reel: 1000 pcs

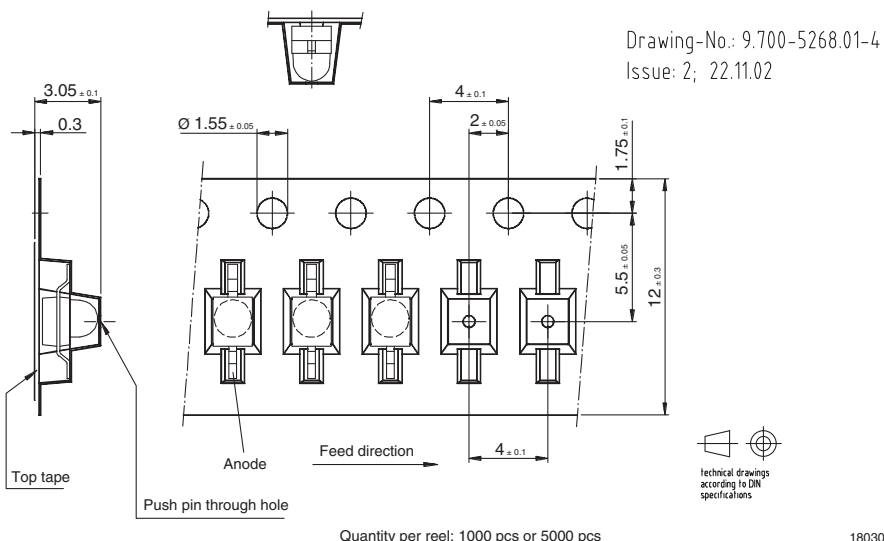


Fig. 18 - Blister Tape of TSMF1000, TSML1000, and TEMD1000

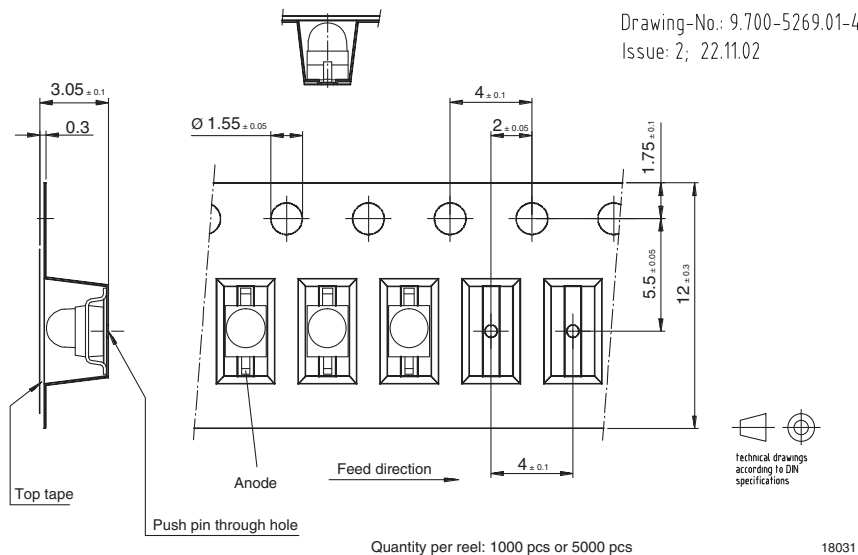


Fig. 19 - Blister Tape of TSMF1020, TSML1020, and TEMD1020

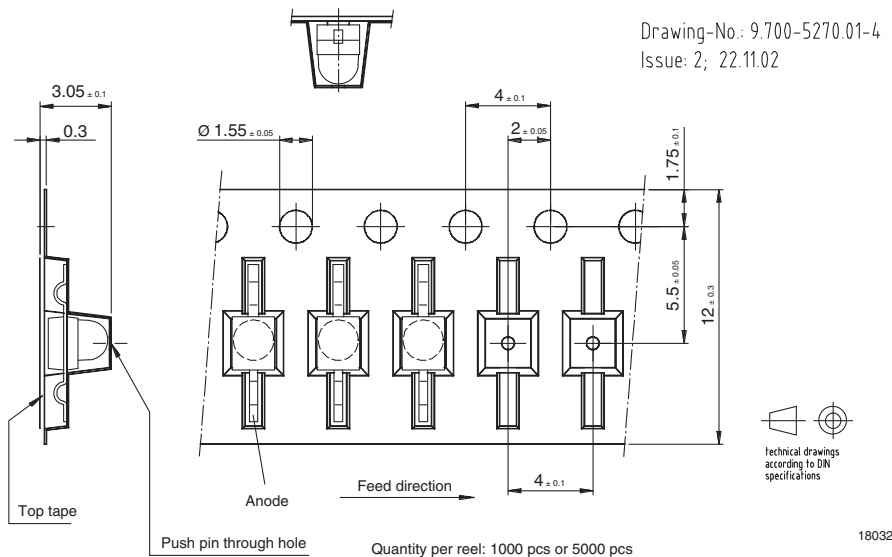


Fig. 20 - Blister Tape of TSMF1030, TSML1030, and TEMD1030

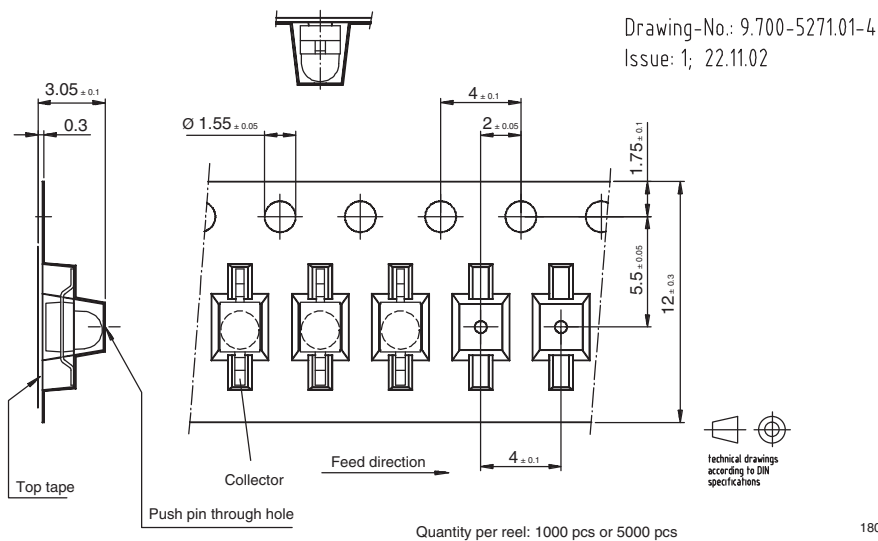


Fig. 21 - Blister Tape of TEMT1000

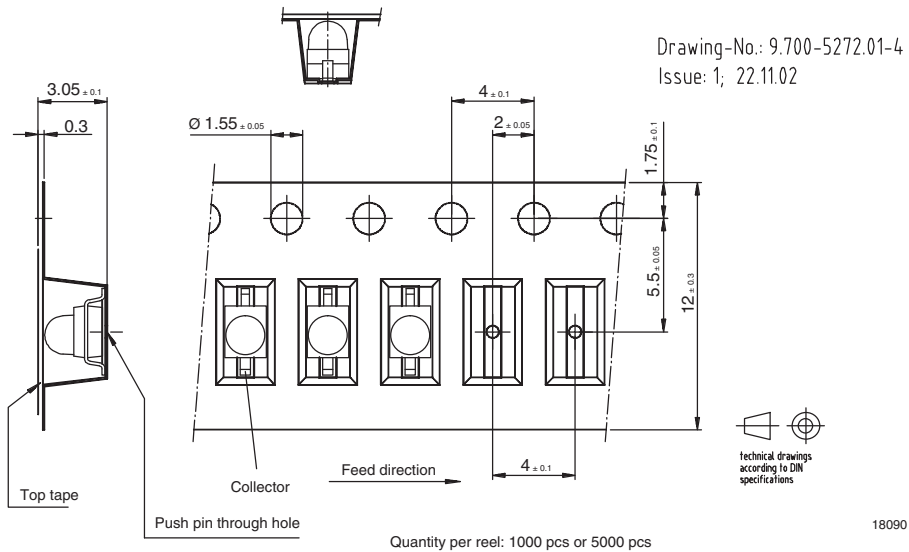


Fig. 22 - Blister Tape of TEMT1020 and TEMT1520

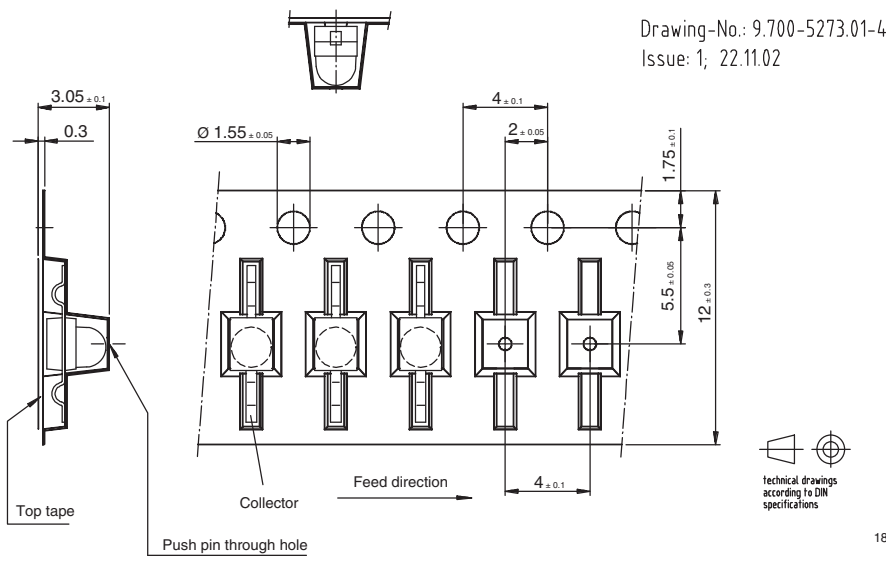


Fig. 23 - Blister Tape of TEMT1030

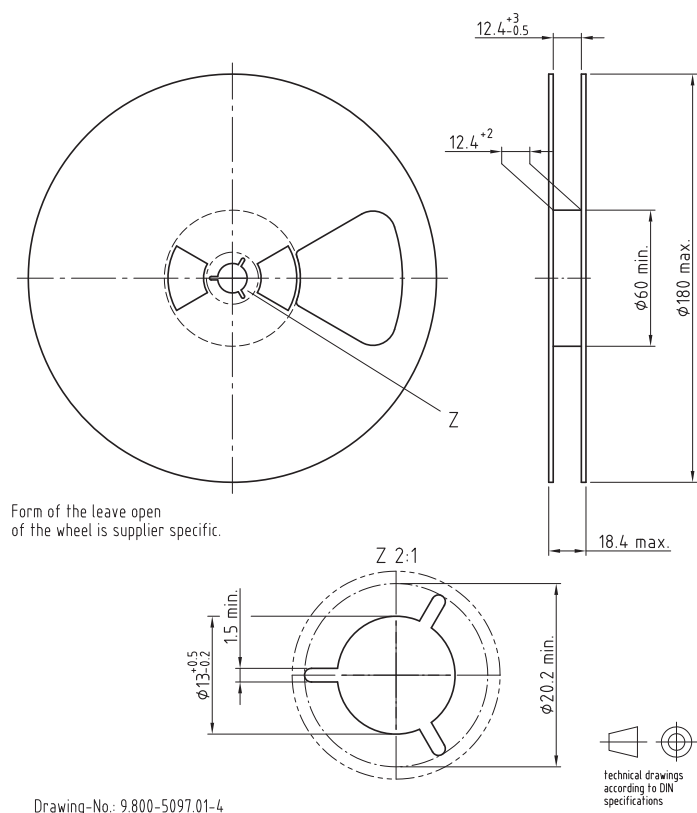
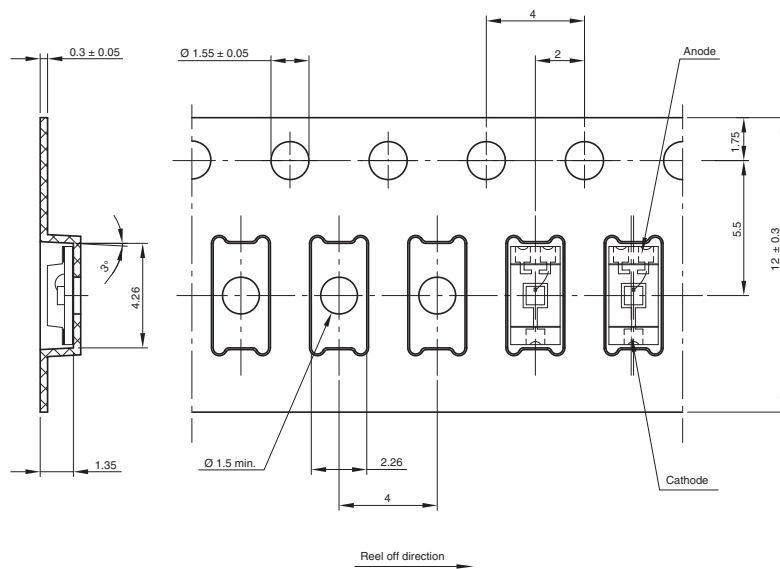


Fig. 24 - Reel of TEMx6000, VEML60x0FX01 Series
Quantity per Reel: 3000 pcs

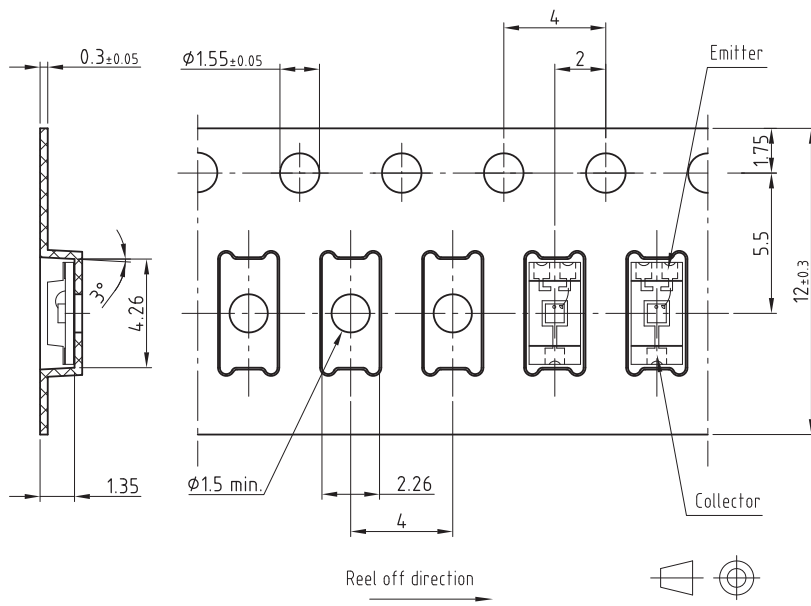


Drawing-No.: 9.700-5329.02-4
Issue: 2; 31.08.09
20877

Not indicated tolerances ± 0.1

technical drawings
according to DIN
specifications

Fig. 25 - Blister Tape of TEMD6010FX01



Drawing-No.: 9.700-5329.01-4
Issue: 1; 05.05.08
20876

Not indicated tolerances ± 0.1

technical drawings
according to DIN
specifications

Fig. 26 - Blister Tape of TEMT6000X01

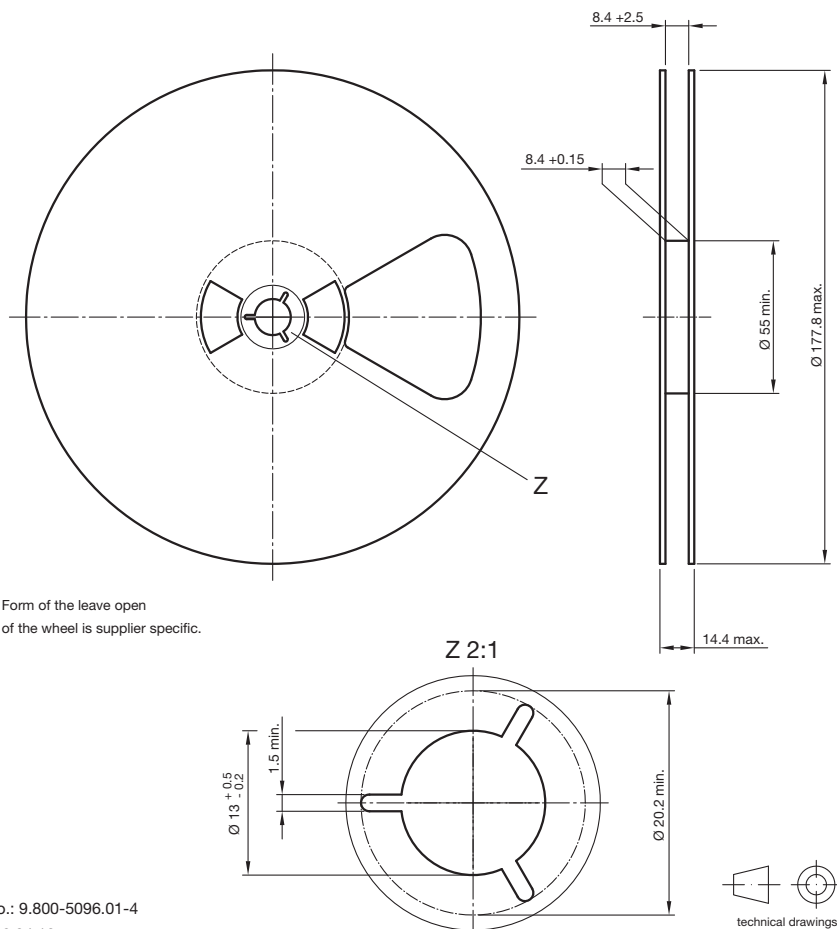
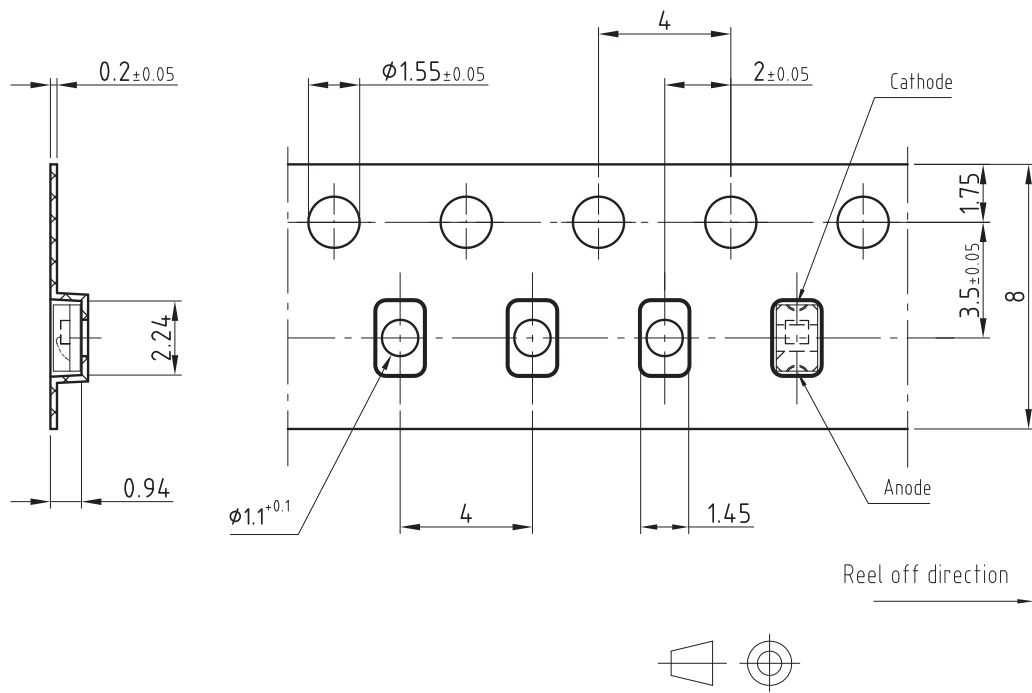


Fig. 27 - Reel of TEMx6200X01, TEMx7x00X01, VSMB1940X01, VSMY1850X01 Series
Quantity per reel: 3000 pcs



Drawing-No.: 9.700-5311.01-4

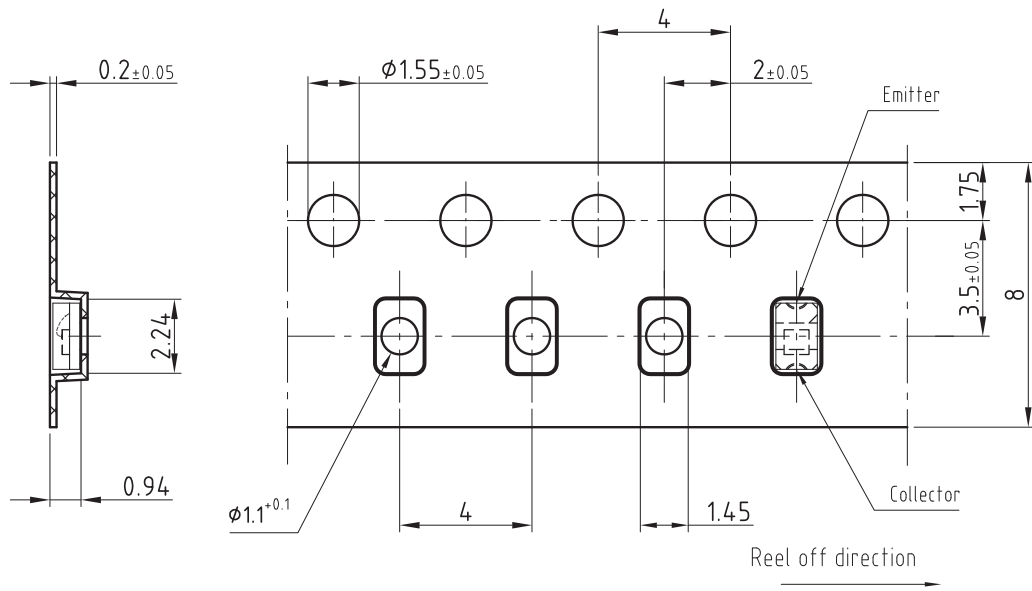
Issue: 1; 23.02.07

21501

technical drawings
according to DIN
specifications

Not indicated tolerances ±0.1

Fig. 28 - Blister Tape of TEMD7x00X01, VSMB1940X01



Drawing-No.: 9.700-5310.01-4

Issue: 2; 14.08.07

20690

Not indicated tolerances ±0.1

Quantity per reel: 3000 pcs

technical drawings
according to DIN
specifications

Fig. 29 - Blister Tape of TEMT7x00X01, TEMT6200FX01

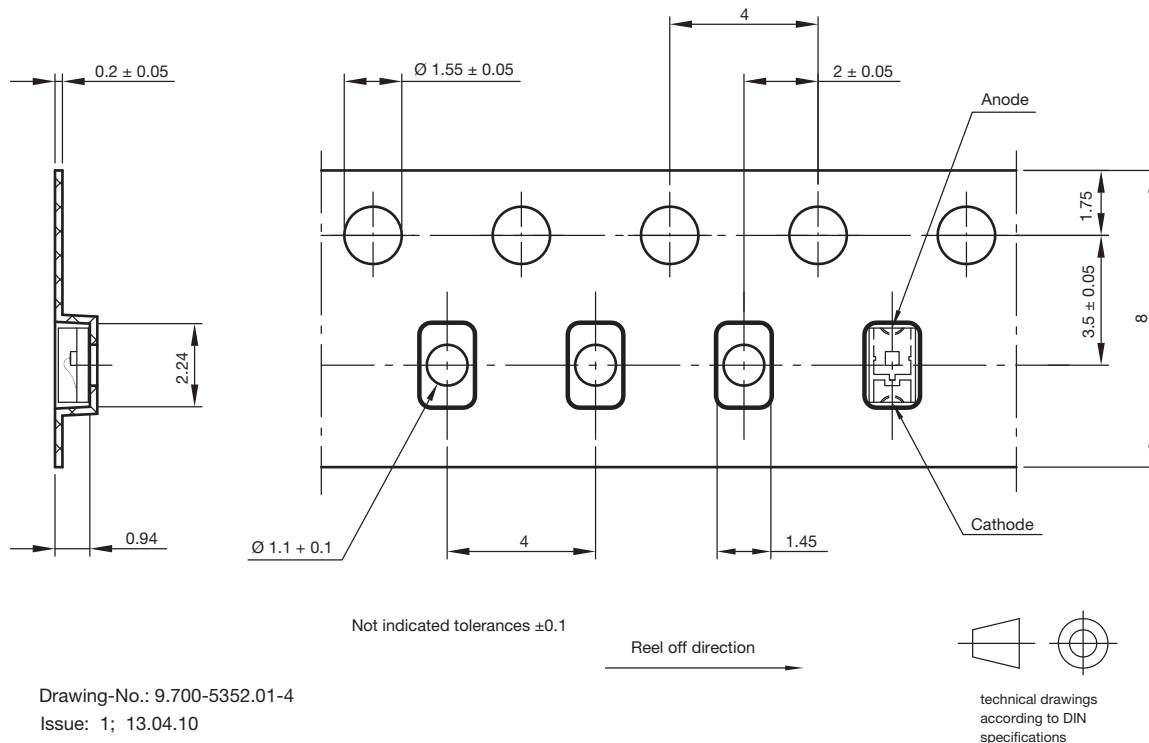


Fig. 30 - Blister Tape of VS MY1850, VS MY1850X01

TAPING OF T-1 (3 mm) AND T-1 $\frac{1}{4}$ (5 mm) DEVICES

The taping specification is based on IEC publication 286, taking into account industrial requirements for automatic insertion.

Absolute maximum ratings, mechanical dimensions, optical and electrical characteristics for taped devices are identical to basic catalog types and can be found in specifications for untaped devices.

Note that the lead wires of taped components may be shorted or bent in accordance to the IEC standard.

PACKAGING

The tapes of components are available on reels or in Ammopack. Each reel and each box is marked with label containing the following information:

- Vishay
- Type
- Group
- Tape code (see figure 24)
- Production code
- Quantity

CODE FOR TAPED DEVICES

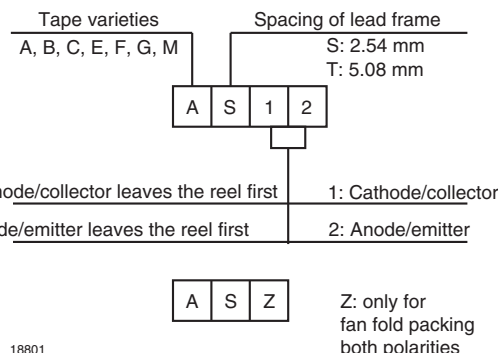


Fig. 31 - Taping Code

Number of Packed Components

T-1 (3 mm): 2000 pcs

T-1 $\frac{1}{4}$ (5 mm): 1000 pcs

MISSING COMPONENTS

Up to 3 consecutive components may be missing but the gap is followed by at least 6 components. A maximum of 0.5 % of components per reel quantity may be missing. At least 5 empty positions are present at the start and the end of the tape to enable tape insertion.

Tensile strength of the tape: $\geq 15\text{ N}$

Pulling force in plane of the tape, at right angles to reel: $\geq 5\text{ N}$

Note

- Shipment in fan-fold packages is standard for radial taped devices.
- Shipment in reel packing is only possible if the customer guarantees removal of empty reels.
- According to what is stated in a German packaging decree (Verpackungsverordnung) we are not able to accept return of reels.

ORDERING CODE

Type designations are extended by a code for the taping standard.

Example:

TSAL6200-AS12 (reel packing)

TSAL6200-ASZ (fan-fold packing)

BPW85-AS12 (reel packing)

TABLE 4 - TAPING SURVEY OF LEADED COMPONENTS

CODE FOR TAPING STANDARD	“H” - HEIGHT OF TAPING IN mm (TOLERANCES $\pm 0.5\text{ mm}$)			PREFERENCES	REMARKS
	3 mm	5 mm	SIDEVIEW'S		
AS12	17.3	17.3	16.0	Standard	Reel, cathode / collector leaves first
AS21					Reel, anode / emitter leaves first
ASZ					Ammopack
KS12	19.3	19.3	-	-	Reel, cathode / collector leaves first
KS21					Reel, anode / emitter leaves first
KSZ					Ammopack
CS12	22.0	22.0	-	-	Reel, cathode / collector leaves first
CS21					Reel, anode / emitter leaves first
CSZ					Ammopack
ES12	-	24.0	24.0	Standard	Reel, cathode / collector leaves first
ES21					Reel, anode / emitter leaves first
ESZ					Ammopack
EGZ	-	-	24.0		Ammopack 2 mm pin distance lead to lead
MS12	25.5	25.5	-		Reel, cathode / collector leaves first
MS21					Reel, anode / emitter leaves first
MSZ					Ammopack
GSZ	-	-	29.0		Ammopack 2 mm pin distance lead to lead
FSZ	-	-	27.0	Standard	Ammopack
FGZ	-	-	27.0		Ammopack 2 mm pin distance lead to lead

REEL DIMENSIONS in millimeters

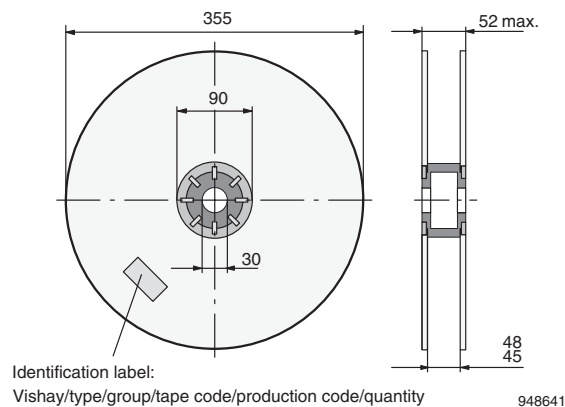


Fig. 32 - Dimensions of the Reel

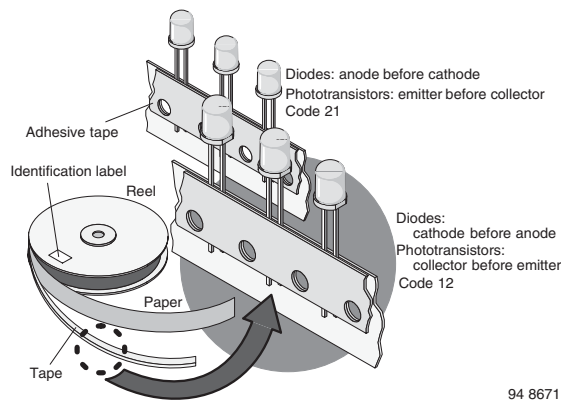


Fig. 33 - Components on Tape and Reel

AMMOPACK

The tape is folded in a concertina arrangement and laid in a cardboard box.

If components are required to have the cathode or collector leave the box first (figure 27), then open the box at the side marked with the “-” symbol. If anode or emitter should leave the box first, then open at the side marked with the “+” symbol.

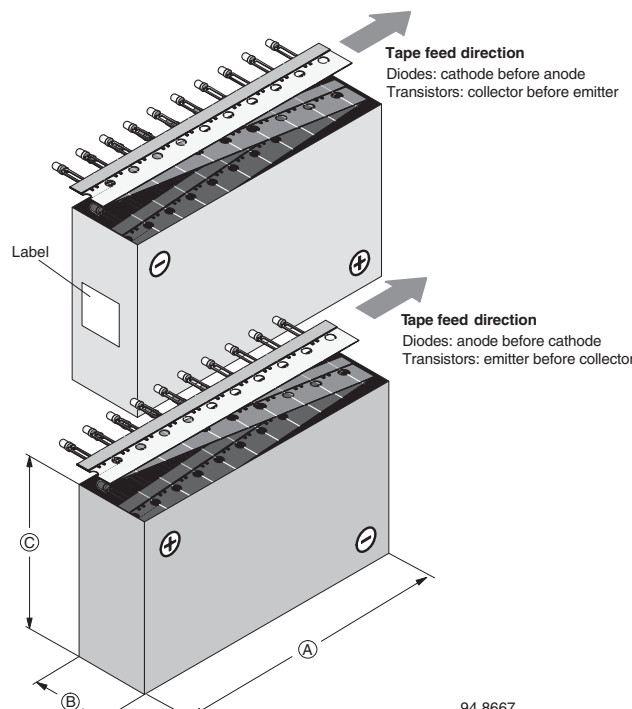


Fig. 34 - Tape Feed Direction

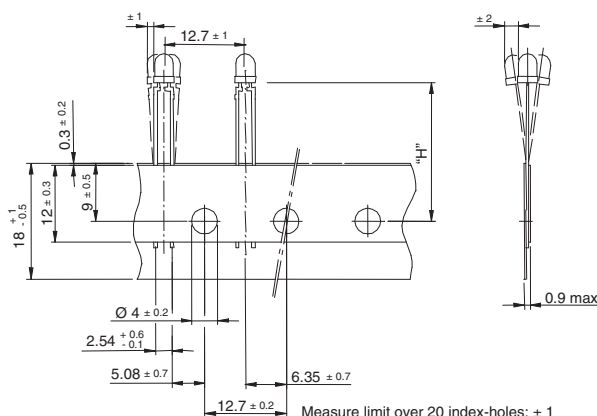
TABLE 5 - INNER DIMENSIONS OF AMMOPACK

A mm	B mm	C mm	COMPONENTS
340	46	125	T-1½ (5 mm)
340	34	140	T-1 (3 mm) AS-taping
340	41	140	T-1 (3 mm) other than AS-taping
348	43	125	FSZ side view lens
348	46	125	GSZ side view lens

TAPING OF T-1 (3 mm) PACKAGES

Polarity options: Z, 12, 21

TABLE 6 - POSITION OF T-1 (3 mm) COMPONENTS IN TAPE		
OPTION	H	PREFERENCE
AS	17.3 ± 0.5 mm	recommended
MS	25.5 ± 0.5 mm	recommended
CS	22.0 ± 0.5 mm	



Quantity per:	Reel (Mat. - No. 1764)
	2000

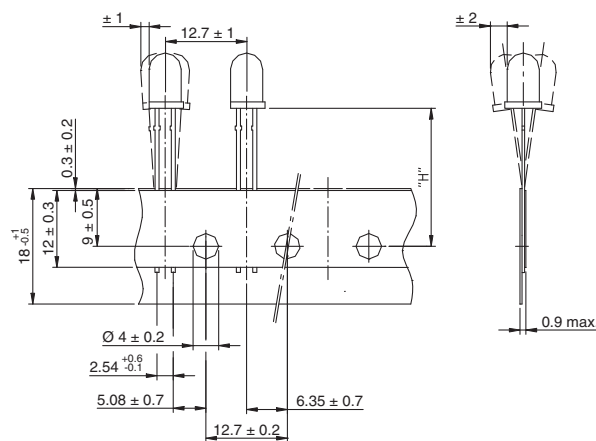
94 8171

Fig. 35 - Taping of T-1 (3 mm) Devices

TAPING OF T-1¾ (5 mm) PACKAGES

Polarity options: Z, 12, 21

TABLE 7 - POSITION OF T-1¾ (5 mm) COMPONENTS IN TAPE		
OPTION	H	PREFERENCE
AS	17.3 ± 0.5 mm	recommended
KS	19.3 ± 0.5 mm	
MS	25.5 ± 0.5 mm	recommended
CS	22.0 ± 0.5 mm	
ES	24.0 ± 0.5 mm	



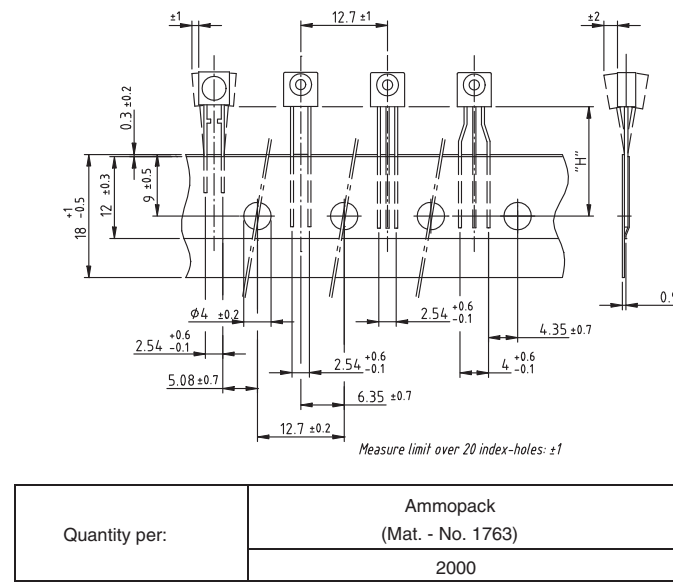
Quantity per:	Reel (Mat.-no. 1764)
	1000

94 8172

Fig. 36 - Taping of T-1¾ (5 mm) Devices

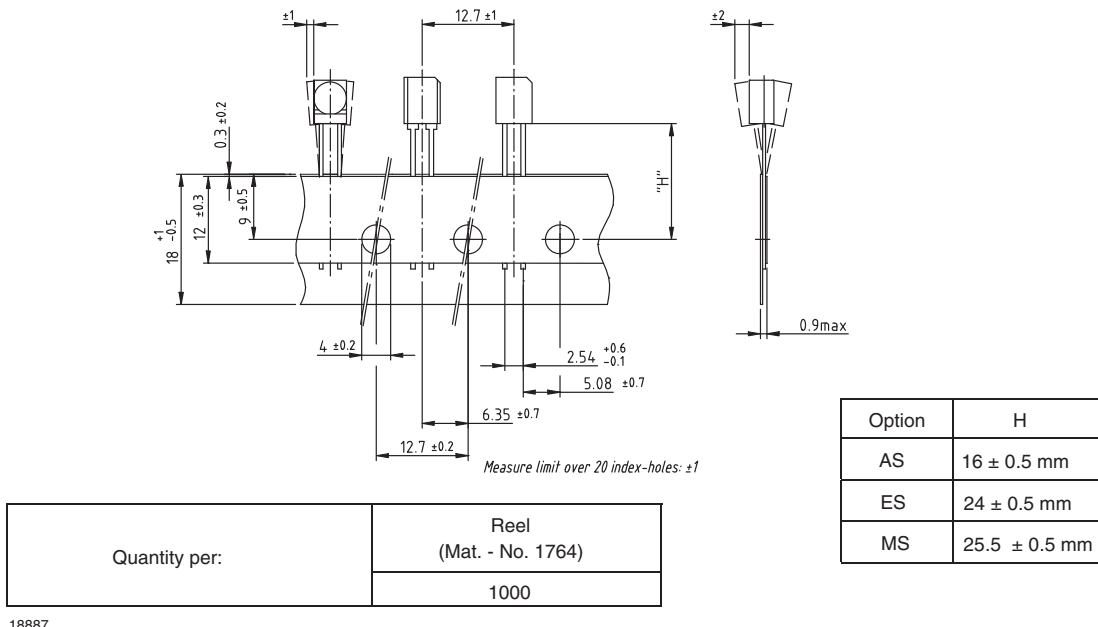
Bend leads:
Lead standard xG
Straight leads:
Lead standard xS

Option	H
AS	16 ± 0.5 mm
ES	24 ± 0.5 mm
FS	27 ± 0.5 mm
GS	29 ± 0.5 mm
EG	24 ± 0.5 mm
FG	27 ± 0.5 mm



18886

Fig. 37 - Taping of Side View Lens Packages



18887

Fig. 38 - Taping of Side View PIN Photodiodes

TUBE PACKAGING OF TOP VIEW PIN PHOTODIODES BP104S AND BPW34S

Dimensions in millimeters

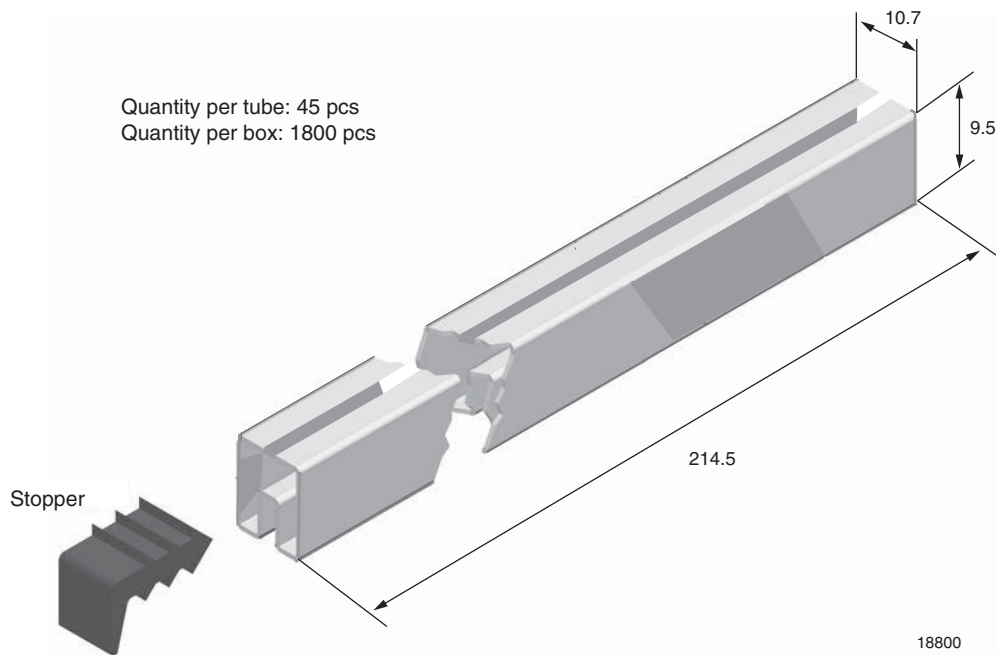


Fig. 39 - Drawing Proportions Not Scaled

Infrared Emitters, Photo Detectors, and Optical Sensors



Infrared Emitters

PIN Photodiodes

Phototransistors

Reflective Sensors – Analog

Transmissive Sensors – Analog

Ambient Light Sensors

Fully Integrated Proximity and Ambient Light Sensors

RESOURCES

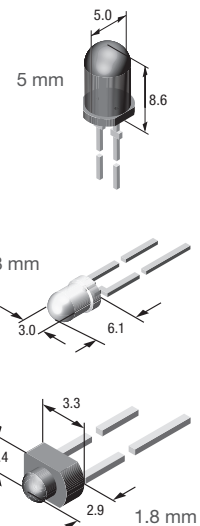
- Optical sensors product portfolio: www.vishay.com/optical-sensors/
- Infrared emitters product portfolio: www.vishay.com/ir-emitting-diodes/
- Photo detectors product portfolio: www.vishay.com/photo-detectors/
- Optoelectronics complete product portfolio: www.vishay.com/optoelectronics/
- Technical support:
 - emittertechsupport@vishay.com
 - sensorstechsupport@vishay.com
 - detectortechsupport@vishay.com
- Sales contacts: www.vishay.com/doc?99914

The DNA of tech.™

Infrared Emitters

Vishay offers emitters in more wavelengths than any other supplier: 830 nm, 850 nm, 870 nm, 890 nm, 940 nm, and 950 nm. Providing fast rise and fall response times, Vishay also has the broadest selection of double hetero infrared emitters. They are the highest power infrared emitters with the lowest forward voltages on the market, making them ideal for high current applications. The latest surface emitter technology based devices, which provide the highest radiant intensities, round out our extensive IR emitter portfolio.

Package	Part Number	Peak Wavelength (nm)	Angle of Half Intensity (\pm °)	Radiant Intensity, I_e (mW/sr) ⁽¹⁾	Rise and Fall Time, t_r / t_f (ns)	Remark
Through-Hole Packages						
5 mm	TSAL6100	940	10	170	15	No stand-off
	TSAL6200	940	17	72	15	No stand-off
	TSAL6400	940	25	50	15	No stand-off
	TSHF5210	890	10	180	30	Stand-off
	TSHF5410	890	22	70	30	Stand-off
	TSHF6210	890	10	180	30	No stand-off
	TSHF6410	890	22	70	30	No stand-off
	TSHG5210	850	10	230	20	Stand-off
	TSHG5410	850	18	90	20	Stand-off
	TSHG6200	850	10	180	20	No stand-off
	TSHG6210	850	10	230	20	No stand-off
	TSHG6400	850	22	70	20	No stand-off
	TSHG6410	850	18	90	20	No stand-off
	VSLY5850	850	3	600	10	Stand-off
	VSLY5940	940	3	600	10	Stand-off
3 mm	TSAL4400	940	25	30	800	No stand-off
	TSHA4400	875	20	20	600	No stand-off
	VSLB3940	940	22	65	15	No stand-off
	VSLB3948	940	22	65	15	No stand-off
	VSLB4940	22	940	65	15	
	VSLY3850	18	850	70	10	
	VSLY3943	17	940	70	5	$I_F = 70 \text{ mA}$
1.8 mm	CQY36N	950	55	1.50	800	No stand-off
	CQY37N	950	12	5	800	No stand-off



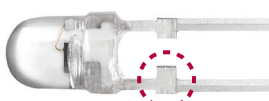
The DNA of tech.™

Infrared Emitters (continued)

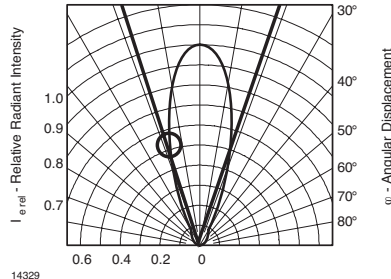
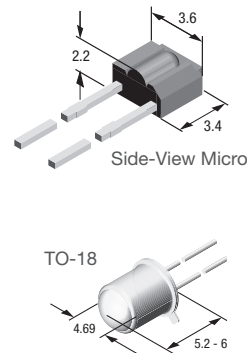
Package	Part Number	Peak Wavelength (nm)	Angle of Half Intensity (\pm °)	Radiant Intensity, I_e (mW/sr) ⁽¹⁾	Rise and Fall Time, t_r / t_f (ns)	Remark
Through-Hole Packages						
Side-View Micro	TSSS2600	950	25 H, 65 V	2.6	800	No stand-off
TO-18	TSTA7100	875	5	50	600	No stand-off
	TSTA7300	875	12	20	600	No stand-off
	TSTA7500	875	30	6	600	No stand-off
	TSTS7100	950	5	18	800	No stand-off
	TSTS7300	950	12	6	800	No stand-off
	TSTS7500	950	30	1.6	800	No stand-off

Note
⁽¹⁾ $I_F = 100$ mA

Stand-Off



To control the height of the emitter when inserted into the PCB for soldering, some leaded emitters and photo detectors feature a stand-off option (shown at left). The stand-off is the tab on the leads. It is sometimes called a stopper.



14329

Angle of Half Intensity, $\Phi_{0.5}$ or θ

In a radiation diagram, the angle of half intensity is the angle within which the radiant intensity is greater than or equal to half of the maximum intensity. In Vishay datasheets, the symbol $\Phi_{0.5}$ is most commonly used for the angle of half intensity. For visible LEDs this is sometimes called the viewing angle. There is still light, be it infrared or visible, outside of this angle.

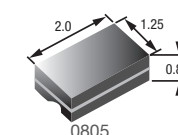
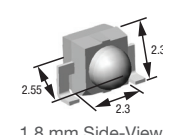
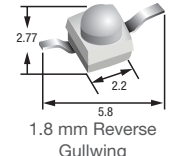
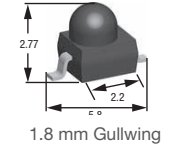
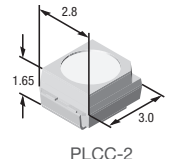
The DNA of tech.™

Infrared Emitters (continued)

Package	Part Number ⁽²⁾	Peak Wavelength (nm)	Angle of Half Intensity (\pm °)	Radiant Intensity, I_e (mW/sr) ⁽¹⁾	Rise and Fall Time, t_r / t_f (ns)	Remark
Surface-Mount Packages						
PLCC-2	VSMB3940X01	940	60	13	15	
	VSMY3940X01	940	60	15	10	
	VSML3710	940	60	6	800	
	VSMY3850	850	60	17	10	
	VSMY385010	850	60	9	10	$I_F = 70$ mA
	VSMY385010X01	60	850	12	7	$I_F = 70$ mA
	VSMY3850X01	60	850	17	10	
	VSMY3890X01	60	890	18	10	
1.8 mm	VSMY2850RG, -G	850	10	100	10	
	VSMY2853RG, -G	850	28	35	10	
	VSMF2890RGX01, -GX01	890	12	40	30	
	VSMY2940RG, -G	940	10	120	10	
	VSMB2000X01, -2020X01	940	12	40	15	
	VSMB2943RGX01, -GX01	940	25	20	15	
	VSMB2948RG, -G	940	25	20	15	
	VSMY2943RG, -G	940	28	35	10	
	VSMY294310RG, -G	940	25	25	10	$I_F = 70$ mA
	VSMY2853SL	850	28	35	10	
1.8 mm Side-View	VSMB2943SLX01	940	25	20	15	Max. pulse current: 1 A
	VSMB2948SL	940	25	20	15	Max. pulse current: 500 mA
	VSMY294310SL	940	25	32	10	$I_F = 70$ mA
	VSMY2943SL	940	28	35	10	
	VSMY1940X01	940	60	10	10	
0805	VSMB1940X01	940	60	6	15	
	VSMY1850	850	60	12	10	
	VSMY1850X01	60	850	10	10	
	VSMY1850ITX01	60	850	10	10	110 °C operating temperature
	VSMY1940ITX01	60	940	10	10	110 °C operating temperature
	VSMY1943X01	60	940	6	5	$I_F = 50$ mA
	VSMY4850X01	60	850	8	7	Black package
	VSMY5850	60	850	13	7	
	VSMY5850X01	60	850	13	7	
	VSMY5890	60	890	13	7	
	VSMY5890X01	60	890	13	7	
	VSMY5940	60	940	13	7	
	VSMY5940X01	60	940	13	7	

Notes

⁽¹⁾ $I_F = 100$ mA unless otherwise stated

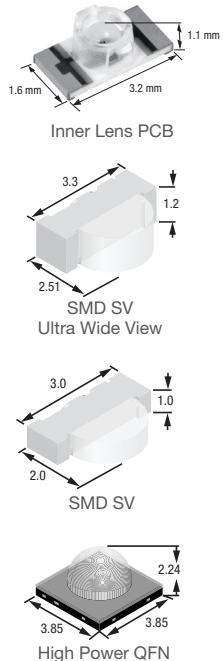
⁽²⁾ Products ending in "X01" are AEC-Q101 qualified


The DNA of tech.TM

Inner Lens PCB

Package	Part Number ⁽²⁾	Peak Wavelength (nm)	Angle of Half Intensity (\pm °)	Radiant Intensity, I_e (mW/sr) ⁽¹⁾	Rise and Fall Time, t_r / t_f (ns)	Remark
Surface-Mount Packages						
Inner Lens PCB	VSMY12850	850	40	16	10	$I_F = 70$ mA
	VSMY12940	940	40	16	10	$I_F = 70$ mA
SMD SV Ultra Wide View	VSMB10940	940	75	1	15	$I_F = 20$ mA
	VSMB10941X01	940	75	1	15	$I_F = 20$ mA
SMD SV	VSMB14940	940	9	35	15	$I_F = 70$ mA
	VSMY14940	940	9	35	15	$I_F = 70$ mA
High Power QFN	VSMY98545	850	45	350	15	$I_F = 1.0$ A

Notes

⁽¹⁾ $I_F = 100$ mA unless otherwise stated⁽²⁾ Products ending in "X01" are AEC-Q101 qualified

The DNA of tech.™

PIN Photodiodes

Vishay has the broadest portfolio of PIN photodiodes on the market. With lower capacitance, they provide high speed response, low noise, and low dark current, along with excellent sensitivity. They are ideal for high speed data transfer, light barriers, alarm systems, and linear light measurement.

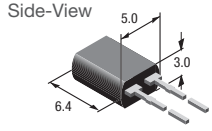
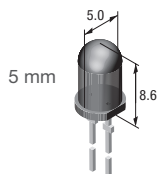
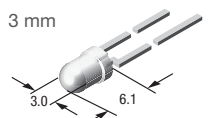
Package	Part Number	Peak Wavelength (nm)	Bandwidth $\lambda_{0.5}$ (nm)	Sensitivity I_{ra} (μA) ⁽¹⁾	Angle of Half Sensitivity (\pm °)	Photo Area (mm)	Rise / Fall Time, t_r / t_f (ns) ⁽²⁾	Remark
Through-Hole Packages								
3 mm	TEFD4300	950	350 to 1120	17	20	0.23	100	
	TEFD4300F	950	770 to 1070	17	20	0.23	100	
5 mm	BPV10	920	380 to 1140 ⁽⁷⁾	70	20	0.78	2.5 ⁽³⁾	Stand-off
	BPV10NF	940	790 to 1050	60	20	0.78	2.5 ⁽³⁾	Stand-off
Side-View	BPW41N	950	870 to 1050	45	65	7.5	100	5 x 4 x 6.8
	BPW46 (L)	900	430 to 1100 ⁽⁷⁾	50	65	7.5	100	5 x 3 x 6.4
	BPW82	950	790 to 1050	45	65	7.5	100	5 x 4 x 6.8
	BPW83	950	790 to 1050	45	65	7.5	100	5 x 3 x 6.4
Side-View, High Performance	BPV22F	950	870 to 1050	80	60	7.5	100	
	BPV22NF	940	790 to 1050	85	60	7.5	100	
	BPV23F	950	870 to 1050	63	60	4.4	70	
	BPV23NF	940	790 to 1050	65	60	4.4	70	
TO-5	BPW20RF	920	400 to 1100 ⁽⁷⁾	42	50	7.5	3600 ⁽⁶⁾	
TO-18	BPW24R	900	430 to 1100 ⁽⁷⁾	60	12	0.78	7 ⁽⁴⁾⁽⁵⁾	
Top-View, Leaded	BP104	950	870 to 1050	45	65	7.5	100	
	BPW34	900	430 to 1100 ⁽⁷⁾	55	65	7.5	100	

Notes

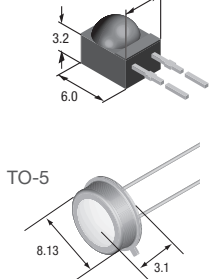
⁽¹⁾ $I_F = 100 \text{ mA}$ unless otherwise stated

⁽²⁾ Products ending in "X01" are AEC-Q101 qualified

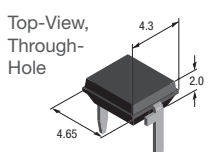
⁽¹⁾ Sensitivity: $V_R = 5 \text{ V}$, $E_e = 1 \text{ mW/cm}^2$, $\lambda = 950 \text{ nm}$;

⁽²⁾ Speed: $R_L = 1 \text{ k}\Omega$, $\lambda = 820 \text{ nm}$, $V_R = 10 \text{ V}$
⁽³⁾ $V_R = 50 \text{ V}$, $R_L = 50 \Omega$, $\lambda = 820 \text{ nm}$
⁽⁴⁾ $R_L = 50 \Omega$
⁽⁵⁾ $V_R = 20 \text{ V}$
⁽⁶⁾ $V_R = 0 \text{ V}$
⁽⁷⁾ Bandwidth $\lambda_{0.1}$ (nm)


Side-View, High Performance

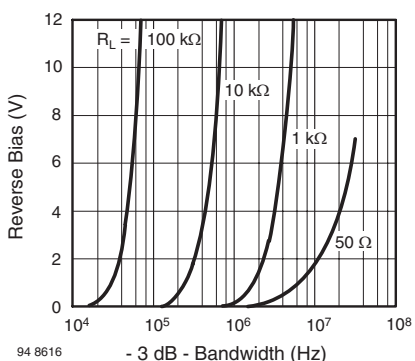


TO-5



Rise and Fall Time

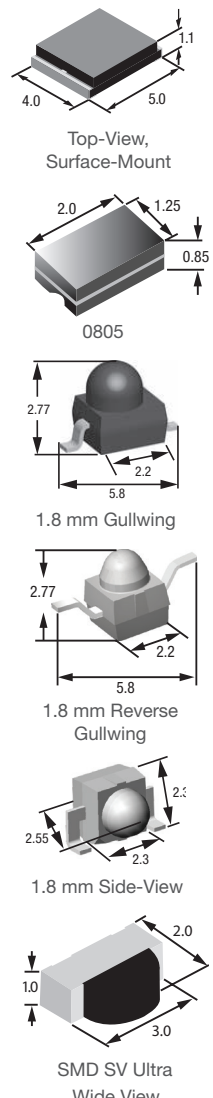
Switching times for photo detectors are strongly dependent on the measurement conditions. Shown in the diagrams are two major conditions: the reverse bias and the value of the load resistor used in the circuit. The switching time of a photodiode varies by two orders of magnitude when the load resistor value changes from 50Ω to $10 \text{ k}\Omega$. The lower the value of the load resistor, the faster the diode becomes. Also, the higher the reverse bias, the faster the switching times.



The DNA of tech.TM

PIN Photodiodes (continued)

Package	Part Number ⁽⁵⁾	Peak Wavelength (nm)	Bandwidth $\lambda_{0.5}$ (nm)	Sensitivity I_{ra} (μ A) ⁽¹⁾	Angle of Half Sensitivity (\pm °)	Photo Area (mm)	Rise / Fall Time, t_r / t_f (ns) ⁽²⁾	Remark
Surface-Mount Packages								
4-Quadrant Photodiode	K857PE	840	730 to 980	5.7	60	4 x 1.6	30	AEC-Q101
Top-View	TEMD5080X01	940	350 to 1100 ⁽⁴⁾	60	65	7.5	40 ⁽⁴⁾	AEC-Q101
	TEMD5020X01	940	430 to 1100 ⁽⁴⁾	35	65	4.4	100	AEC-Q101
	TEMD5120X01	940	790 to 1050	35	65	4.4	100	AEC-Q101
	TEMD5010X01	940	430 to 1100 ⁽⁴⁾	55	65	7.5	100	AEC-Q101
	TEMD5110X01	940	790 to 1050	55	65	7.5	100	AEC-Q101
	VBP104S	940	430 to 1100 ⁽⁴⁾	35	65	4.4	100	Gullwing
	VBP104SR	940	430 to 1100 ⁽⁴⁾	35	65	4.4	100	Reverse gullwing
	VBP104FAS	950	780 to 1050	35	65	4.4	100	Gullwing
	VBP104FASR	950	780 to 1050	35	65	4.4	100	Reverse gullwing
	VBPW34S	940	430 to 1100 ⁽⁴⁾	55	65	7.5	100	Gullwing
	VBPW34SR	940	430 to 1100 ⁽⁴⁾	55	65	7.5	100	Reverse gullwing
	VBPW34FAS	950	780 to 1050	55	65	7.5	100	Gullwing
	VBPW34FASR	950	780 to 1050	55	65	7.5	100	Reverse gullwing
1206	VEMD6010X01	900	430 to 1100	9.5	60	0.85	100	
	VEMD6110X01	950	750 to 1050	9.5	60	0.85	100	
QFN	VEMD5010X01	940	430 to 1100	48	65	7.5	100	
	VEMD5110X01	940	790 to 1050	48	65	7.5	100	
0805	TEMD7000X01	900	350 to 1120 ⁽⁴⁾	3	60	0.23	100	
	TEMD7100X01	950	750 to 1050	3	60	0.23	100	
	VEMD4010X01	910	550 to 1040	2.4	55	0.42	100	AEC-Q101
	VEMD4110X01	910	740 to 1040	2.4	55	0.42	100	AEC-Q101
1.8 mm	VEMD2000X01	940	750 to 1050	12	15	0.23	100	Reverse gullwing
	VEMD2020X01	940	750 to 1050	12	15	0.23	100	Gullwing
	VEMD2500X01	900	350 to 1120 ⁽⁴⁾	12	15	0.23	100	Reverse gullwing
	VEMD2520X01	900	350 to 1120 ⁽⁴⁾	12	15	0.23	100	Gullwing
	VEMD2503X01	900	350 to 1120 ⁽⁴⁾	10	30	0.23	100	Reverse gullwing
	VEMD2523X01	900	350 to 1120 ⁽⁴⁾	10	30	0.23	100	Gullwing
	VEMD2003X01	940	750 to 1050	10	30	0.23	100	Reverse gullwing
	VEMD2023X01	900	750 to 1050	10	30	0.23	100	Gullwing
1.8 mm Side-View	VEMD2523SLX01	900	350 to 1120 ⁽⁴⁾	10	30	0.23	100	
	VEMD2023SLX01	940	750 to 1050	10	30	0.23	100	
SMD SV Ultra Wide View	VEMD10940F	920	780 to 1050	3	75	0.23	100	Side-view
	VEMD11940FX01	950	780 to 1050	1.13	75	0.053	1000	Side-view


Notes
⁽¹⁾ Sensitivity: $V_R = 5$ V, $E_e = 1$ mW/cm², $\lambda = 950$ nm

⁽²⁾ Speed: $R_L = 1$ k Ω , $\lambda = 820$ nm, $V_R = 10$ V

⁽³⁾ $R_L = 50$ Ω
⁽⁴⁾ Bandwidth $\lambda_{0.1}$ (nm)

⁽⁵⁾ Products ending in "X01" are AEC-Q101 qualified

The DNA of tech.™

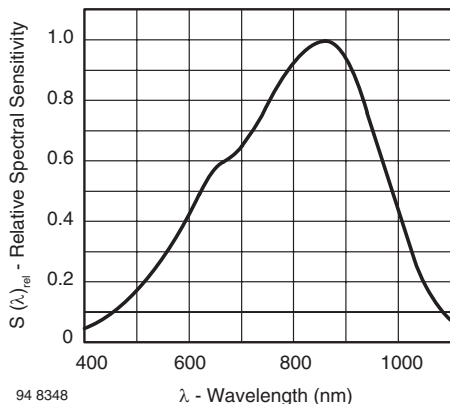
Phototransistors

Vishay provides the industry's widest selection of phototransistors. Offered in over 10 different packages, Vishay's phototransistors are exceptionally sensitive and simplify circuit design by eliminating the need for a separate amplifier.

Package	Part Number	Peak Wavelength (nm)	Bandwidth $\lambda_{0.5}$ (nm)	Collector Light Current, I_{ca} (mA) ⁽¹⁾	Angle of Half Sensitivity (\pm °)	Rise / Fall Time, t_r / t_f (ns) ⁽²⁾	Remark
Through-Hole Packages							
5 mm	BPV11	850	450 to 1080 ⁽³⁾	10	15	6	With base pin
	BPV11F	930	900 to 980	9	15	6	With base pin
	BPW96C	850	450 to 1080 ⁽³⁾	8	20	2	Stand-off
3 mm	BPW85C	850	450 to 1080 ⁽³⁾	5	25	2	Stand-off
	TEFT4300	925	875 to 1000	3.2	30	2	No stand-off
1.8 mm	BPW16N	825	450 to 1040 ⁽³⁾	0.14	40	4.8	
	BPW17N	825	450 to 1040 ⁽³⁾	1	12	4.8	
Side-View Micro	TEST2600	920	850 to 980	2.5	30 H, 60 V	6	
Side-View Lens	TEKT5400S	920	850 to 980	4	37	6	
TO-18	BPW76B	850	450 to 1080 ⁽³⁾	1.2	40	6	
	BPW77NB	850	450 to 1080 ⁽³⁾	20	10	6	

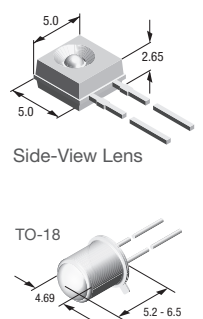
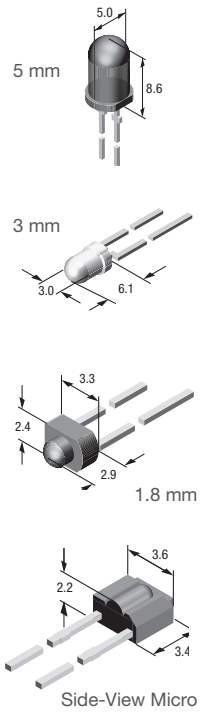
Notes

⁽¹⁾ Collector light current: $V_{CE} = 5$ V, $E_e = 1$ mW/cm², $\lambda = 950$ nm, typical

⁽²⁾ Speed: $V_S = 5$ V, $I_C = 5$ mA, $R_L = 100 \Omega$
⁽³⁾ Bandwidth $\lambda_{0.1}$ (nm)


Bandwidth: $\lambda_{0.5}$ and $\lambda_{0.1}$

The diagram to the left shows the relative spectral sensitivity of the BPV11 phototransistor. The peak sensitivity is found at 850 nm. The bandwidth of the detector can be defined by using a relative spectral sensitivity value of 0.5 or 0.1. Vishay datasheets will show one of these values. In the case of the BPV11, the bandwidth in the datasheet is 450 nm to 1080 nm, $\lambda_{0.1}$.



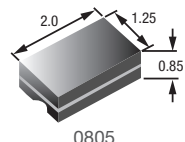
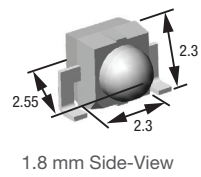
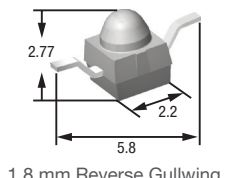
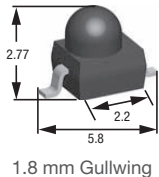
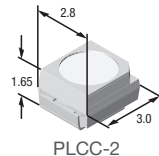
The DNA of tech.™

Phototransistors (continued)

Package	Part Number	Peak Wavelength (nm)	Bandwidth $\lambda_{0.5}$ (nm)	Collector Light Current, I_{ca} (mA) ⁽¹⁾	Angle of Half Sensitivity ($\pm ^\circ$)	Rise / Fall Time, t_r / t_f (ns) ⁽²⁾	Remark
Through-Hole Packages							
PLCC-2	VEMT3700	850	450 to 1080 ⁽³⁾	0.5	60	2	
	VEMT3700F	940	850 to 1050	0.5	60	2	
	VEMT4700	850	450 to 1080 ⁽³⁾	0.5	60	2	With base pin
1.8 mm	VEMT2000X01	860	790 to 970	6	15	2	Reverse gullwing
	VEMT2020X01	860	790 to 970	6	15	2	Gullwing
	VEMT2500X01	850	470 to 1090 ⁽³⁾	6	15	2	Reverse gullwing
	VEMT2520X01	850	470 to 1090 ⁽³⁾	6	15	2	Gullwing
	VEMT2503X01	860	470 to 1090 ⁽³⁾	4	30	10	Reverse gullwing
	VEMT2523X01	860	470 to 1090 ⁽³⁾	4	30	10	Gullwing
	VEMT2003X01	860	790 to 970	4	30	10	Reverse gullwing
	VEMT2023X01	860	790 to 970	4	30	10	Gullwing
1.8 mm Side-View	VEMT2523SLX01	850	470 to 1090 ⁽³⁾	4	30	10	
	VEMT2023SLX01	860	790 to 970	4	30	10	
0805	TEMT7000X01	850	470 to 1090 ⁽³⁾	0.45	60	2	
	TEMT7100X01	870	750 to 1010	0.45	60	2	

Notes
⁽¹⁾ Collector light current: $V_{CE} = 5$ V, $E_e = 1$ mW/cm², $\lambda = 950$ nm, typical

⁽²⁾ Speed: $V_s = 5$ V, $I_c = 5$ mA, $R_L = 100 \Omega$
⁽³⁾ Bandwidth $\lambda_{0.1}$ (nm)

⁽⁴⁾ Products ending in "X01" are AEC-Q101 qualified


Reflective Sensors, Analog Output

Part Number ⁽¹⁾⁽³⁾	Package		Peak Operating Range (mm) ⁽²⁾	Peak Operating Distance (mm)	Typical Output Current (mA)
	L x W (mm)	H (mm)			
TCND5000(3)	6.0 x 4.3	3.75	2 to 25	6.0	0.0015
TCRT1000, TCRT1010	7.0 x 4.0	2.5	0.2 to 4.0	1.0	0.5
TCRT5000(L)	10.2 x 5.8	7.0	0.2 to 15	2.5	1
CNY70	7.0 x 7.0	6.0	0 to 5.0	0	1

Notes
⁽¹⁾ All optical sensors have phototransistor output except where noted

⁽²⁾ Relative collector current > 20 %

⁽³⁾ TCND5000 has a PIN photodiode output


TCND5000

TCRT1000

TCRT1010

TCRT5000(L)

CNY70

The DNA of tech.™

Transmissive Sensors, Analog Output

Part Number ⁽¹⁾⁽³⁾	Package		Gap (mm)	Aperture (mm)	Typical Output Current (mA)	On / Off Time t_{on} / t_{off} (μs)	Max. Operating Temperature
	L x W (mm)	H (mm)					
TCPT1300X01	5.5 x 4.0	4.0	3.0	0.3	0.6	20 / 30	+105 °C
TCUT1300X01 ⁽²⁾	5.5 x 4.0	4.0	3.0	0.3	0.6	20 / 30	+105 °C
TCPT1350X01	5.5 x 4.0	4.0	3.0	0.3	1.6	9 / 16	+125 °C
TCUT1350X01 ⁽²⁾	5.5 x 4.0	4.0	3.0	0.3	1.6	9 / 16	+125 °C
TCPT1600X01	5.5 x 4.0	5.7	3.0	0.3	1.6	9 / 16	+105 °C
TCUT1600X01 ⁽²⁾	5.5 x 4.0	5.7	3.0	0.3	1.6	9 / 16	+105 °C
TCUT1630X01 ⁽⁴⁾	5.5 x 5.85	7.0	3.0	0.3	1.3	9 / 16	+105 °C
TCUT1800X01 ⁽⁵⁾	5.5 x 5.85	7.0	3.0	0.3	1.3	9 / 16	+105 °C
TCST1030	8.3 x 4.7	8.15	3.1	none	2.4	15 / 10	+85 °C
TCST1103	11.9 x 6.3	10.8	3.1	1.0	4.0	10 / 8	+85 °C
TCST1202	11.9 x 6.3	10.8	3.1	0.5	2.0	10 / 8	+85 °C
TCST1230	9.2 x 4.8	5.4	2.8	0.5	2.0	15 / 10	+85 °C
TCST1300	11.9 x 6.3	10.8	3.1	0.25	0.5	10 / 8	+85 °C
TCST2103	24.5 x 6.3	10.8	3.1	1.0	4.0	10 / 8	+85 °C
TCST2202	24.5 x 6.3	10.8	3.1	0.5	2.0	10 / 8	+85 °C
TCST2300	24.5 x 6.3	10.8	3.1	0.25	0.5	10 / 8	+85 °C
TCST5250	14.3 x 6.0	9.5	2.7	0.5	1.5	15 / 10	+85 °C

Notes
⁽¹⁾ All optical sensors have phototransistor output

⁽²⁾ Dual channel

⁽³⁾ Products ending in "X01" are AEC-Q101 qualified

⁽⁴⁾ Triple channel

⁽⁵⁾ Quad channel


The DNA of tech.™

Ambient Light Sensors

Ambient light sensors are used to detect light or brightness in a manner similar to the human eye. They are most commonly found in industrial lighting, consumer electronics, and automotive systems, where they allow settings to be adjusted automatically in response to changing ambient light conditions. By turning on, turning off, or adjusting features, ambient light sensors can conserve battery power or provide extra safety, while eliminating the need for manual adjustments.

Package	Part Number ⁽²⁾	Peak Wavelength (nm)	Bandwidth $\lambda_{0.5}$ (nm)	Angle of Half Sensitivity ($\pm ^\circ$)	Light Current Incandescent (μA) ⁽¹⁾	Remark
Photodiodes						
0805, SMD	TEMD6200FX01	540	430 to 610	60	0.04	Stand-off
1206, SMD	TEMD6010FX01	540	430 to 610	60	0.04	
Top-View SMD	TEMD5510FX01	540	430 to 610	65	1	
	VEMD5501FX01	540	420 to 620	65	0.7	
TO-5, Leaded	BPW21R	565	420 to 675	50	0.9	
Phototransistors						
0805, SMD	TEMT6200FX01	550	450 to 610	60	12	
1206, SMD	TEMT6000X01	570	430 to 800	60	50	
5 mm, flat top	TEPT5700	570	430 to 800	50	75	Leaded
5 mm	TEPT5600	570	430 to 800	20	350	Leaded
3 mm	TEPT4400	570	430 to 800	30	200	Leaded

Notes
⁽¹⁾ $E_V = 100 \text{ lux}, V_{CE} = 5 \text{ V}, \text{CIE illuminant A, typical}$
⁽²⁾ Products ending in "X01" are AEC-Q101 qualified

F	Part numbers with an F contain an infrared filtering epoxy to further improve the ambient light sensing performance	X01	Part numbers with an X01 are qualified to the AEC-Q101 standard and support operating temperatures from -40 °C to +100 °C
---	---------------------------------------------------------------------------------------------------------------------	-----	---------------------------------------------------------------------------------------------------------------------------


[TEMD5510FX01](#)
[TEMT6200FX01](#),
[TEMD6200FX01](#)
[TEMD6010FX01](#),
[TEMT6000X01](#)
[TEPT5600](#)
[TEPT4400](#)
[TEPT5700](#)
[BPW21R](#)

The DNA of tech.™

High Accuracy Digital Light Sensors

Based on patented Filtron™ technology implementation, digital light sensors introduced by Vishay provide red, green, blue, IR, and UVAB light sensing for precise color measurement. All digital light sensors have 16-bit resolution and feature miniature transparent OPLGA packages. These are fully integrated sensors – including a high sensitivity photodiode, a low noise amplifier, and a 16-bit A/D converter – with support for easy to use I²C bus communication.

Features and Benefits

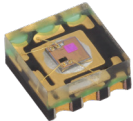
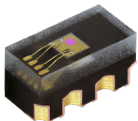
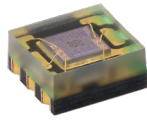
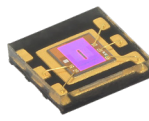
- On-chip coating provides best spectral sensitivity to cover visible and UV spectrum (Filtron™ technology)
- Shutdown mode with < 1 µA power consumption
- 16-bit range for ambient light detection, RGB, and UV
- ALS output tolerance < 10 %
- I²C interface

Applications

- Health monitoring
- AWB correction
- Control display brightness
- Home lightning control

Ambient Light Sensors

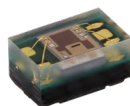
Part Number	Package Dimensions L x W x H (mm)	Ambient Light Resolution (lx)	Operating Voltage (V)	Operating Temperature Range (°C)	Output Code	AEC-Q101 Qualified
VEML3235	2 x 2 x 0.87	0.0021	2.6 to 3.6	-40 to +85	16 bit, I ² C	-
VEML3235SL	2.95 x 1.5 x 1.5	0.0021	2.6 to 3.6	-40 to +85	16 bit, I ² C	-
VEML6030	2 x 2 x 0.87	0.0036	2.5 to 3.6	-25 to +85	16 bit, I ² C	-
VEML6035	2.0 x 2.0 x 0.4	0.0004	1.7 to 3.6	-25 to +85	16 bit, I ² C	-
VEML7700	6.8 x 2.35 x 3.0	0.0036	2.5 to 3.6	-25 to +85	16 bit, I ² C	-


VEML3235

VEML3235SL

VEML6030

VEML6035

VEML7700

Color Sensors

Part Number	Package Dimensions L x W x H (mm)	Peak Sensitivity (nm)	Operating Voltage (V)	Operating Temperature Range (°C)	Output Code	AEC-Q101 Qualified
VEML3328	2.0 x 1.25 x 1.0	590, 610, 560, 470, 825 (C, R, G, B, IR)	2.6 to 3.6	-40 to +85	16 bit, I ² C	-
VEML3328SL	2.95 x 1.50 x 1.50	590, 610, 560, 470, 825 (C, R, G, B, IR)	2.6 to 3.6	-40 to +85	16 bit, I ² C	-
VEML6040	2.0 x 1.25 x 1.0	650, 550, 450 (R, G, B)	2.5 to 3.6	-40 to +85	16 bit, I ² C	-


VEML6040

VEML3328

VEML3328SL

The DNA of tech.™

Fully Integrated Proximity and Ambient Light Sensors

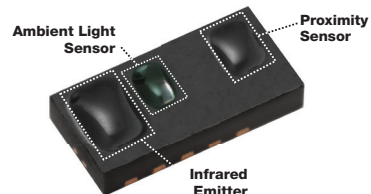
To simplify the design process, Vishay has integrated the infrared emitter, proximity photodiode, ambient light sensor, and signal processing IC in one package. Window design and sensor placement are no longer geometric puzzles and the need for mechanical crosstalk barriers is eliminated. Each sensor is a leadless surface-mount package with standard I²C communication and features an interrupt function. Interrupts reduce power consumption by eliminating polling traffic between the sensor and microcontroller.

Features and Benefits

- Low profile; height less than 0.83 mm
- 16-bit dynamic range
- Programmable emitter drive current
 - 10 mA to 200 mA (in 10 mA steps)
- Detection range up to 1.5 m
- Light sensing from 0.004 lx to 16 klx
- I²C interface

Applications

- Mobile devices (smart phones, tablets, gaming controllers)
- Consumer (white goods, cameras, game systems)
- Computing devices (notebooks, tablet PCs)
- Automotive and industrial devices (presence detection and displays)
- Health monitoring


VCNL4020X01

VCNL4200

VCNL4020

VCNL4010

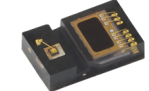
VCNL3020

VCNL36687S

VCNL4035X01

VCNL4030X01

**VCNL3030X01,
VCNL3036X01**

VCNL3040

VCNL36825T

VCNL36826S

Proximity Sensors

Part Number	Package Dimensions L x W x H (mm)	Integrated Components			Operating Temperature Range (°C)	AEC-Q101 Qualified
		Infrared Emitter	Proximity Detector	Ambient Light Sensor		
VCNL4020X01	4.90 x 2.40 x 0.83	x	x	x	-40 to +105	x
VCNL4035X01	4.0 x 2.36 x 0.75	-	x	x	-40 to +105	x
VCNL4030X01	4.0 x 2.36 x 0.75	x	x	x	-40 to +105	x
VCNL3020	4.90 x 2.40 x 0.83	x	x	-	-25 to +85	-
VCNL36687S	3.05 x 2 x 1.0	VCSEL	x	-	-40 to +85	-
VCNL4010	3.95 x 3.95 x 0.75	x	x	x	-25 to +85	-
VCNL4020	4.90 x 2.40 x 0.83	x	x	x	-25 to +85	-
VCNL4040	4.0 x 2.0 x 1.1	x	x	x	-25 to +85	-
VCNL4200	8.0 x 3.0 x 1.1	x	x	x	-40 to +85	-
VCNL3030X01	4.0 x 2.36 x 0.75	x	x	-	-40 to +105	x
VCNL3036X01	4.0 x 2.36 x 0.75	-	x	-	-40 to +105	x
VCNL3040	4.0 x 2.0 x 1.1	x	x	-	-40 to +85	-
VCNL36825T	2.0 x 1.25 x 0.5	VCSEL	x	-	-40 to +85	-
VCNL36826S	2.55 x 2.05 x 1.0	VCSEL	x	-	-40 to +85	-

Reliability and Statistics Glossary

DEFINITIONS

Accelerated Life Test: A life test under conditions that are more severe than usual operating conditions. It is helpful, but not necessary, that a relationship between test severity and the probability distribution of life be ascertainable.

Acceleration Factor: Notation: $f(t)$ = the time transformation from more severe test conditions to the usual conditions. The acceleration factor is $f(t)/t$. The differential acceleration factor is $df(t)/dt$.

Acceptance Number: The largest numbers of defects that can occur in an acceptance sampling plan and still have the lot accepted.

Acceptance Sampling Plant: An accept/reject test the purpose of which is to accept or reject a lot of items or material based on random samples from the lot.

Assessment: A critical appraisal including qualitative judgments about an item, such as importance of analysis results, design criticality, and failure effect.

Attribute (Inspection by): A term used to designate a method of measurement whereby units are examined by noting the presence (or absence) of some characteristic or attribute in each of the units in the group under consideration and by counting how many units do (or do not) possess it. Inspection by attributes can be two kinds: either the unit of product is classified simply as defective or not defective or the number of defects in the unit of product is counted with respect to a given requirement or set of requirements.

Attribute Testing: Testing to evaluate whether or not an item possesses a specified attribute.

Auger Electron Spectrometer: An instrument, that identifies elements on the surface of a sample. It excites the area of interest with an electron beam and observes the resultant emitted Auger electrons.

These electrons have the specific characteristics of the near surface elements. It is usually used to identify very thin films, often surface contaminants.

Availability (Operational Readiness): The probability that at any point in time the system is either operating satisfactorily or ready to be placed in operation on demand when used under stated conditions.

Average Outgoing Quality (AOQ): The average quality of outgoing product after 100 % inspection of a rejected lot, with replacement by good units of all defective units found in inspection.

Bathtub Curve: A plot of the failure rate of an item (whether repairable or not) vs. time. The failure rate initially decreases, then stays reasonably constant, then begins to rise rather rapidly. It has the shape of bathtub. Not all items have this behavior.

Bias:

1. The difference between the s-expected value of an estimator and the value of the true parameter
2. Applied voltage.

Burn-in: The initial operation of an item to stabilize its characteristics and to minimize infant mortality in the field.

Confidence Interval: The interval within which it is asserted that the parameters of a probability distribution lie.

Confidence Level:

Equals $1 - \alpha$

where

α = the risk (%).

Corrective Action: A documented design, process, procedure, or materials change to correct the true cause of a failure. Part replacement with a like item does not constitute appropriate corrective action. Rather, the action should make it impossible for that failure to happen again.

Cumulative Distribution Function (CDF): The probability that the random variable takes on any value less than or equal to a value x , e.g.

$$F(x) = CDF(x) = \Pr(x \leq X).$$

Defect: A deviation of an item from some ideal state. The ideal state usually is given in a formal specification.

Degradation: A gradual deterioration in performance as a function of time.

Derating: The intentional reduction of the stress/strength ratio in the application of an item, usually for the purpose of reducing the occurrence of stress-related failures.

Duty Cycle: A specified operating time of an item, followed by a specified time of no operation.

Early Failure Period: That period of life, after final assembly, in which failures occur at an initially high rate because of the presence of defective parts and workmanship. This definition applies to the first part of the bathtub curve for failure rate (infant mortality).

EDX Spectrometer: Generally used with a scanning electron microscope (SEM) to provide elemental analysis of X-rays generated on the region being hit by the primary electron beam.

Effectiveness: The capability of the system or device to perform its function.

EOS - Electrical Overstress: The electrical stressing of electronic components beyond specifications. May be caused by ESD.

ESD - Electrostatic Discharge: The transfer of electrostatic charge between bodies at different electrostatic potentials caused by direct contact or induced by an electrostatic field. Many electronic components are sensitive to ESD and will be degraded or fail.

Expected Value: A statistical term. If x is a random variable and $F(x)$ its CDF, the $E(x) = \int x dF(x)$, where the integration is over all x . For continuous variables with a pdf, this reduces to $E(x) = \int x pfd(x) dx$. For discrete random variables with a pfd, this reduces to

$$E(x) = \sum x_n p(x_n) \text{ where the sum is over all } n.$$

Exponential Distribution: A 1 parameter distribution ($\lambda > 0$, $t \leq 0$) with: $pfd(t) = \lambda e^{-\lambda t}$; $Cdf(t) = 1 - e^{-\lambda t}$; $Sf(t) = e^{-\lambda t}$; failure rate = λ ; mean time-to-failure = $1/\lambda$. This is the constant failure-rate-distribution.

Failure: The termination of the ability of an item to perform its required function.

Failure Analysis: The identification of the failure mode, the failure mechanism, and the cause (i.e., defective soldering, design weakness, contamination, assembly techniques, etc.). Often includes physical dissection.

Failure, Catastrophic: A sudden change in the operating characteristics of an item resulting in a complete loss of useful performance of the item.

Failure, Degradation: A failure that occurs as a result of a gradual or partial change in the operating characteristics of an item.

Failure, Initial: The first failure to occur in use.

Failure, Latent: A malfunction that occurs as a result of a previous exposure to a condition that did not result in an immediately detectable failure. Example: Latent ESD failure.

Failure Mechanism: The mechanical, chemical, or other process that results in a failure.

Failure Mode: The effect by which a failure is observed. Generally, describes the way the failure occurs and tells "how" with respect to operation.

Failure Rate: (A) The conditional probability density that the item will fail just after time t , given the item has not failed up to time t ; (B) The number of failures of an item per unit measure of life (cycles, time, miles, events, etc.) as applicable for the item.

Failure, Wearout: Any failure for which time of occurrence is governed by rapidly increasing failure rate.

FIT: Failure Unit; (also, Failures In Time) Failures per 109 h.

Functional Failure: A failure whereby a device does not perform its intended function when the inputs or controls are correct.

Gaussian Distribution: A 2 parameter distribution with:

$$pfd(x) = \frac{1}{\sigma\sqrt{2\pi}} \cdot e^{-\frac{(x-u)^2}{2\sigma^2}}$$

$Cdf(x) = \text{gauf}(x)$. $SF(x) = \text{gaufc}(x)$. "Mean value of x " u , "standard deviation of x " = σ

Hazard Rate: Instantaneous failure rate.

Hypothesis, Null: A hypothesis stating that there is no difference between some characteristics of the parent populations of several different samples, i.e., that the samples came from similar populations.

Infant Mortality: Premature catastrophic failures occurring at a much greater rate than during the period of useful life prior to the onset of substantial wear out.

Inspection: The examination and testing of supplies and services (including when appropriate, raw materials, components, and intermediate assemblies) to determine whether they conform to specified requirements.

Inspection by Attributes: Inspection whereby either the unit of product or characteristics thereof is classified simply as defective or not defective or the number of defects in the unit of product is counted with respect to a given requirement.

Life Test: A test, usually of several items, made for the purpose of estimating some characteristic(s) of the probability distribution of life.

Lot: A group of units from a particular device type submitted each time for inspection and/or testing is called the lot.

Lot Reject Rate (LRR): The lot reject rate is the percentage of lots rejected from the lots evaluated.

Lot Tolerance Percent Defective (LTPD): The percent defective, which is to be accepted a minimum or arbitrary fraction of the time, or that percent defective whose probability of rejection is designated by b .

Mean: (A) The arithmetic mean, the expected value; (B) As specifically modified and defined, e.g., harmonic mean (reciprocals), geometric mean (a product), logarithmic mean (logs).

Mean Life: $R(t)dt$; where $R(t)$ = the s-reliability of the item; t = the interval over which the mean life is desired, usually the useful life (longevity).

Mean-Life-Between-Failures: The concept is the same as mean life except that it is for repaired items and is the mean up-time of the item. The formula is the same as for mean life except that $R(t)$ is interpreted as the distribution of up-times.

Mean-time-between-failures (MTBF): For a particular interval, the total functioning life of a population of an item divided by the total number of failures within the population during the measurement interval. The definition holds for time, cycles, miles, events, or other measure of life units.

Mean-Time-To-Failure (MTTF): See "Mean Life".

Mean-Time-To-Repair (MTTR): The total corrective maintenance time divided by the total number of corrective maintenance actions during a given period of time.

MTTR: = $G(t)dt$; where $G(t)$ = CDF of repair time; T - maximum allowed repair time, i.e., item is treated as no repairable at this echelon and is discarded or sent to a higher echelon for repair.

Reliability and Statistics Glossary

Vishay Semiconductors

Reliability and Statistics
Glossary



Operating Characteristic (OC) Curve: A curve showing the relation between the probability of acceptance and either lot quality or process quality, whichever is applicable.

Part Per Million (PPM): PPM is arrived at by multiplying the percentage defective by 10 000.

Example: 0.1 % = 1.000 PPM.

Population: The totality of the set of items, units, measurements, etc., real or conceptual that is under consideration.

Probability Distribution: A mathematical function with specific properties, which describes the probability that a random variable will take on a value or set of values. If the random variable is continuous and well behaved enough, there will be a pdf. If the random variable is discrete, there will be a pmf.

Qualification: The entire process by which products are obtained from manufacturers or distributors, examined and tested, and then identified on a Qualified Product List.

Quality: A property, which refers to the tendency of an item to be made to specific specifications and / or the customer's express needs. See current publications by Juran, Deming, Crosby, et al.

Quality Assurance: A system of activities that provides assurance that the overall quality control job is, in fact, being done effectively. The system involves a continuing evaluation of the adequacy and effectiveness of the overall quality control program with a view to having corrective measures initiated where necessary. For a specific product or service, this involves verifications, audits, and the evaluation of the quality factors that affect the specification, production inspection, and use of the product or service.

Quality Characteristics: Those properties of an item or process, which can be measured, reviewed, or observed and which are identified in the drawings, specifications, or contractual requirements. Reliability becomes a quality characteristic when so defined.

Quality Control (QC): The overall system of activities that provides a quality of product or service, which meets the needs of users; also, the use of such a system.

Random Samples: As commonly used in acceptance sampling theory, the process of selecting sample units in such a manner that all units under consideration have the same probability of being selected.

Reliability: The probability that a device will function without failure over a specified time period or amount of usage at stated conditions.

Reliability Growth: Reliability growth is the effort, and the resource commitment, to improve design, purchasing, production, and inspection procedures to improve the reliability of a design.

Risk: α : The probability of rejecting the null hypothesis falsely.

Scanning Electron Microscope (SEM): An instrument which provides a visual image of the surface features of an

item. It scans an electron beam over the surface of a sample while held in a vacuum and collects any of several resultant particles or energies. The SEM provides depth of field and resolution significantly exceeding light microscopy and may be used at magnifications exceeding 50 000 times.

Screening Test: A test or combination of tests intended to remove unsatisfactory items or those likely to exhibit early failures.

Significance: Results that show deviations between hypothesis and the observations used as a test of the hypothesis, greater than can be explained by random variation or chance alone, are called statistically significant.

Significance Level: The probability that, if the hypothesis under test were true, a sample test statistic would be as bad as or worse than the observed test statistic.

SPC: Statistical Process Control.

Storage Life (Shelf Life): The length of time an item can be stored under specified conditions and still meet specified requirements.

Stress: A general and ambiguous term used as an extension of its meaning in mechanics as that which could cause failure. It does not distinguish between those things which cause permanent damage (deterioration) and those things which do not (in the absence of failure).

Variance: The average of the squares of the deviations of individual measurements from their average. It is a measure of dispersion of a random variable or of data.

Wearout: The process of attrition which results in an increase of hazard rate with increasing age (cycles, time, miles, events, etc.) as applicable for the item.

ABBREVIATIONS

AQL	Acceptable quality level
CAR	Corrective action report/request
DIP	Dual in-line package
ECAP	Electronic circuit analysis program
EMC	Electro magnetic compatibility
EMI	Electro magnetic interference
EOS	Electrical overstress
ESD	Electrostatic discharge
FAR	Failure analysis report/request
FIT	(Failure in time) Failure unit; Failures/109 h
FMEA	Failure mode and effects analysis
FTA	Fault tree analysis
$h(t)$	Hazard rate
LTPD	Lot tolerance percent defective
MOS	Metal oxide semiconductor
MRB	Material review board
MTBF	Mean-time-between-failures
MTTF	Mean-time-to-failure



Reliability and Statistics Glossary

Reliability and Statistics Glossary

Vishay Semiconductors

MTTR Mean-time-to-repair

PPM Parts per million

PRST Probability ratio sequential test

QA Quality assurance

QC Quality control

QPL Qualified products list

RPM Reliability planning and management

SCA Sneak circuit analysis

SEM Scanning electron microscope

TW Wearout time

Z (t) Hazard rate

λ Failure rate (Lambda)



Disclaimer

ALL PRODUCT, PRODUCT SPECIFICATIONS AND DATA ARE SUBJECT TO CHANGE WITHOUT NOTICE TO IMPROVE RELIABILITY, FUNCTION OR DESIGN OR OTHERWISE.

Vishay Intertechnology, Inc., its affiliates, agents, and employees, and all persons acting on its or their behalf (collectively, "Vishay"), disclaim any and all liability for any errors, inaccuracies or incompleteness contained in any datasheet or in any other disclosure relating to any product.

Vishay makes no warranty, representation or guarantee regarding the suitability of the products for any particular purpose or the continuing production of any product. To the maximum extent permitted by applicable law, Vishay disclaims (i) any and all liability arising out of the application or use of any product, (ii) any and all liability, including without limitation special, consequential or incidental damages, and (iii) any and all implied warranties, including warranties of fitness for particular purpose, non-infringement and merchantability.

Statements regarding the suitability of products for certain types of applications are based on Vishay's knowledge of typical requirements that are often placed on Vishay products in generic applications. Such statements are not binding statements about the suitability of products for a particular application. It is the customer's responsibility to validate that a particular product with the properties described in the product specification is suitable for use in a particular application. Parameters provided in datasheets and / or specifications may vary in different applications and performance may vary over time. All operating parameters, including typical parameters, must be validated for each customer application by the customer's technical experts. Product specifications do not expand or otherwise modify Vishay's terms and conditions of purchase, including but not limited to the warranty expressed therein.

Hyperlinks included in this datasheet may direct users to third-party websites. These links are provided as a convenience and for informational purposes only. Inclusion of these hyperlinks does not constitute an endorsement or an approval by Vishay of any of the products, services or opinions of the corporation, organization or individual associated with the third-party website. Vishay disclaims any and all liability and bears no responsibility for the accuracy, legality or content of the third-party website or for that of subsequent links.

Except as expressly indicated in writing, Vishay products are not designed for use in medical, life-saving, or life-sustaining applications or for any other application in which the failure of the Vishay product could result in personal injury or death. Customers using or selling Vishay products not expressly indicated for use in such applications do so at their own risk. Please contact authorized Vishay personnel to obtain written terms and conditions regarding products designed for such applications.

No license, express or implied, by estoppel or otherwise, to any intellectual property rights is granted by this document or by any conduct of Vishay. Product names and markings noted herein may be trademarks of their respective owners.